SCOTT POLAR RESEARCH INSTITUTE, UNIVERSITY OF CAMBRIDGE

Characterising Sikussak and Other Forms of Ice Melange in Greenland Fjords

M.Phil Dissertation

Clare Fraser

Supervised by Poul Christoffersen

JUNE 2012

Abstract

The term ‘sikussak’ has a complex and disordered history of use in glaciological literature, and no dedicated studies of sikussak characteristics have yet been carried out. Using ATM elevation data from the NASA Operation IceBridge campaign, profiles of pro-glacial sikussak and ice melange are derived. Sikussak structures are found to be approximately 15 – 150 m thick and 1 – 35 km long, with surface slopes in the range ⁻0.1 – ⁻0.7°. These structures are therefore larger than is generally perceived, and may have a greater impact on the sensitive terminal zone of tidewater glaciers than previously considered. This study aims to characterise pro-glacial sikussak and melange structures and their importance at the calving front of tidewater terminating glaciers using a dataset of 13 glaciers around the Greenland Ice Sheet. Based on observations from these data, a classification system is proposed for the different pro-glacial structures found in Greenlandic fjords, and the geographical location of these various structures is delimited using a fast-ice index based on the ratio between positive and freezing degree days. The primary controls affecting sikussak morphology are investigated, and a hierarchy of glacio-dynamic, environmental and topographic factors are identified. Finally, it is proposed that there exists a stabilising feedback between rapid glacier flow and sikussak formation, and that this may be threatened under future climate change.

Acknowledgements

The data on which this project is based was collected by the NASA Operation IceBridge Campaign. I would like to thank my supervisor, Poul Christoffersen, for his guidance and advice, Steven Palmer for his technical assistance, my fellow MPhil students for their encouragement, and my parents for their support. Special thanks go to Joe Todd for his endless patience in explaining programming techniques.

Contents

1. Introduction

1. 1. Etymological evolution

The etymology and definition of the term 'sikussak' (alternatively: sikkusak, sikussaq, sikusaaq, sikosaq) has been variously contested since its first appearance in glaciological literature in the scientific report of the First Thule Expedition of 1912 by Peter Freuchan and Knud Rasmussen (Freuchan, 1915; Rasmusssen, 1915). Even these two early authors did not achieve a consensus on the primary characteristics of this phenomenon, though their two descriptions comprised parts of the same report. Rasmussen used the spelling 'sikussaq', and defined it as "fragments of inland ice packed on the fjord in the course of years" whereas Freuchan alternatively claimed that "this ice is called by the Eskimos 'Sikosaq'... i.e. fresh-water ice formed on the sea". He explained that "this kind of ice originates from the same causes as the glaciers, viz; excessive rainfall or thaw, and differs only from ordinary glacier ice in the fact that it is formed not on land, but on the sea ice". This puzzling (and little explained) description by Freuchan of "fresh-water ice formed on the sea" is elucidated by Lauge Koch (1926; 1928) who claims sikussak "was originally sea ice that has become rougher and rougher in the course of successive summers. After two to five years the ice has become quite fresh, and its structure is increasingly granular until it cannot be distinguished from glacier ice", a theory of formation which more recent glaciological research has proved false (Joughin et al., 2008b). Although this, and the assertion that sikussak is the reason icebergs float on the sea, do not fit with modern interpretation, he also notes that sikussak forms only in calm fjords, and helps prevent the calving of icebergs, both concepts which are still investigated in current glaciological research. Koch used yet another permutation of the name, and allows a somewhat broader etymological description; "sikussak is an Eskimo name meaning 'very old ice'".

Later still, Wadhams (1981) used the same spelling of the word, but claimed it was a Greenlandic Eskimo word meaning "fjord ice like ocean ice". Following these early definitions, the term 'sikussak' was included in the Arctic, Desert, Tropic Information Centre Glossary of Arctic and Subarctic Terms (ADTIC, 1955) as 'an Eskimo name for very old sea ice, resembling glacier ice, trapped in a fjord, having a snow accumulation on its surface which contributes to its formation and perpetuation'.

Investigation of modern Inuit dictionaries does not yield any definition for the term in any of its various spellings, the closest modern word is sikuaq, thin ice (sikkusat, floes of thin ice), which implies that sikussak may mean 'floes of thick ice'. In Arctic Canada, Laidler (2007) investigated the use of different terms for sea ice around the three Nunavut communities of Cape Dorset, Igloolik

and Pangnirtung, and records ‘sikusaaq’ as being the description for ice which is ‘newly formed land-fast ice, thick enough for travel’, part of a progression of terms describing increasing thickness of land-fast ice, the terminology evolving with the progressive development of ice. Laidler proposes that ‘sikusaaq’ in Igloolik is equivalent to ‘sikujuq’ in the Cape Dorset and Pangnirtung communities.

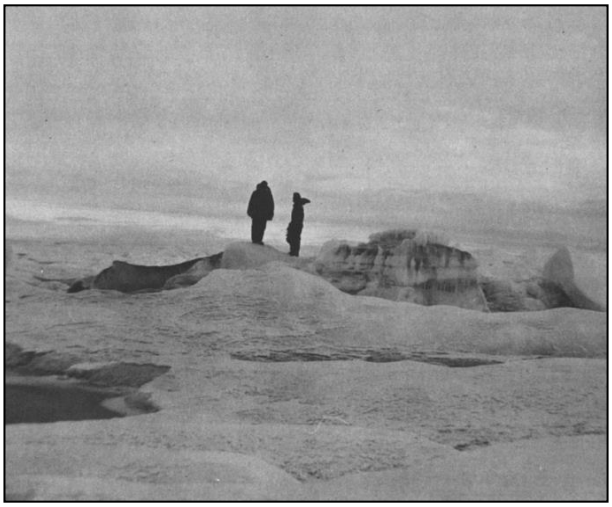

Figure 1.1: Photograph of sikussak according to Wadhams (1981)

The root ‘siku’, however, is found in most Inuit dictionaries, and is always defined as meaning ‘sea ice’, or merely even ‘ice’ in all its permutations and contexts. Krupnik et al. (2010) note that the third person singular intransitive ending ‘juq’ could have a range of meanings (e.g. It’s icy), but is actually highly specific in Inuit nomenclature, meaning ‘ice that is travelable’, as documented by Laidler (2007) in the Cape Dorset community.

In these Nunavut communities, the definition of this feature is heavily influenced by the concerns of these societies; the definition is intrinsically related to the interaction between people and ice, and its usage fundamentally practical, “thick enough to travel”. In glaciological literature, however, this term may serve a very different purpose, relating to a specific structure which plays an important role in the glacial terminal environment. The term is not listed in the World Meteorological Organisation glossary of sea ice nomenclature, although this document does not list an equivalent descriptive term, indicating that the term ‘sikussak’ is not superfluous, but merely relates to a structure which has not as of yet been definitively characterised.

Wadhams (1981) and the ADTIC Glossary (1955) support the description by Koch of ‘fjord ice’; generally smooth, with irregularities from old floes, brash ice and bergy bits, which forms seasonally in constricted channels, and may survive the summer to become a multi-year feature. This ice fills the width of the channel, and achieves a kind of quasi-stability in winter, where a degree of movement and deformation may still occur. However, his description of this form of ice is distinct

from sikussak, for which Wadhams (1981) follows the description of Koch (1945), of "undeformed ice floes of exceptional thickness".

Up until about a decade ago, the term is scarcely found in glaciological literature since early expedition reports. Since these early, vague descriptions, however, which tended to follow the observations of Koch (1928), its definition has evolved somewhat. More recent definitions of 'sikussak' exhibit a seasonal evolution more comparable to Koch's 'fjord ice', which forms and melts in situ, and may have old floes, brash and bergy bits frozen within the ice matrix. Andrews et al. (1994) use sikussak to mean a "chaotic melange of icebergs, sea ice, and bergy bits that extend several kilometres from the actual calving margin" (shown in Figure 1.2, below), and state that this structure is characteristic of some Greenlandic fjord environments, including Kangerdlugssuaq. However, some papers have retained the definition according Wadhams (1981), such as Fox and Squire (1991), and this has led to some confusion over the meaning of the term.

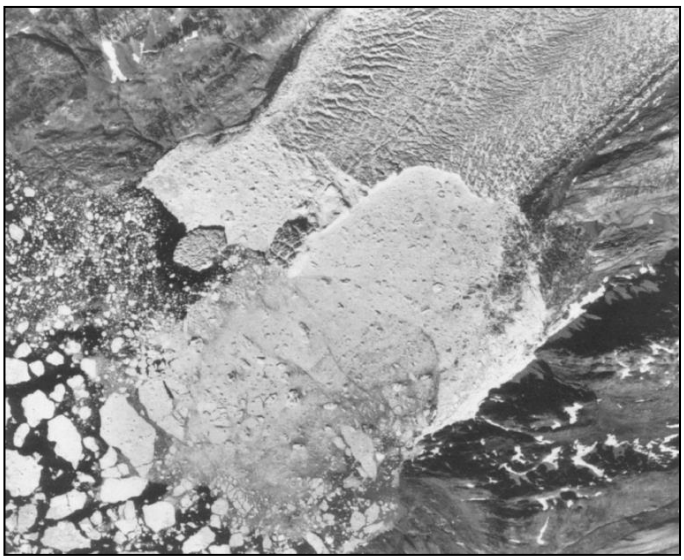

Figure 1.2: Air photograph of ' an ice melange or sikussak' at the calving face (width approximately 2.1 km) of Fredricksborg Gletcher, Watkins Fjord, according to Andrews et al. (1994)

Figure 1.3: Landsat multispectral scanner image (path/row 231/012) acquired on 13/08/1987 depicting 'sikussak or multi-year shore-fast sea ice' in Kangerdlugssuaq Fjord, according to Dowdeswell et al. (2000). Scale is 50 km across image.

Early definitions include a requirement for sikussak to have extreme thickness and great age. Koch (1928) stated that "to be called sikussak the ice must be at least 25 years old", though more recent permutations have tended to refer to increasingly transient structures. Dowdeswell et al., (2000) state that sikussak is a multi-year phenomenon which prevented the evacuation of icebergs from Greenlandic fjords during the Younger Dryas stadial and Little Ice Age cold periods, and this phenomenon may still be present in areas of the high Arctic. However, the most recent definitions do not tend to include a minimum age for sikussak structures (Joughin et al., 2008b).

'Mélange', French for 'mixture' (anglicised in most literature to 'melange'), is a useful general term for any collection of different forms of ice formed either in fjords or open sea, regardless of thickness, cohesion or age. This term has also been used for the collection of ice debris found within ice shelf rifts in Antarctica (Rignot and MacAyeal, 1998; Larour et al., 2004; Fricker et al., 2005), whereas it has been suggested that the term 'sikussak' may not be applicable to other ice marginal areas (Amundsen et al., 2010). The geographical distribution of sikussak has been delimited to various geographical zones, but the limited geographical distribution postulated by early authors may be the result of the highly specific definitions which they applied to the term. Koch (1928) specified that sikussak is generally limited to the central north coast of Greenland (Figure 1.4), the fjords of which (including Frederick Hyde, Bessels, and Humboltd) are (or, at least, were) filled with sikussak, although Wadhams (1981) speculated that sikussak may be present in other high Arctic locations where fjord conditions are sufficiently calm and glacier activity sufficiently low.

Figure 1.4: Location of sikussak and other forms of multi-year ice in northern Greenland according to Koch (1928)

Joughin et al. (2008b) applied a very broad description to the phenomenon, merely stating that it refers to "icebergs frozen together by sea ice". From then on, the terms sikussak and melange tend to be alternatively or synonymously used, for example by Seale (2011), who states that "both are semi rigid mixtures consisting of icebergs, ice fragments and sea ice". A distinctive feature of recent descriptions is the element of seasonal rigidity, although this has been applied to both ice melange (Howat et al., 2010) and sikussak (Christoffersen et al., 2011).

Another term which appears to have some overlap with the structure which this report seeks to investigate is that of an 'icefoot', which is defined by Petersen (1977) as "a bridge or transition zone of tidal cracks or leads where ice floes contract and expand with the tide, and mobile floating sea ice", and seems to be largely applied to arctic beaches (Wiseman et al., 1981), though this feature appears to be additionally relevant to pro-glacial environments (Syvitski et al., 1987). These features are described as being up to 2 m thick in their first year, with both duration and thickness dependent upon, and increasing with, latitude (Syvitski et al., 1987).

1. 2. Sikussak in modern glaciology

Although historically, the term 'sikussak' was reserved for thick, multi-year features in the high northern latitudes, recent descriptions indicate that the term sikussak may be more useful in an alternative glaciological context as a more specific term under the larger heading of melange. Where melange may be used to mean "any material composed of a heterogeneous mixture of ice types" (O'Leary, personal communication), sikussak may be used to refer to a more specific mixture of ice types, where icebergs and sea ice cohere to form a seasonally rigid pro-glacial structure in glacial fjords, such as Reeh et al. (1999), "sikussaq: frozen-together icebergs and sea ice attached to the glacier terminus". The important features of this structure are the aspect of seasonal rigidity, and role as a transitional structure between the calving glacier and seasonal sea ice.

Amundsen et al. (2010) champion the term 'ice melange' over 'sikussak' as these authors feel that 'sikussak' is prohibitively Greenland specific. However, although the etymological investigation in Section 1.1 shows that this word was derived from Greenlandic nomenclature, it has since evolved in scientific literature to become not only unbound from specific locations, but also to refer to a highly specific seasonally rigid transitional structure. The term 'melange' is therefore too broad, used as it is to describe any mixture of ice types, whether rigid or loose. The aspect of rigidity evolved in observations in scientific literature out of an evident necessity to describe the observed pro-glacial structure which seasonally inhibited glacier calving, and therefore a specific term is needed to refer

to this structure. Sikussak is presented as an appropriate term, since it has already evolved to be used in this context in glaciological literature.

The word 'sikussak' is consistently used whenever authors find that a criterion of rigidity is required. Syvitski et al. (1996) refer to this rigidity, describing a "complex of fused icebergs and sea ice attached to the glacier terminus", as do Reeh et al. (1999), "frozen-together icebergs and sea ice attached to the glacier terminus, and Christoffersen et al. (2012), "semi-persistent melange of icebergs and shore-fast sea ice". All of these authors use the term 'sikussak' (although Reeh et al. 1999 use Rasmussen's 1915 spelling of 'sikussaq'), and include sea ice as the mechanism for bonding the clasts. Howat et al. (2010) make reference to a "dense mix of icebergs and sea ice within the fjord", and Amundsen et al. (2010) to "a dense pack of calved ice bergs". Neither of these papers refers to the seasonal formation of sea ice which binds the clasts together, and therefore do not make a distinction between loose melange and rigid sikussak, both preferring the term 'ice melange'. Joughin et al. (2008) include an aspect of seasonal rigidity, describing "sea ice [which] bonds glacier ice in the fjord to produce a nearly rigid mass" in front of Jakobshavn Isbrae, and although this is termed a 'transient winter ice tongue', it is recognisably the same feature which is referred to as 'sikussak' by Syvitski et al. (1996), Reeh et al. (1999) and Christoffersen et al. (2012).

Even in 2011, 'sikussak' is still being used after the description by Koch (1945) to refer to pro-glacial multi-year calf ice at Zachariae Isstrom and Nioghalvfjerdsfjorden (Box and Decker, 2011). However, this definition is now much less pervasive, and it is recognised that the term 'multi-year land-fast ice' is much more frequently used to refer to these thick, old structures in the fjords of the high north of Greenland.

1. 2. 2. Effect on glacier stability

It has been noted that the calving front transition zone in which melange and sikussak structures are found is particularly important for tidewater glacier flow due to their sensitive dependence on longitudinal stress gradients, which are likely to increase towards the terminus (Joughin et al., 2008c). The stress at the ice front is made up of: slope stress (shear stress); gradient stress (the longitudinal gradient in normal stress), a function of terminus geometry (Meier and Post, 1987); and basal and lateral shear stresses from the bed and walls of the fjord (van der Veen, 1996). At the terminus of calving tidewater glaciers, the outward cryostatic pressure can exceed the hydrostatic pressure from the water, leading to a response in the longitudinal stress gradient (Benn et al., 2007).

The term tidewater glacier stems from the effect of tides on the stresses at the calving ice front, which can trigger tidal modulation of calving as well as flow. Changes to the balance of driving and resistive stresses at the terminus cause flow variations, resulting in thinning and acceleration inland

(Joughin et al., 2008c). Since fast-ice structures in fjords have the potential to transmit non-local lateral and basal drag as a resistive force onto the calving face, once these structures are weakened or removed, this loss of resistance must be accounted for through an adjusted strain rate, resulting in extensional or accelerated flow up-glacier (Joughin et al., 2010; Nick et al., 2010).

Many studies have observed that fjord systems tend to become choked with icebergs during the calving season, and this can have the effect of constraining calved icebergs at the terminus. The effect has been compared to the buttressing effect of Antarctic Ice Shelves (Geirsdottir et al., 2008), although most authors concede that the back-stress effect is probably not sufficient to restrain the interior ice. It is therefore more likely that sikussak affects discharge rate by preventing calved icebergs from drifting down-fjord, thereby maintaining the structural integrity of the calving front (Reeh et al. 2001), and acting as a control on the rate of calving (Sohn et al., 1998). The presence of a resistive ice melange reduces the rotational torque at the calving face, which prohibits capsize of calved icebergs, and thereby prevents new icebergs from calving off (Nick et al., 2010, Joughin et al., 2008b). This seasonal suppression of calving affects the length of the calving season, and enables post-melt-season advance, which in turn controls the total annual calving flux (Box and Decker, 2011). Since sikussak likely affects calving front dynamics, it is therefore an important structure to understand. The importance and seasonal variability of this structure has long been identified, though not definitively characterised, in a long history of glaciological literature.

Reeh et al. (2001) construct a series of hypotheses on the role of fast ice (of which sikussak is a seasonally evolving form) proposing that these structures may exert one of a spectrum of effects on the calving front of tidewater glaciers. The weakest and least direct of these is the effect of suppressing the effect of oceanic forcing by damping long ocean and wind-generated waves, thereby reducing bending stresses which lead to fracture, and inhibiting mixing of water masses in the fjord thereby potentially preventing warm saline water from coming into contact with the calving face. At the other end of the scale, it is proposed that sikussak structures may be sufficiently rigid and coherent to apply a back-stress on the calving terminus and in some cases prevent crevasse formation and calving events (Joughin et al., 2008b). Between these two potential effects is the role that fast ice may have in maintaining the integrity of the glacier calving face, preventing icebergs and glacial debris from drifting away and consequently suppressing calving. In addition to these hypotheses, it is also proposed that sikussak formation may facilitate the advance of tidewater glaciers into deep water, in some cases overcoming the stabilising effect of topographic pinning points (Andrews et al., 1994; Warren et al., 1991).

The factors affecting processes in the terminal environment of Greenland's tidewater glaciers are highly interdependent, which makes it difficult to assign causality, but means that a change to any one part of the fjord environment is likely to precipitate a response in the dynamics of the glacier system (Walter et al., 2012). A reduced extent of floating ice results in a reduction of back-stress on the calving front, causing a front-stress perturbation which may destabilise the glacier tongue and trigger calving events (Nick et al., 2009; Andresen et al., 2011). Conversely, increased formation of fjord ice has been linked to reduced calving (Sohn et al., 1988). These processes are all highly sensitive to the overriding climatic and oceanic changes which force the dynamic system (Nick et al., 2009).

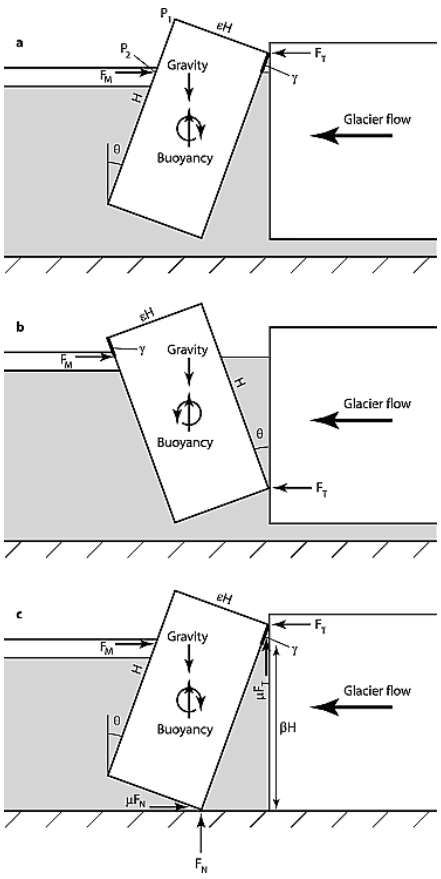

Figure 1.5: Diagrams used for the force balance analysis of calving icebergs. Here *γ* is indicated by thick black lines (Amundsen et al., 2010).

Amundsen (2010) notes that the resistance afforded by pro-glacial melange structures may be sufficient to counteract the rotational moment of the glacier calving face, and thereby cause bottom-out rotation of calved icebergs. This may make the glacier more susceptible to factors causing fracturing and crevasses at the bed of the ice sheet. Amundsen (2010) found that at reasonably small tilt angles (Θ) the melange resistive force (F_M) required to prevent a calved iceberg from rotating bottom-out was at least an order of magnitude greater than that required to prevent top-out rotation, indicating that the changes of bottom-out rotation are greatly increased when a pro-glacial ice melange is present (Figure 1.5). The melange resistive force required to hold a block in static equilibrium is a function of the height, geometry and tilt angle of the calved block, and in order to investigate this, the thickness and shear strength of the structure must be determined. However, it must be considered that the shear strength of melange will not be comparable to that of pure ice, since melange is a highly fractured and heterogeneous mixture.

1. 2. 3. Shear strength

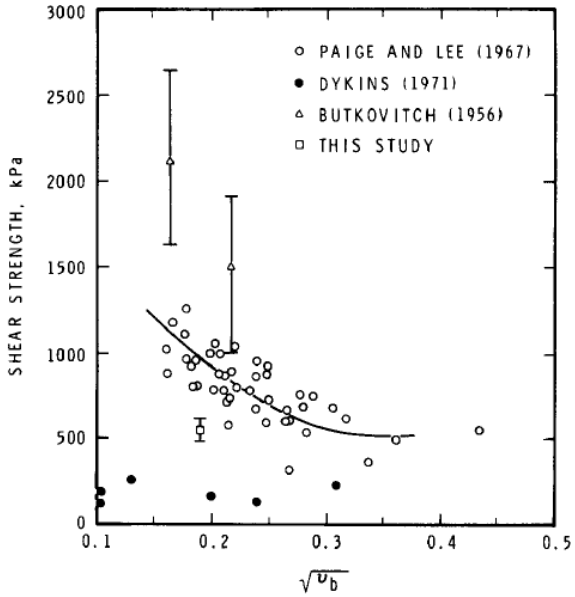

Figure 1.6: Shear strength as a function of the square root of brine volume. Note that the data from the literature are for columnar-grained ice, whereas the results of this study are for granular ice. (Frederking and Timco, 1984)

The shear strength of ice is a function of several interrelated factors, the most important of which are thickness, salinity and temperature. Brine volume (υ_b) is a function of both temperature and salinity, and therefore the relationship of shear strength to this variable reflects changes in both of these factors (Paige and Lee, 1967). Frederking and Timco (1986) note that the shear strength of ice tends to decrease with increasing temperature, though as can be seen from Figure 1.6, the relationship between shear strength and brine volume is highly variable across different studies.

Walter et al. (2012) state that variable iceberg concentration may cause the thickness of pro-glacial melange structures to vary by hundreds of metres. The thickness, strength, and extent of melange structures varies seasonally with peak extent in late April, just prior to summer break-up in June or July (Howat et al., 2010; Walter et al., 2012). This is thought to be a function of some combination of sea ice concentration, climatic and oceanic variables, and glacier dynamic processes (Seale et al., 2011).The winter rigidity of sikussak is facilitated by the formation of sea ice within the fjord systems, and therefore temporal and spatial variations in sikussak strength are inherently dependent upon the thickness and seasonality of sea ice formation within the glacial fjords (Walter et al., 2012).

It is important to make a distinction between the compaction of ice melange and cohesion of sikussak. Unconsolidated melange, such as is present after mobilisation of the ice melange (Walter et al., 2012) may clog a fjord system but is unlikely to exert a substantial resistive stress on the calving front unless it becomes highly compacted and compressed. Sikussak, on the other hand, becomes structurally sound once sea ice freezes the clasts together, and therefore may be forced down-fjord as a cohesive mass, and may become detached from the glacier front due to turbid upwelling of water at the glacier front (Motyka et al., 2003). Due to their different properties and dynamic characteristics, these structures must be considered independently. Defining them as

melange/sikussak respectively enables a distinction to be drawn between them, and the back-stress they exert on the calving front investigated individually.

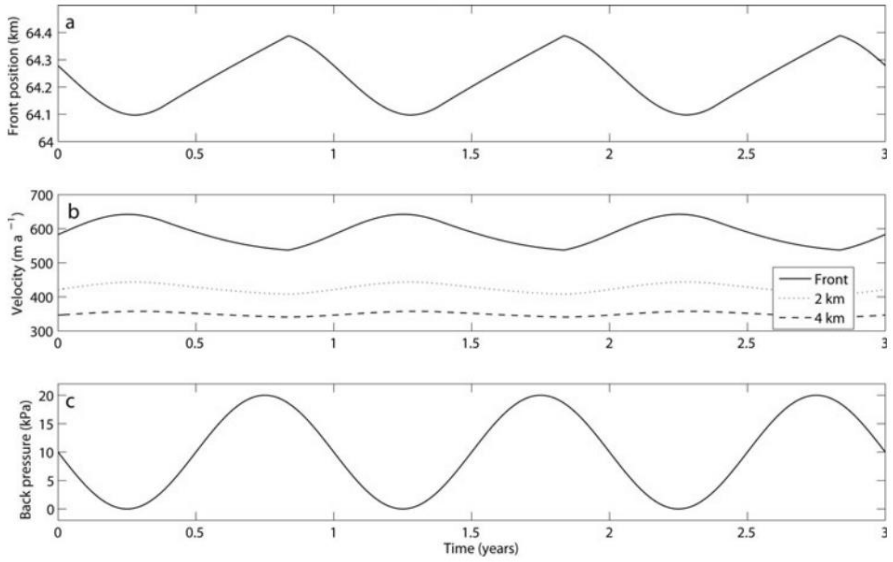

Figure 1.7: Seasonal variations in a) Calving front position; b) Velocity variations 0, 2 and 4 km from the calving front, and c) The seasonal variation in back pressure from sea ice and sikussak thought to be forcing these changes in the model (Nick et al., 2010).

In the Nick et al. (2010) calving model of marine outlet glaciers, sikussak and sea ice were incorporated into the boundary conditions as a backpressure (σ_B). Nick et al. (2010) propose that these boundary conditions produce a sinusoidal seasonal pattern of back-stress on the calving front of tidewater glaciers in Greenland, which effects seasonal variations in position of the calving front, and near-front velocity changes (Figure 1.7).

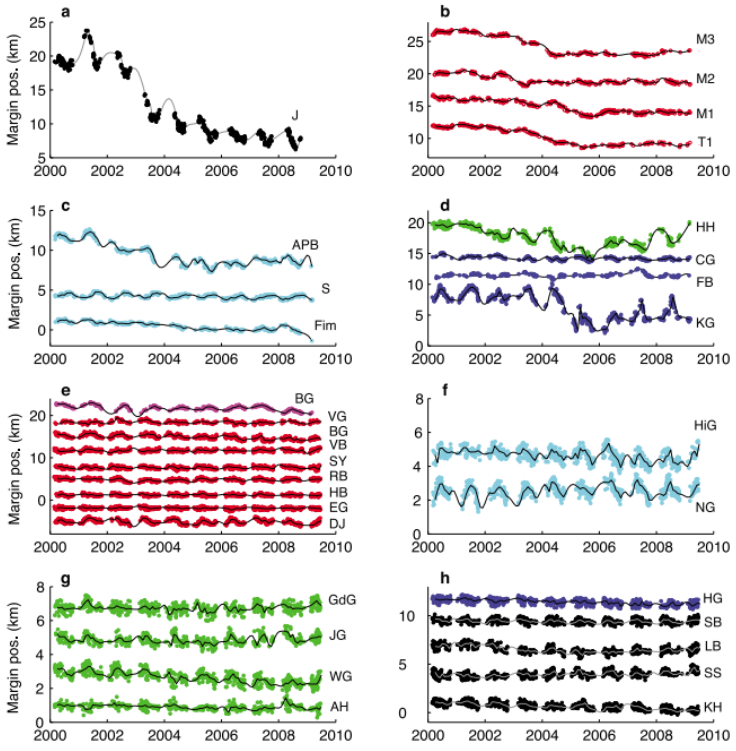

Figure 1.8: Changes in calving front position for glaciers of East Greenland, derived from automatic edge detection and brightness in MODIS imagery. Notable glaciers include (a) J: Jakobshavn Isbrae,(d) HH: Helheim Glacier and KL: Kangerdlugssuaq Glacier (Seale et al., 2011).

These seasonal variations in calving front positions were empirically derived for a set of tidewater glaciers in East Greenland by Seale et al. (2011). Shown in Figure 1.8 are variations in calving front position of 30 glaciers. The degree to which this seasonal cycle is affected by changes in the sikussak and sea ice thickness and extent is unknown, but a good correlation between loss of sikussak rigidity and initiation of margin retreat for yearly records of East Greenland glaciers indicates that these factors are either related, or dependent on a common forcing factor (Seale et al., 2011).

Walter et al. (2012) used GPS and photogrammetry techniques to monitor changes in glacier flow velocity in response to observations of ice melange disintegration, tidal fluctuations and quantified calving events. The influence of these factors on velocity perturbations further up-glacier from the terminus is inferred from longitudinal coupling (Echelmeyer and Kamb, 1986). Qualitative observations made in this paper indicate that during the period of ice melange stability (until late May/ early June) when air temperatures were predominantly below freezing, the calving front was stable and the glacier extended down-fjord. Once the melange mobilises, it rapidly disintegrates into a loose melange of small bergs and brash ice, which does not appear to have the same stabilising influence as rigid sikussak. The break-up is thought to have been influenced by the wind gusts of >25 m s^{-1} which were observed simultaneously.

Comparison of these observations with measured ice velocity shows a close correlation between the timing of melange disintegration and a subsequent ice flow acceleration of 1.5 m d^{-1} (14%) over ~2 days. This is attributed to the effect of a loss of buttressing from the ice melange, indicating that the ice melange exerted sufficient back-stress to inhibit ice flow, in a manner similar to that of buttressing ice shelves (Geirsdottir et al., 2008). After the melange disintegration, the glacier flow velocity exhibits large diurnal and smaller semi-diurnal fluctuations, thought to be the result of a hydrological connection with the bed routing daily peaks in surface meltwater to the bed.

A correlation is also found between the timing of ice melange break-up and clearance and the calving activity record, which indicates a link between episodes of calving activity and ice flow acceleration, both of which are more frequent after melange disintegration. However, causality of flow acceleration cannot be definitively attributed to the influence of a single factor such as melange clearance without considering the simultaneous influences of tidal variations and calving. Instead, estimates based on flow speed variations when the melange is present are made.

Longitudinal coupling theory (Echelmeyer and Kamb, 1986) is based on a consideration of the force balance of the glacier and the interaction between the driving stress, lateral shear stress and basal shear stress to evaluate how the glacier responds to dynamic changes such as stretching at the

terminus. It is assumed that the forces at the calving front, comprised of driving stress (τ_d), longitudinal stress (τ_L) and basal shear stress (τ_b), balance, such that:

$$\tau_d - \tau_L - \tau_b = 0$$

[1]

This was then used to estimate tidally-forced flow perturbations using an extension to this theory by Walters (1989), which considers glacier flow response to tidally-induced hydrostatic stress variations at the terminus, using the equation below:

$$u_1(x) = \frac{p_{T\mathrm{L}}}{\bar{\eta}} \exp(-|x - x_0|/L)$$

[2]

Where p_{T} is the variation in pressure caused by a 2 m tide level change, η the effective viscosity, *x* the distance along-flow, and *L is* the longitudinal coupling length-scale (Walter et al., 2012).

From observations of a ~1.5m d^{-1} 'ramped' step-change in ice flow velocity, $u_1(x)$, near the terminus coincident with the disintegration of the pro-glacial ice melange, Walter et al. (2012) estimated the pressure due to the presence of the ice melange ($p_{melange}$):

$$p_{melange} = \frac{u_1(x_0)\bar{\eta}}{L}$$

[3]

The values for $p_{melange}$ calculated from this range from 30 to 60 kPa which is comparable to the back-stress effect of measured tidal perturbations (~20 kPa).

Despite the preponderance of observations indicating that melange in fjord systems is an important control upon tidewater calving, many models still assume rapid evacuation of icebergs from the fjord system, or do not consider the role of melange structures in force balance analysis (Geirsdottir et al., 2008; Vieli et al., 2001; Bassis and Walker, 2012). An exception to this is the study by MacAyeal et al.

(2012), who idealise ice melange as a set of 20 separate and evenly spaced icebergs of identical dimensions (1km wide, 200m thick) within the fjord . This is an extremely simplified representation of ice melange, and does not take into account any cohesion or compression between the icebergs.

However, the role of pro-glacial structures is contested, as Luckman et al. (2006) disregard fjord ice as an important multi-annual influence on calving front retreat. These authors state that although seasonal sikussak formation may affect abrupt frontal changes, the primary driver affecting frontal position is glacier flow velocity, controlled by regional climatic and oceanic factors. Contrarily, Joughin et al. (2008a) state that flow velocity is controlled by the ice front position, indicating the importance of bi-directional forcings in the terminal environment. Since causality has not been definitively established, it is possible that the seasonal consolidation of sikussak and the annual advance and retreat cycle are synchronous not because they are causally linked, but because they are reacting independently to some external forcing, such as atmospheric/oceanic temperatures, wind or meltwater production.

1. 3. Environmental forcing

The tidewater terminating glaciers of Greenland are highly sensitive to changes at the ice/ocean interface (Nick et al., 2009), and in particular variations in the temperature of coastal waters (Hanna et al., 2009). Since melange and sikussak structures are located in this sensitive terminal zone, they are similarly affected by the environmental factors which force changes in tidewater glaciers. Warm surface water affects the duration and extent of fjord ice, thereby influencing the period of sikussak rigidity which controls the length of the calving season at tidewater glaciers (Murray et al., 2009).

In recent years, many of Greenland's tidewater terminating glaciers have undergone frontal retreat, dynamic thinning, and accelerated flow velocity (Joughin et al., 2008a). In the southeast, a notable synchronicity in frontal retreat and flow acceleration, especially between Helheim and Kangerdlugssuaq glaciers, indicates a common regional forcing, likely climatic or oceanic in origin (Walsh et al, 2012; Andresen et al., 2012; Luckman et al., 2006). This, linked with the close correlation between timings of frontal change of southern Greenland tidewater glaciers and periods of ocean warming in the late 1990s and early 2000s, as shown for Helheim glacier in Figure 1.9 (Andresen et al., 2011), indicates that ocean temperatures are of vital importance to the dynamics of tidewater glaciers. Greenland's location at the northern edge of the Subpolar Gyre makes the properties of its coastal waters dependent on the variations of this circulation (Stein, 2005). It has been proposed by Nick et al. (2009) that observations linking oceanic temperature changes to

fluctuations of the calving face of Jakobshavn Isbrae and other glaciers are merely ephemeral changes and do not reflect a long-term trend. However, research from benthic foraminiferal data from Disko Bay, in front of Jakobshavn Isbrae, shows that a correlation between ice margin position and oceanic conditions has persisted for at least 100 years (Lloyd et al., 2011).

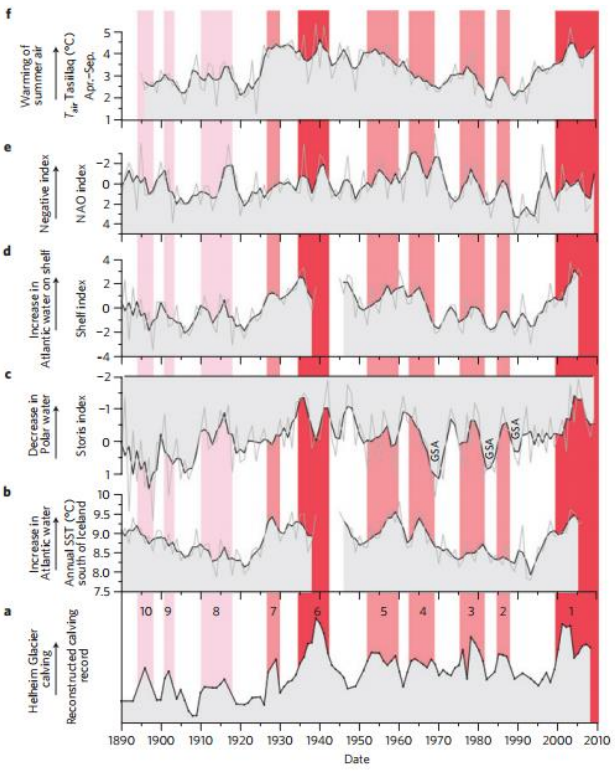

Figure 1.9: Comparison between calving record and climate indices (Andresen et al., 2011)

Along the eastern coast, there is a strong disparity between the highly synchronous retreat behaviour of tidewater glaciers south of 69°N and the much smaller and more variable pattern of retreat for glaciers north of 69°N (Christoffersen et al., 2011). 69°N corresponds to the northern limit of the Irminger current, part of the subpolar gyre, which brings incursions of warm, saline Atlantic water to Greenland's shores (Walsh et al., 2012), the path of which is shown in Figure 1.10 (Hanna et al., 2009).

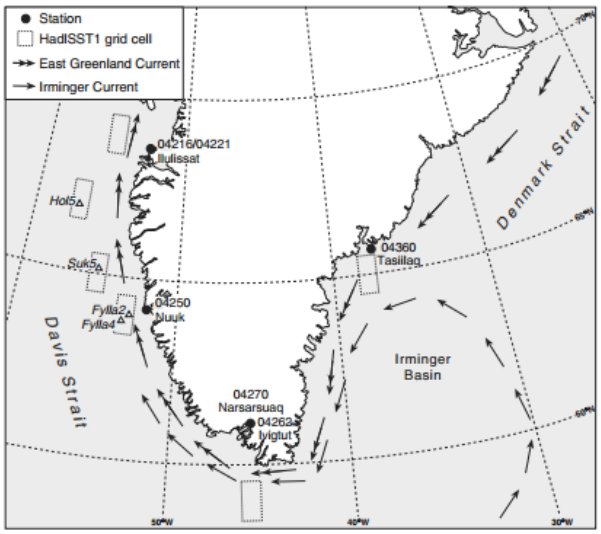

Figure 1.10: Map of southern Greenland showing the path of the East Greenland and Irminger Currents. Produced by Paul Coles, University of Sheffield (Hanna et al., 2009).

The subpolar gyre is highly dependent upon the strength of the NAO, as illustrated by the switch in the winters of 1994/1995 and 1995/1996 from a strongly positive phase to a negative phase, resulting in a dramatic weakening and contraction of the subpolar gyre (Hakkinen and Rhines, 2004), enabling a greater quantity of warmer subtropical waters to spread westward to the Irminger Sea and on over the continental shelf of West Greenland (Holland et al., 2008). Similarly, in the winter of 2009/2010, an extremely negative NAO index resulted in anomalously warm conditions

(Ribergaard, 2011). This indicates that the oceanic heat flux towards the fjords of southern Greenland is highly dependent on the state of the NAO.

Strong winds along the eastern coast of Greenland cause incursion of these warm subtropical waters over the continental shelf, and control the renewal rate of fjord waters (Straneo et al., 2010). This wind stress is determined by the atmospheric pressure gradient between the Greenland high-pressure system and the Icelandic low-pressure system (Christoffersen et al., 2011). In addition, a stratification of water masses within Greenlandic fjords has been observed, with the warmer and more saline subtropical waters overlain by colder and fresher Arctic waters (Straneo et al., 2011), as shown schematically in Figure 1.11. Straneo et al. (2011) propose that this water stratification may cause variable heat transport and melting at the calving face of Greenland's tidewater glaciers, and therefore to some extent control the structure and stability of their floating sections. Murray et al. (2010) suggest that a negative feedback may occur when increased transport of warm subtropical waters to tidewater glaciers results in increased calving. Cold water from glacier discharge strengthens the East Greenland Coastal Current (EGCC), which prevents incursion of warm subtropical water, and thereby inhibits the continued large mass loss from these tidewater terminating glaciers. However, this feedback mechanism is not confirmed as it has been suggested that these observations of increased calving and flow at tidewater glaciers may be controlled by changes in the properties of the warm subtropical water masses, rather than their increased transport across the coastal shelf of Greenland (Christoffersen et al., 2011).

The west Greenland current, which brings warmer subsurface waters to the southwest of Greenland, is formed of a combination of the Irminger Current from the Atlantic and the colder East Greenland Current from the Arctic. These water masses become increasingly mixed as they flow around the southern tip of Greenland (Lloyd et al., 2011), shown in Figure 1.10. It has been observed that ice conditions are well correlated with the strength of the NAO, but a distinct delay is observed between the same-year response in the southeast and the next-year response in the southwest, as shown in Figure 1.12 (Stern and Heide-Jorgensen, 2003). This indicates that sea ice concentration in the southeast is well correlated with this

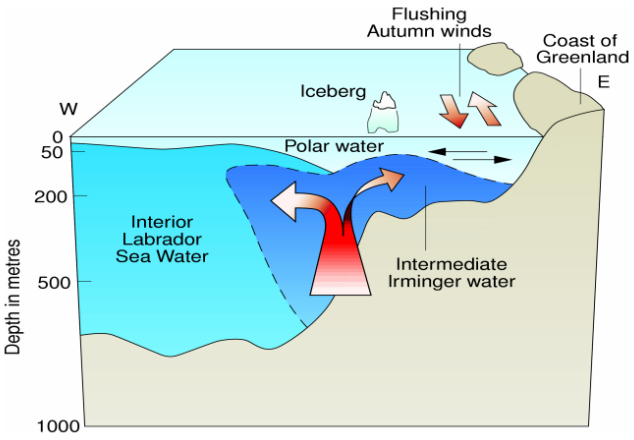

Figure 1.11: Schematic diagram showing stratification of water masses off the coast of West Greenland (Ribergaard, 2011)

year's NAO index, whereas in the southwest it shows a good correlation with the previous year's NAO index (Stern and Heide-Jorgensen, 2003).

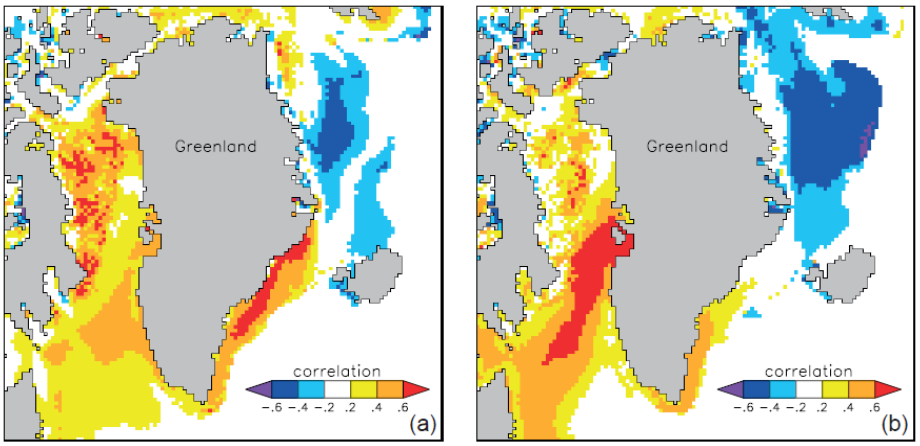

Figure 1.12: Correlation of winter (December to March) sea ice concentration (SMMR+SSMI 1979-1999) with (a) Winter NAO indiex (1979-1999) and (b) previous winter's NAO index (1978-1998). (Stern and Heide-Jorgensen, 2003).

The seasonal formation of sea ice within fjords such as Jakobshavn Isfjord, which may exert an important control upon the calving rate and length of calving season of Greenland's most prolific exporter of ice, is controlled by regional air and ocean temperatures (Nick et al., 2009; Germe et al., 2011). Therefore the heat flux of waters breaching the continental shelf of Greenland may have important effects for the timing of seasonal melange formation and disintegration. A pro-glacial sikussak may inhibit atmosphere-ocean heat exchange, affect wind-driven mixing, and thereby alter the temperature of water reaching the glacier calving face (Walter et al., 2012).

The duration of sea ice and melange formation in glacial fjords, thought to influence the length of the glacier calving season, may be controlled by ocean/air warming (Andresen et al. 2012). In the far north, ocean water properties may have a critical effect on the remains of thick multi-year ice (sikussak) in the Lincoln Sea and around the northeast edge of Greenland (Munchow et al., 2011). The length of the land-fast sea ice season is contracting, which may have implications for the glaciers of this northern region.

A major challenge currently facing researchers is distinguishing between the effect of atmospheric and oceanic changes, which together constitute a primary forcing in the dynamic terminal zone of tidewater glaciers (Bamber et al., 2007). Maslinik et al. (1996) notes that variations in the thickness and extent of regional sea ice are well correlated to air temperature anomalies, though Andresen et al. (2011) note that ocean temperature anomalies can also affect the growth and decay of sea ice and sikussak.

Air temperature has long been identified as a control, or at least major indicator of the location of regions of fast-ice. This was most explicit in the work of Reeh et al. (1999), who developed a fast ice index which estimated the latitudinal range of fast-ice growth and persistence based on the

annually-summed number of days above and below freezing. Based on the assumption that air temperature is a primary control on the location of fast-ice, it is likely that regions of fast-ice were much more extensive during previous cold periods, including the Younger Dryas (YD) and Little Ice Age (LIA) (Dowdeswell et al., 2000). Therefore, fast-ice location is expected to vary both temporally and spatially with variations in air temperature.

1. 3. Topographic control

The concept that fjord topography exerts a control on the location of tidewater calving margins is well-established (Warren, 1991), and it has been suggested that this control is strong enough to cause hysteresis in glacier response to climate forcings (Meier and Post, 1987). Syvitski et al. (1996) suggest that this theory may be applied to sikussaks, and assert that this acts as an important factor in determining when and where sikussak structures form. This is attributed to two factors. Firstly, that topographic constrictions or bathymetric rises cause large icebergs to ground and trap the melange material behind them. This theory is based on the assumption that in the absence of a seaward iceberg 'trap', the material would simply drift away. The second theory is that smaller channels or embayments represent a sheltered area where the sikussak is protected from oceanic influences (Syvitski et al., 1996). These two theories differ from the idea of 'pinning points' as applied to the calving front of tidewater glaciers, which attribute long-term stability at topographic constrictions and terminal moraines to the effect that a wider calving face and greater water depth has upon the calving rate, and therefore mass balance of the glacier (Warren, 1991). Glaciers therefore tend to retreat to locations with a relatively small width and water depth, where mass balance is reduced, and to move from these 'pinning point' locations, the glacier must overcome a threshold of stability in gradient stress (Meier and Post, 1987). If the same theory was applied to pro-glacial sikussak structures, it would imply that these structures had sufficient rigidity to become dependent on gradient stress, and it may therefore be appropriate to apply glacio-dynamic theories of gradient stress and calving to their growth, persistence, and decay.

Once the primary characteristics of melange and sikussak structures in Greenland have been identified, it is necessary to establish the major controls on sikussak formation in order to apply an appropriate system of classification. If sikussak features are primarily a function of climate, it may be appropriate to group them latitudinally. However, if these structures are primarily controlled by glacio-dynamic factors, a classification system based on these controls is required.

1. 4. Aim and Objectives

The aim of this project is to classify melange and sikussak structures in Greenlandic fjords based on an understanding of their primary physical characteristics.

The objectives of this study are to indentify the extent to which the physical characteristics of sikussak and other forms of ice melange are controlled by:

(a) Climatic factors

(b) Glaciological factors

(c) Topographic factors

2. Methods

2. 1. Study Area

The locations for this study were chosen with a consideration for a wide spread of latitudes along both the East and West coasts of Greenland in order to achieve a wider picture of the behaviour of melange structures. However, the choice of glaciers was constrained by the availability of laser altimeter data, collected by Operation IceBridge.

Therefore, glaciers were chosen by overlaying the IceBridge flight paths for all available years on a base map of Greenland and selecting glaciers from a range of locations around the Greenland Ice Sheet (GrIS) where flight paths indicated that data was available for at least two of the years 2009-2011. An additional consideration was to choose larger and faster flowing glaciers, as these are most likely to have a considerable impact on the future of the ice sheet.

Glacier Name	Abbreviation	Latitude	Longitude	Side	Velocity (m/a)	Width (km)
Kangiata Nunata Sermia	KNS	64.3	310.4	W	6090	4.45
Helheim Gletscher	HH	66.4	321.9	E	7987	5.6
Kangerdlugssuaq Gletscher	KL	68.6	327.1	E	9901	7.5
Jakobshavn Isbrae	JI	69.2	309.3	W	13316	9.1
Kangerlussuaq Sermerssua	KS	71.5	308.6	W	2210	4.3
Rink Isbrae	RI	71.7	308.3	W	4629	4.5
Umiamako Isbrae	UM	71.7	307.6	W	2228	3.2
Daugaard-Jensen Glacier	DJ	71.9	331.4	E	3621	5.9
Ingia Isbrae	II	72	307.4	W	1056	2.8
Tracy Glacier	TG	77.5	293.9	W	1760	5
Zachariae Isstrom	ZI	78.9	339.5	W	1874	22.8
Nioghalvfjerdsfjorden	79N	79.3	337.6	W	1305	31.2
Petermann Glacier	PM	81	298	E	1045	15.6

Table 2.1: List of glaciers of this study

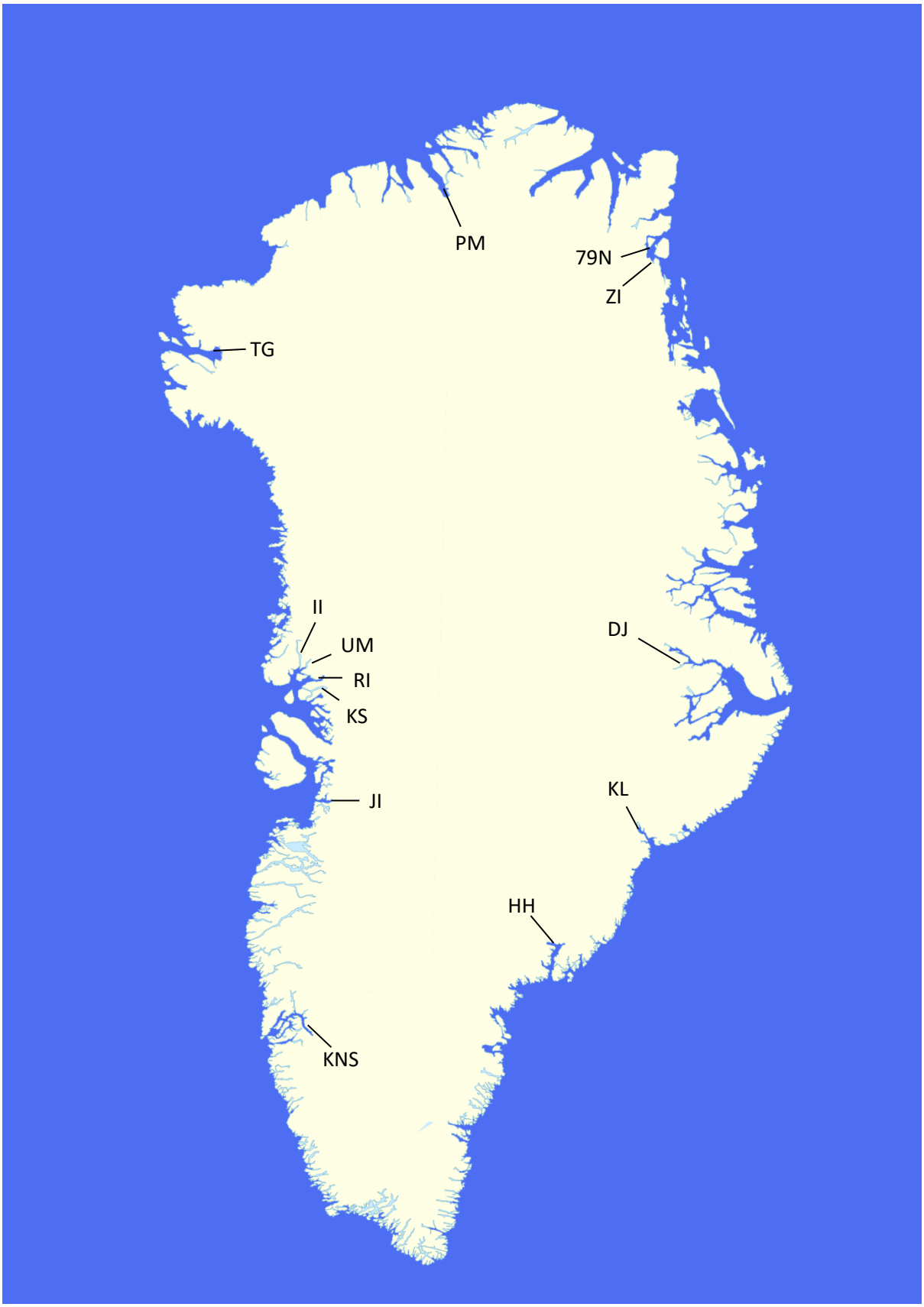

Figure 2.1: Locations of study sites around the Greenland Ice Sheet. (Map made with Natural Earth)

2. 2. IceBridge ATM

2. 2. 1. Overview

One of the properties of sikussak, which has not been successfully characterised by previous studies, is its thickness. This is of vital importance, as the thickness and structural integrity of the sikussak formation is a critical control on its buttressing effect upon the glacier calving front. Joughin et al. (2008b) used ICESat data to track elevation changes for JI, but observations were limited to a single period (Nov/03 to Feb/07). Reeh et al. (2001) identified a spectrum of possible effects of seasonal sikussak formation, which are highly dependent upon the thickness of the structure. If the sikussak is sufficiently thick, it may exert enough back-stress upon the glacier to prevent the formation and subsequent propagation of crevasses or merely be sufficiently coherent to stabilise the calving front by preventing calved icebergs from rotating or drifting away from the glacier front, thereby preventing new icebergs from calving off (Reeh et al., 2001). Therefore, a better understanding of the thickness and morphology of pro-glacial structures will better constrain force balance equations for which it is an important control (Amundsen et al., 2010).

2. 2. 2. Data acquisition

NASA Operation Ice Bridge Airborne Topographic Mapper (ATM) L2 Icessn Elevation, Slope, and Roughness (ILATM2) data collected in survey campaigns between March-May in the years 2009-2011 were used to obtain the elevation (h_e) referenced to WGS84 ellipsoid. These elevation data have a spatial resolution of 80 m across-track nadir platelet width with 40 m spacing along track. Elevation is measured by a LIDAR to an accuracy of 10-20 cm, through the use of GPS receivers and inertial navigation system (INS) attitude sensors to account for pitch and roll of the plane.

These data represent an improvement on the ICESAT data used in studies by Joughin et al (2008b) and Kwok and Cunningham (2008), which were constrained by relatively poor temporal resolution and spatial extent. As such, these data enable investigation of the morphology of pro-glacial melange structures, the thickness of which has not been able to be accurately constrained previously.

The ice melange thicknesses in the fjords of the glaciers listed in Table 2 were investigated for each of the years for which IceBridge data was available.

2. 2. 3. Data processing

The data for the individual glaciers were clipped from the ATM dataset for each year in the Linux package PuTTy, which enabled each glacier to be analysed individually. Since the equation used to ascertain ice thickness of the floating melange assumes hydrostatic equilibrium, the data was subsequently clipped to the calving front, which was identified by overlaying the flight-path on a Landsat (if available) or MODIS image from the time of data acquisition, then cross referencing with the elevation data in Excel, where a significant change in height was usually a good indication of the location of the calving front. Once the calving front was identified, the latitude and longitude of its location was used as fixed points from which to calculate distance down the fjord.

Potential errors in the reference ellipsoid were accounted for through the use of tie-points to derive the freeboard (*fb*) from ice surface elevation (h_{ice}) above sea level (h_{sl}) (Kwok et al., 2010).

$$fb = h_{ice} - h_{sl} \quad [4]$$

From calculation of freeboard, the relative elevation to sea level was established, despite bias in absolute elevation (Zwally et al., 2008). In order to establish an accurate sea-level tie point, the method of Zwally et al. (2008) was utilised, whereby long-wavelength geoid error, tidal error, and dynamic ocean topography are compensated for by using a mean over at least 2 km of sea level beyond the end of the sikussak as the tie-point, rather than a single value. There was some difficulty in establishing tie-points at the high northern glaciers, where it was unclear whether the flight path encompassed any open water, or whether flat sea ice extended to the end of the dataset.

The freeboard is composed of the height of ice above sea level (h_{ice}) and the snow depth (h_s).

$$fb = h_{ice} - h_s \quad [5]$$

However, for the purposes of studying sikussak and melange, snow cover was examined and found to be negligible. The thickness of the floating melange ($h_{melange}$) could then be derived from Equation

6 (Kurtz and Harbeck (2012), assuming hydrostatic equilibrium according to the Archimedes buoyancy principle (Kwok and Cunningham, 2008) :

$$h_{melange} = \frac{p_w}{p_w - p_i} fb - \frac{p_w}{p_w - p_i}$$

[6]

Variable	Description	Constant values
$h_{melange}$	Melange thickness	
fb	Freeboard height	
p_w	Water density	1023.9 kg m-3
p_i	Sea ice density	915.1 kg m-3

Table 2.2: Variables and constants used in equation to derive ice thickness from freeboard data.

The densities used for p_w and p_i are based on those derived by Kurtz and Harbeck (2012). Once these constants are incorporated, h_i may be expressed as;

$$h_i = 9.411 \times fb - 1.3312$$

[7]

2. 2. 4. Smoothing function

Once ice thickness and distance from calving front had been calculated, the irregular distances from the calving front were assigned to a regular vector so that a smoothing function of moving averages could be applied. This accounts for variability resulting from measurement inaccuracies and smoothes out irregular values. The ice surface (freeboard) and bottom depth (freeboard minus ice thickness) were then plotted for each glacier to obtain the melange profile, and these are shown in Section 3. 1.

Once the thickness data were obtained from the glacier calving front, a first degree polynomial line fitting was applied to each set in order to establish the vertical extent and slope of the pro-glacial melange.

2. 3. ERA-Interim

The European Centre for Medium-Range Weather Forecasts (ECMWF) meteorological reanalysis product ERA-Interim was used for daily sea surface temperature (SST) and surface air temperature (SAT) data. The 1.5° grid cells yield a much better spatial resolution than meteorological data from weather stations in Greenland. Consequently, time series can be extracted for the locations of the glaciers themselves, rather than relying on data from the nearest possible weather station. A comparison between the ERA-Interim data and data from weather stations, obtained from NASA Goddard Institute for Space Studies (GISS) surface temperature analysis, was made to establish the correspondence between these two records. This was done for two weather stations with relatively long and complete records, Aasiaat (formerly Egedesminde) and Nuuk (formerly Godthab), which are proximate to Jakobshavn Isbrae and Kangiata Nunata Sermia respectively. When a comparison was made between the GISS station records and the time series extracted from ERA-Interim for these two glaciers, a good fit was found between these data, shown in the figures 2.2 and 2.3 below.

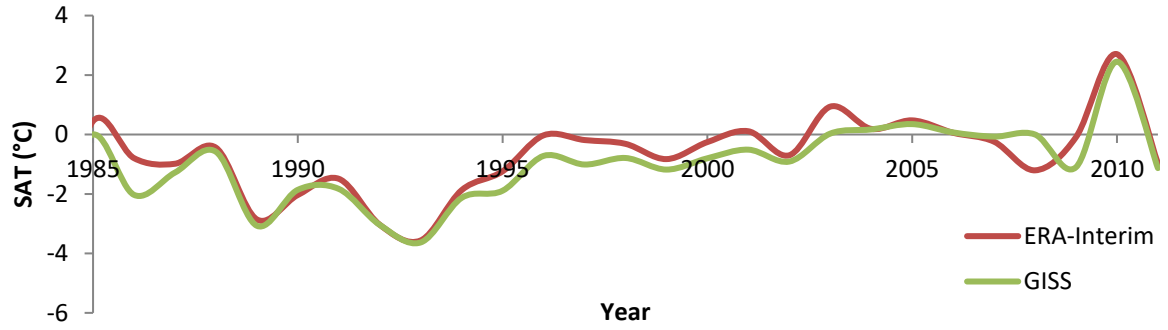

Figure 2.2: Comparison between ERA-Interim data from KNS and GISS station data from Nuuk for the years 1985-2011

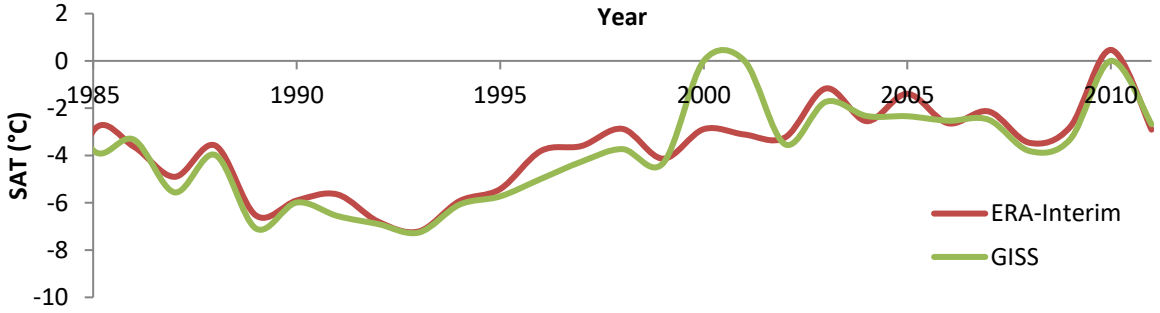

Figure 2.3: Comparison between ERA-Interim data from JI and GISS station data from Aasiaat for the years 1985-2011

However, it was noted that in order to achieve this close correlation, it was necessary to extract data from sites at coastal locations, rather than further inland. This was attributed to the effect of atmospheric lapse rate over the GrIS, an annual average of approximately −6.8 °C km^{-1}, with a minimum in July of −4.6°C km^{-1} , and maximum in February of −8.9°C km^{-1} (Fausto et al., 2009). Therefore, time series extracted from ERA-Interim data at locations more inland, when averaged over the 1.5° grid cell, show significantly lower temperatures than the data from these coastal locations.

2. 4. Satellite Imagery

2. 4. 1. MODIS

High temporal resolution data from the Moderate Resolution Imagine Spectrometer (MODIS) aboard the Terra and Aqua satellites from the years 2000-2011 were used to analyse seasonal changes to pro-glacial melange structures at a high level of temporal detail. Image stacks created and converted into movie form by Seale (2009) facilitated close analysis of seasonal variations in melange structure, rigidity and movement.

Limitations of MODIS data include the winter 'blackout' period which restricted analysis of winter changes to melange and sikussak, and instances of cloud cover which inhibited the identification of precise timings of melange weakening and disintegration. Although the 250 m spatial resolution of MODIS data is reasonable, and sufficient to identify significant changes in the size and movement of the melange, it is not possible from these data to make detailed analysis of changes in form and structure. These data were obtained from RISCO (Rapid Ice Sheet Change Observatory) RapidIce survey, the Danish Meteorological Institute (DMI) Centre for Ocean and Ice collection of MODIS imagery, or data previously collected by Seale (2009).

2. 4. 2. Landsat

Landsat data was used in order to establish the more detailed characteristics of the structure at discrete moments in time. These data were obtained from the United States Geological Survey (USGS) satellite image database or the Global Land Cover Facility (GLCF) database. Landsat 7 provides 15-60 m high resolution multispectral data from 1999 though Landsat ETM+ (Enhanced Thematic Mapper Plus). True-colour composites were produced by merging layers 1-3 in ERDAS Imagine, and geo-corrected to Universal Transverse Mercator (UTM) co-ordinates. True-colour composites from GLCF imagery were produced by merging layers 1-3 in ERDAS Imagine, and geo-corrected to Universal Transverse Mercator (UTM) co-ordinates.

2. 5. RADARSAT

The velocity data used in this project is derived from RADARSAT synthetic aperture radar data obtained by Joughin et al. (2010) for the winter 2005/2006. These data have been processed using SAR, speckle-tracking and interferometric algorithms (Joughin, 2002) from which velocities for the major Greenlandic glaciers were derived. This dataset was chosen as, although it does not encompass the 2009/2011 time period which this study focuses upon, it is the most recent compete set of velocity data. Additionally, although velocities may have altered slightly since these data were acquired, they still give a reasonable dataset from which to compare the relative speeds of these glaciers. The period from 2005-06 to 2010-11 is furthermore associated with limited glacier change on a regional scale.

3. Results

3. 1. Sikussak and melange profiles

These profiles were derived from the Operation IceBridge ATM elevation data, from which the freeboard (blue line) and bottom depth (green line) were calculated using the techniques explained in Section 2. 2. Here, each glacier of this study is presented, along with a Landsat image, with quantitative and qualitative observations of the nature of the pro-glacial structures of each. In this section, all pro-glacial structures are referred to as melange until a definite characterisation is made. Distance is measured from the same location on the glacier in each year, and so changes in terminus position and melange extent are directly comparable between the plots.

3. 1. 1. Kangiata Nunata Sermia (KNS)

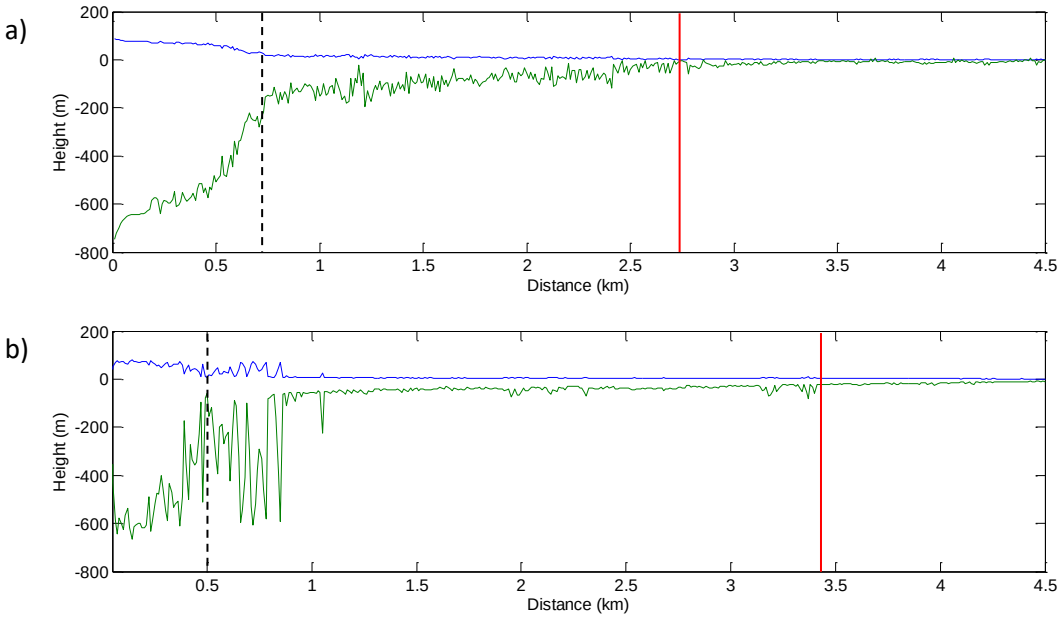

Figure 3.1: Melange profiles derived from freeboard (blue line) and bottom depth (green line) for KNS, in the years (a) 2010; (b) 2011. Black dashed line shows the calving front and red line shows the extent of pro-glacial material.

Figure 3.2: Landsat ETM+ image of the calving front of KNS from 11/03/2009. Scale is 10 km across the image, and north is aligned with the long axis.

The pro-glacial melange of KNS is 35 – 53 m thick at the calving margin, with an extent of 2 – 3 km and a surface slope of ⁻0.2°. In 2009 (Figure 3.1a), KNS develops a sikussak-type structure, characterised by peak thickness at the glacier calving face which gradually reduces away from the calving face. However, this structure is not present in the 2010 profile (Figure 3.1b), where a chaotic melange is present at a retreated calving front. Observation from MODIS imagery shows that the pro-glacial melange is not seasonally bonded with sea ice, and the lack of seasonal rigidity means that this structure is defined as melange.

3. 1. 2. Helheim Gletscher (HH)

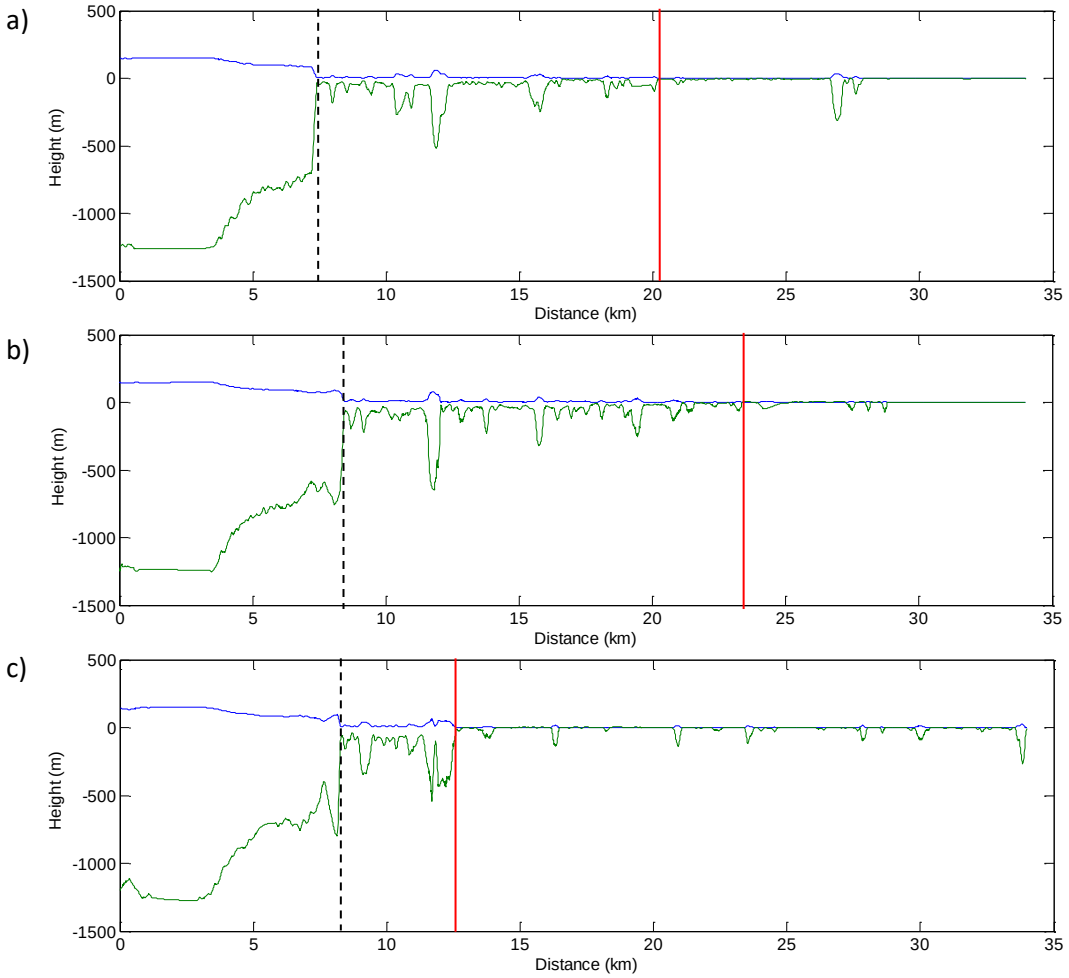

Figure 3.3: Melange profiles derived from freeboard (blue line) and bottom depth (green line) for HH, in the years (a) 2009; (b) 2010; (c) 2011. Black dashed line shows the calving front and red line shows the extent of pro-glacial material. Note the short (~5 km) floating tongue of HH glacier.

The pro-glacial melange of HH is 115 – 146 m thick at the calving margin with an extent of 5 – 16 km and a surface slope of ⁻0.6 – ⁻0.8°. This melange is loose and unconsolidated, widely differing in extent in each year. Observations from MODIS imagery show that this structure is absent through winter and early spring, forming only when the glacier starts to calve in late spring/early summer. The smallest melange extent occurs at the before the start and after the end of the calving season. Due to these characteristics, it is inferred to be unconsolidated melange material rather than a pro-glacial sikussak.

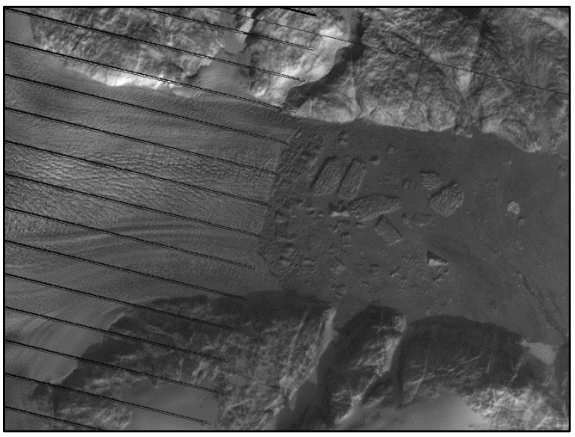

Figure 3.4: Landsat ETM+ image of the calving front of HH from 23/03/2011. Scale is 20 km across the image, and north is aligned with the long axis.

3. 1. 3. Kangerdlugssuaq Gletscher (KL)

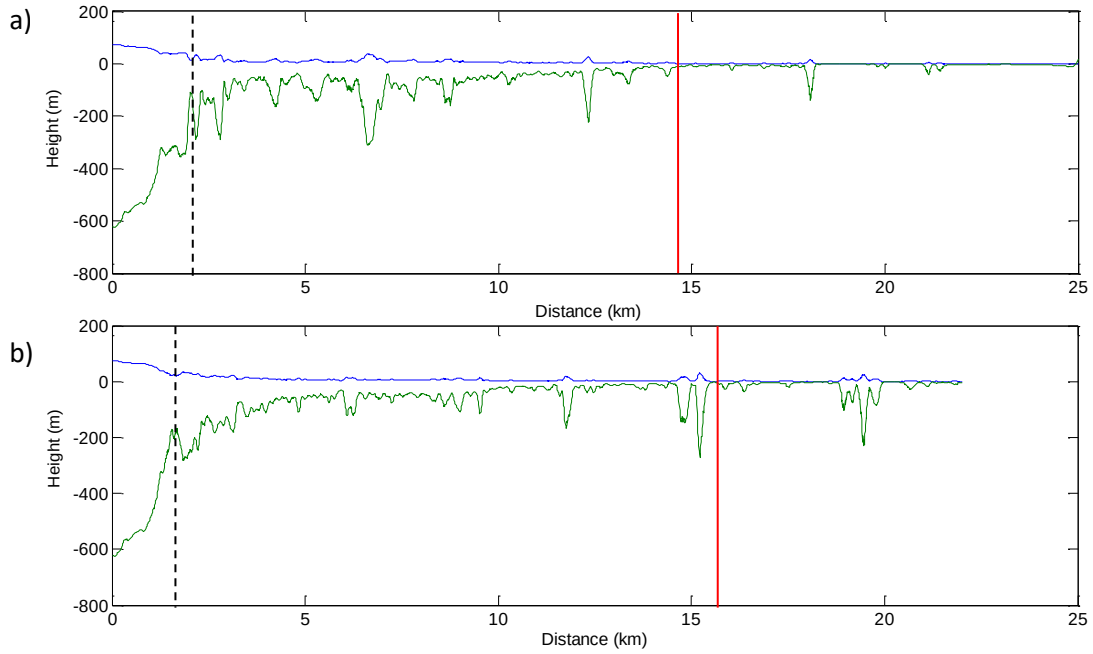

Figure 3.5: Melange profiles derived from freeboard (blue line) and bottom depth (green line) for KL, in the years (a) 2010; (b) 2011. Black dashed line shows the calving front and red line shows the extent of pro-glacial material.

The pro-glacial melange of KL is 99 – 169 m thick at the calving margin with an extent of 13 – 14 km and a surface slope of ⁻0.6 – ⁻0.7°. This melange is consolidated into a pro-glacial sikussak. Peak thickness is seen at the calving face and reduces steeply away from the glacier front. The sikussak extends approximately 15 km from the calving margin each year, beyond which loose melange and individual icebergs can be identified in the profiles.

Figure 3.6: Landsat ETM+ image of the calving front of KL from 14/04/2010. Scale is 20 km across the image, and north is aligned with the long axis. Note the large tabular berg trapped against the calving front.

The calving front of KL glacier has remained stable over both years (2009, 2010), and though the sikussak is not typically multi-year, it has built up to the same thickness of up to 250 m at the calving front over successive years. The large peaks seen in Figure 3.5 are suggestive of the tabular icebergs which can be seen trapped in the ice melange in the Landsat image (Figure 3.6).

The sikussak of KL has a defined seasonal cycle: the fjord is packed with over-winter sea ice, which disintegrates and blows out of the fjord at the beginning of the calving season. Discharge occurs in bursts throughout the summer, though there is usually at least 2 km of sikussak maintained at the front of the glacier calving face.

3. 1. 4. Jakobshavn Isbrae (JI)

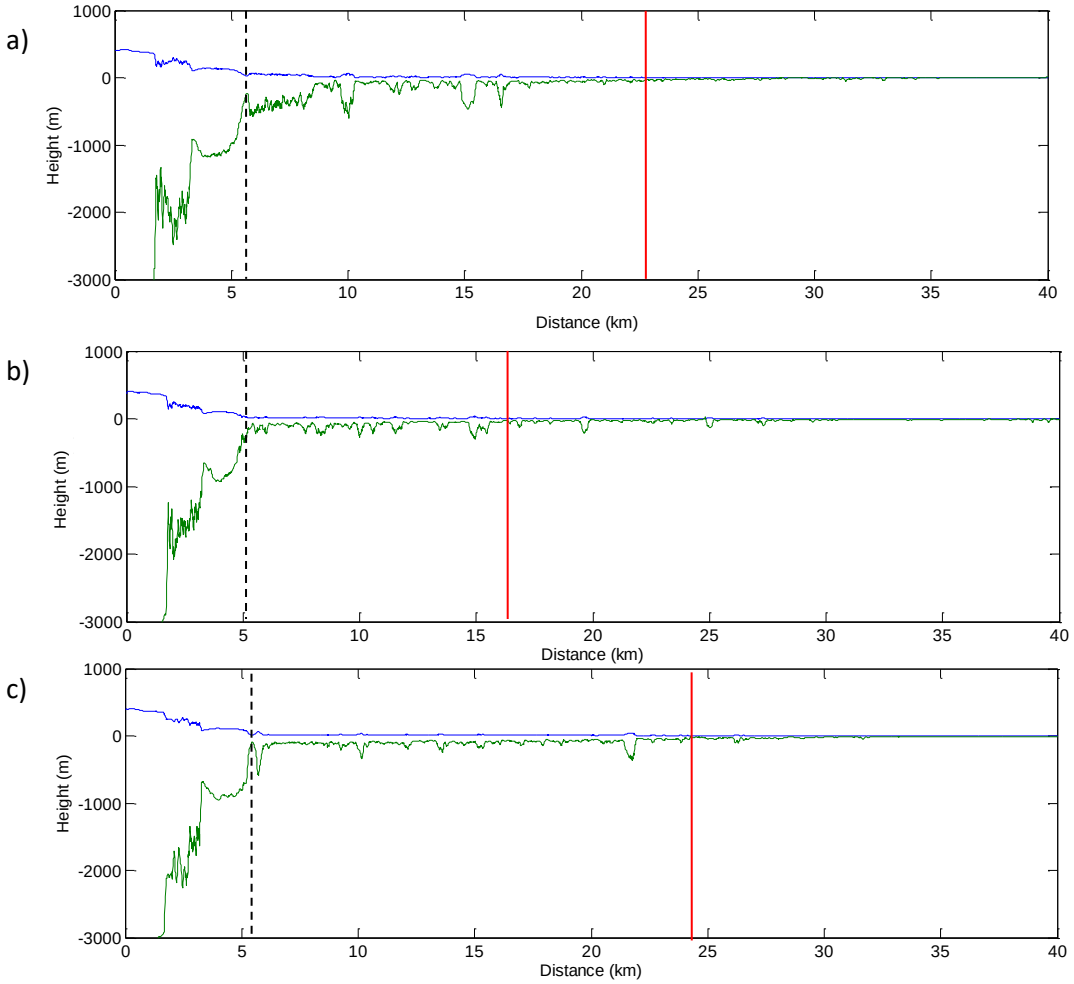

Figure 3.7: Melange profiles derived from freeboard (blue line) and bottom depth (green line) for JI, in the years (a) 2009; (b) 2010; (c) 2011. Black dashed line shows the calving front and red line shows the extent of pro-glacial material.

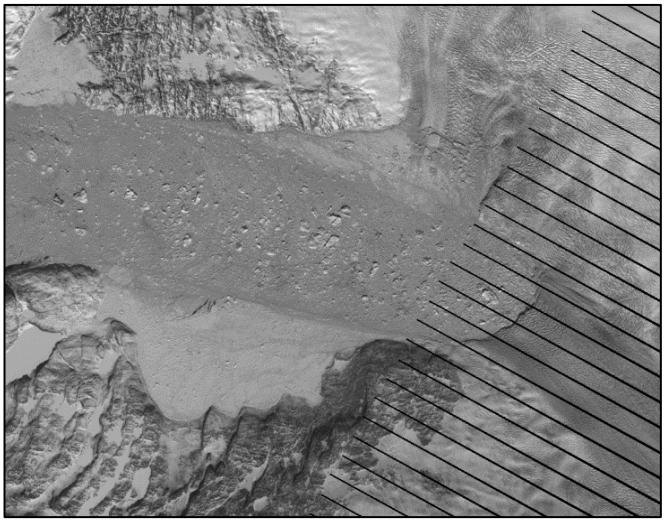

Figure 3.8: Landsat ETM+ image of the calving front of JI from 11/04/2011. Scale is 20 km across the image, and north is aligned with the long axis.

The pro-glacial melange of JI is 126 – 172 m thick at the calving margin with an extent of 12 – 18 km and a surface slope of ¯0.4 – ¯0.6°. An exceptionally thick section is seen in 2009 (Figure 3.7a). The sikussak is thickest at the calving front, and declines in thickness away from the glacier. Observations from MODIS show that this structure obtains seasonal rigidity with the formation of sea ice between the clasts. The concentration of icebergs in the JI sikussak is exceptionally high, as can be clearly seen in the Landsat image (Figure 3.8).

3. 1. 5. Kangerlussuaq Sermerssua (KS)

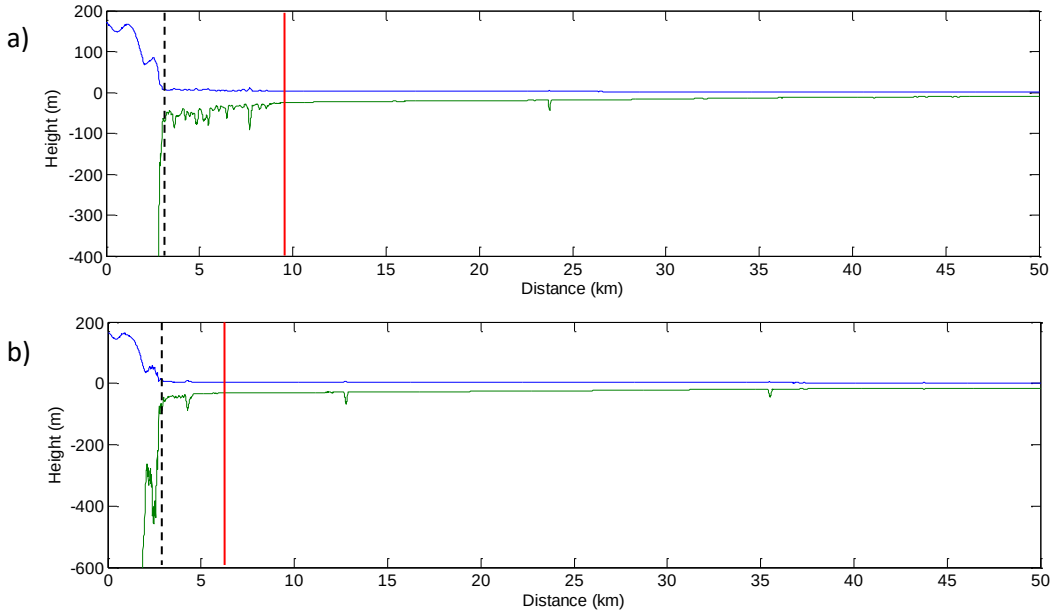

Figure 3.9: Melange profiles derived from freeboard (blue line) and bottom depth (green line) for KS, in the years (a) 2010; (b) 2011. Black dashed line shows the calving front and red line shows the extent of pro-glacial material.

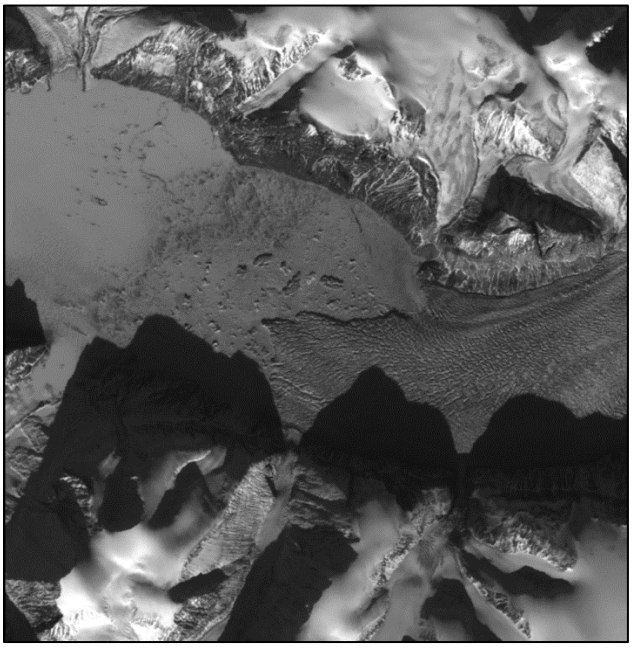

Figure 3.10: Landsat ETM+ image of the calving front of KS from 23/03/2010. Scale is 15 km across the image, and north is aligned with the long axis.

The pro-glacial melange of KS is 23 – 33 m thick at the calving margin with an extent of 3 – 6 km and a surface slope of ⁻ 0.05 – ⁻ 0.08°. A sikussak is seen in 2009, but this structure is much reduced in the subsequent year. The Landsat image from 23/03/2010 (Figure 3.10) shows very little accumulated icebergs and bergy bits trapped pro-glacially, and the melange profiles show no indication of a floating tongue (Figure 3.9).

3. 1. 6. Rink Isbrae (RI)

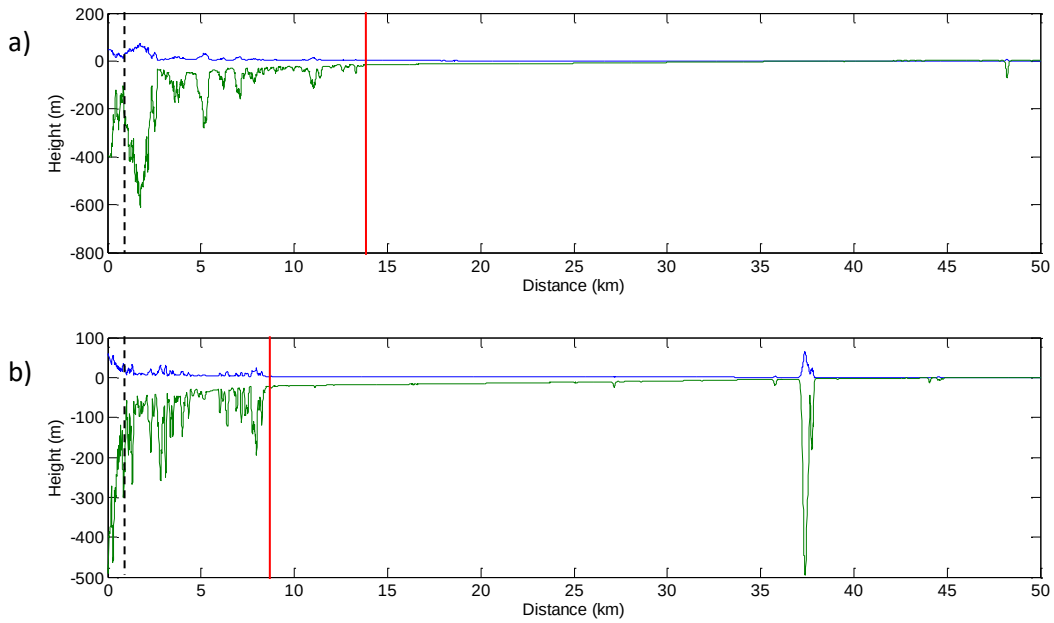

Figure 3.11: Melange profiles derived from freeboard (blue line) and bottom depth (green line) for RI, in the years (a) 2010; (b) 2011. Black dashed line shows the calving front and red line shows the extent of pro-glacial material.

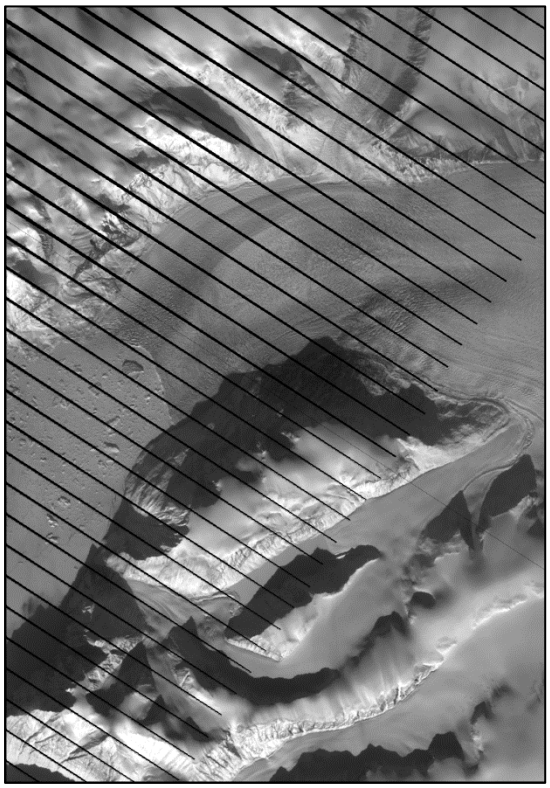

Figure 3.12: Landsat ETM+ image of the calving front of RI from 03/04/2011. Scale is 20 km across the image, and north is aligned with the long axis.

The pro-glacial melange of RI is 78 – 123 m thick at the calving margin with an extent of 8 – 13 km and a surface slope of ¯ 0.2 – ¯ 0.4°. RI has a short pro-glacial sikussak, which is more pronounced in 2011 than 2010. The distinction between sikussak and sea ice is very clear at this glacier, which allows the extent to be easily demarcated. Thick sea ice can be seen past the end of the sikussak in 2011 (Figure 3.11b), although this appears very smooth in the melange profile, indicating that it does not contain any calved material, and is therefore not interpreted as an extension of the sikussak.

3. 1. 7. Umiamako Isbrae (UM)

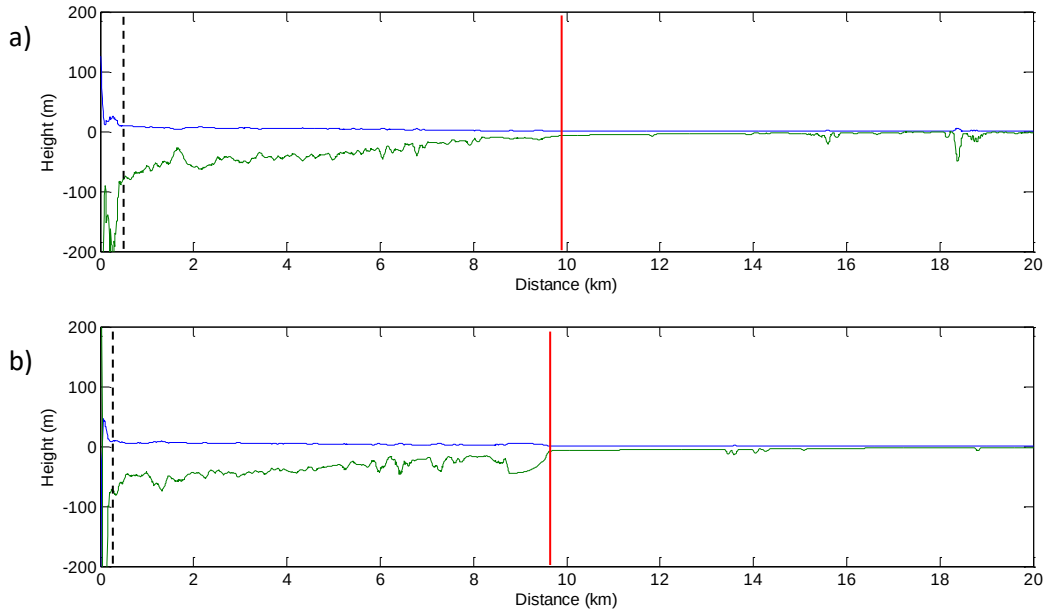

Figure 3.13: Melange profiles derived from freeboard (blue line) and bottom depth (green line) for UM, in the years (a) 2009; (b) 2010. Black dashed line shows the calving front and red line shows the extent of pro-glacial material.

Figure 3.14: Landsat ETM+ image of the calving front of UM from 23/04/2010. Scale is 10 km across the image, and north is aligned with the long axis.

The pro-glacial melange of UM is 34 – 35 m thick at the calving margin, with an extent of 8 – 10 km and a surface slope of ¯ 0.1°. This sikussak structure clearly shows a peak thickness at the calving face, with a gradual slope away from the glacier to a distinct point where sikussak ends and the sea ice with occasional bergs begins. This sikussak structure is relatively smooth, indicating that it has few large bergs trapped in the matrix, and is instead primarily comprised of smaller clasts and bergy bits.

3. 1. 8. Daugaard-Jensen Glacier (DJ)

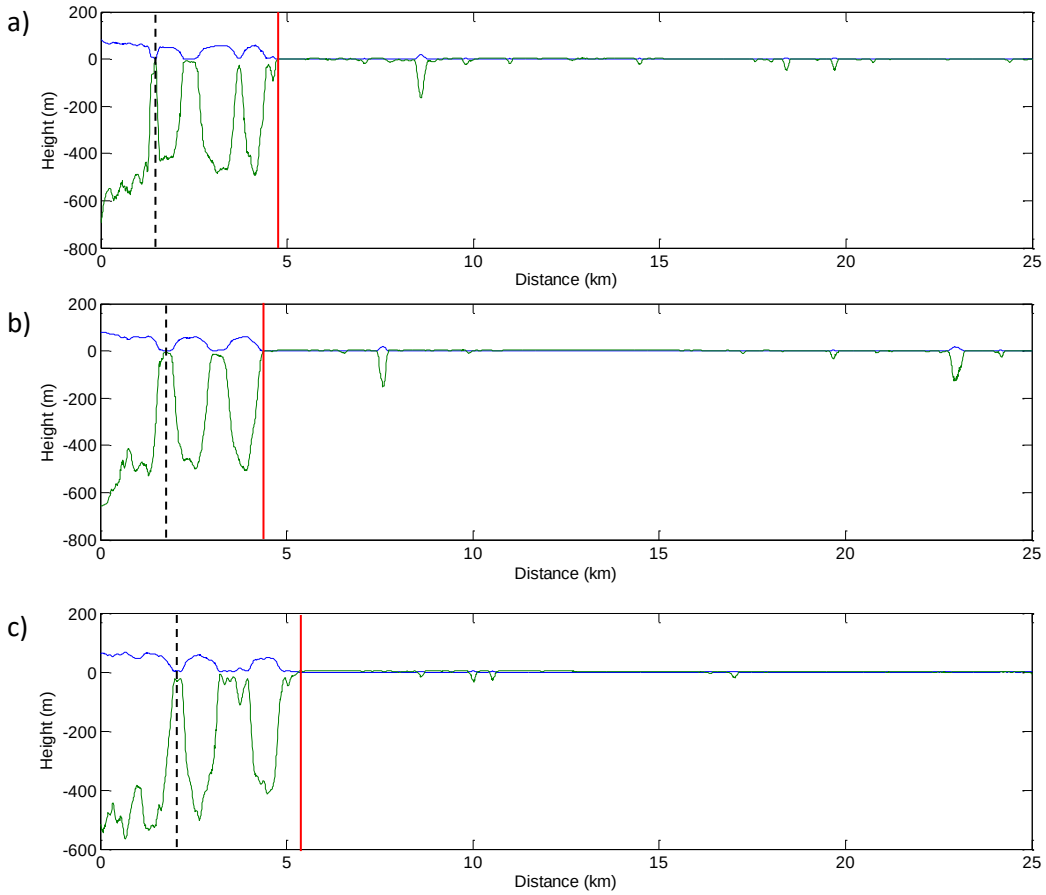

Figure 3.15: Melange profiles derived from freeboard (blue line) and bottom depth (green line) for DJ, in the years (a) 2009; (b) 2010; (c) 2011. Black dashed line shows the calving front and red line shows the extent of pro-glacial material.

Figure 3.16: Landsat ETM+ image of the calving front of DJ from 01/06/2010. Scale is 10 km across the image, and north is aligned with the long axis.

The pro-glacial melange of DJ is 97 – 110 m thick at the calving margin, with an extent of 2 – 4 km and a surface slope of ¯ 0.4 – ¯ 0.5°. At DJ, huge tabular bergs which have been calved from the front remain in close proximity to the glacier as they are trapped within the sikussak matrix, seen in Figure 3.16. Observation from MODIS imagery show a clear cycle of fjord sea ice weakening, breakup and export immediately preceding the onset of movement in the sikussak. Freeze-up occurs in early October, and it is inferred that this remains throughout the winter, suppressing calving.

3. 1. 9. Ingia Isbrae (II)

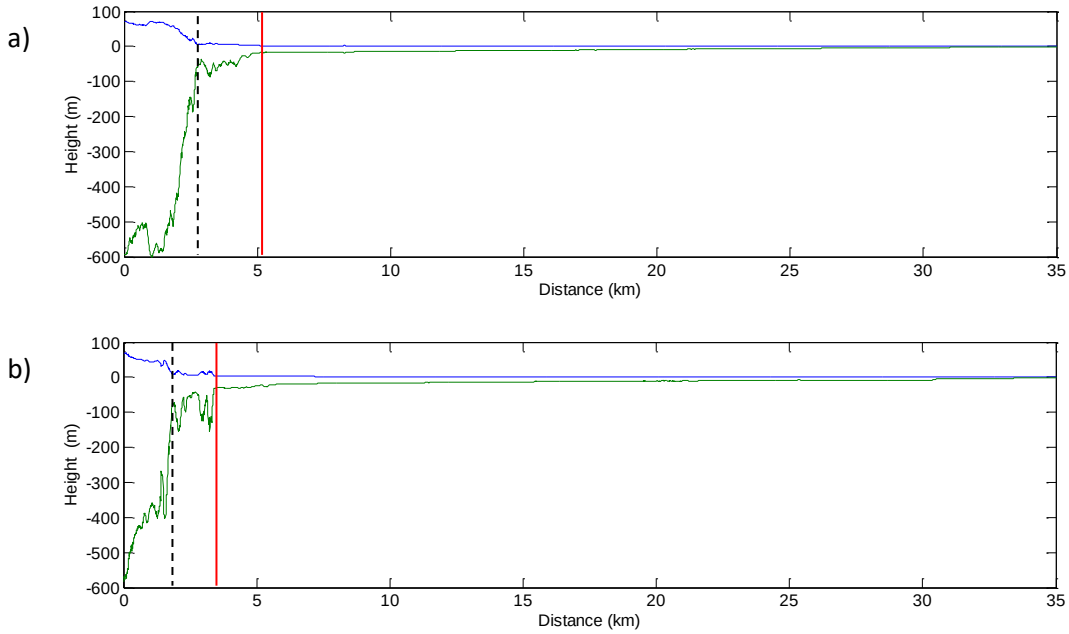

Figure 3.17: Melange profiles derived from freeboard (blue line) and bottom depth (green line) for II, in the years (a) 2009; (b) 2010. Black dashed line shows the calving front and red line shows the extent of pro-glacial material.

Figure 3.18: Landsat ETM+ image of the calving front of II from 23/04/2010. Scale is 10 km across the image, and north is aligned with the long axis.

The pro-glacial melange of II is 36 – 47 m thick at the calving margin with an extent of 1.5 – 2.5 km and a surface slope of ¯ 0.2°. Although this structure is very short, it is identified it as a sikussak, which traps calved ice next to the calving front. There is a very sharp definition between the sikussak and the sea ice, seen in the melange profiles as an abrupt change in roughness and thickness.

3. 1. 10. Tracy Glacier

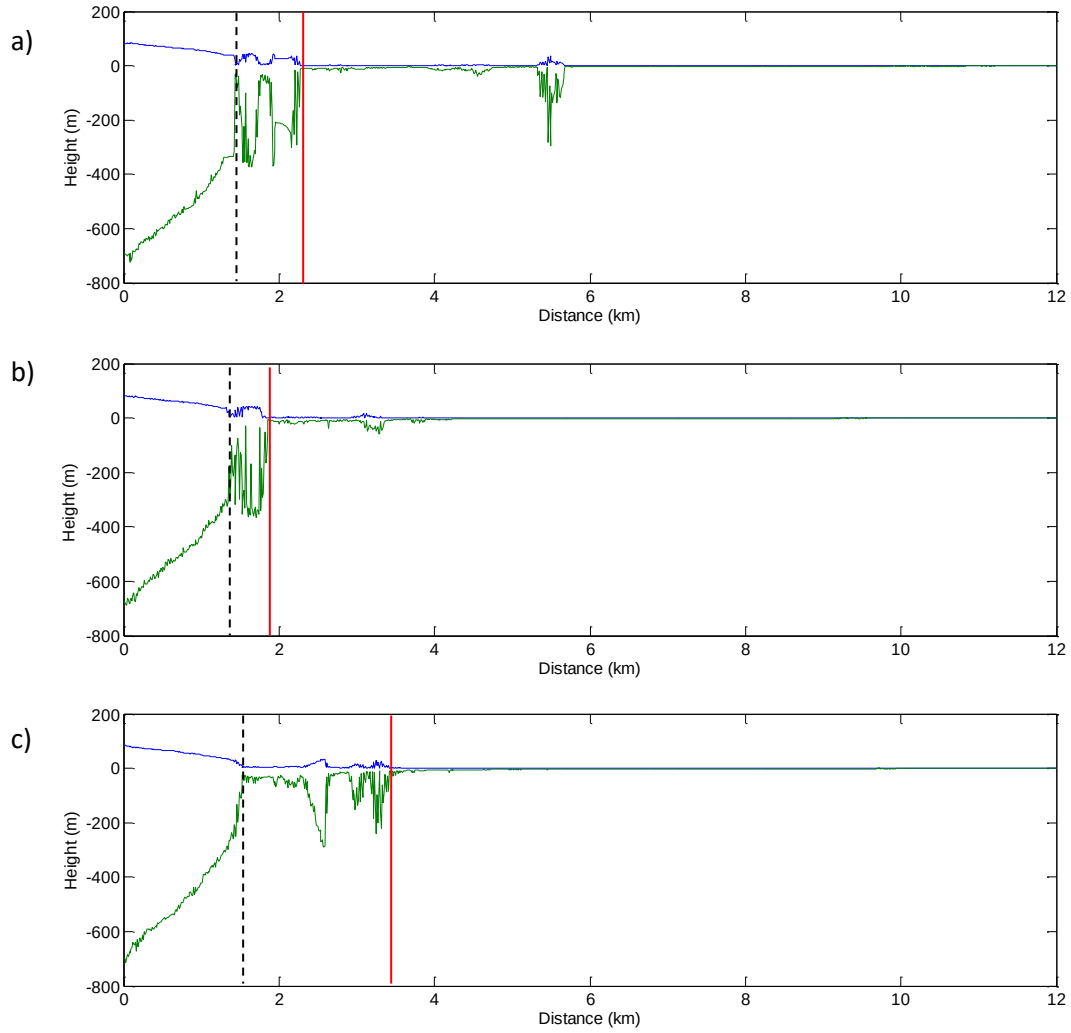

Figure 3.19: Melange profiles derived from freeboard (blue line) and bottom depth (green line) for TG, in the years (a) 2009; (b) 2010; (c) 2011. Black dashed line shows the calving front and red line shows the extent of pro-glacial material.

Figure 3.20: Landsat ETM+ image of the calving front of TG from 18/06/2011. TG is the larger glacier shown. Scale is 10 km across the image, and north is aligned with the long axis.

The pro-glacial melange of TG is 36 – 47 m thick at the calving margin with an extent of 1.5 – 2.5 km and a surface slope of ¯ 0.2°. This is identified as a short, seasonally rigid sikussak, distinct in the Landsat image (Figure 3.20) as a radar-bright region, packed against the glacier calving face by the formation of seasonal sea ice, which appears much darker in the image. Large tabular icebergs trapped in the matrix are evident in both the melange profiles and Landsat image.

3. 1. 11. Zachariae Isstrom (ZI)

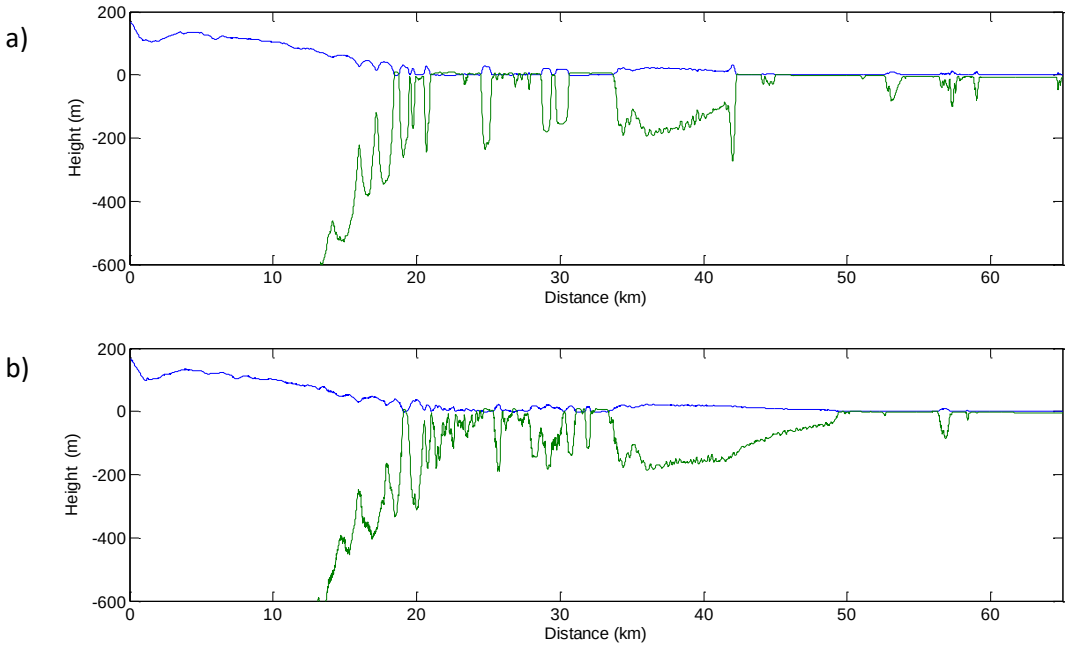

Figure 3.21: Pro-glacial profiles derived from freeboard (blue line) and bottom depth (green line) for ZI, in the years (a) 2009; (b) 2010.

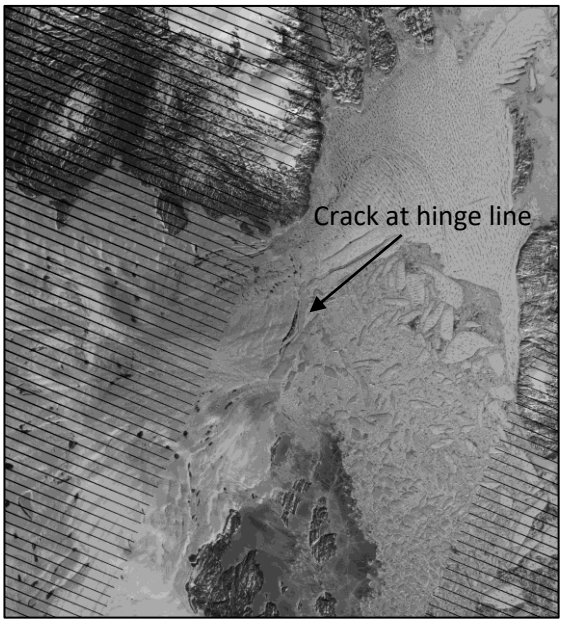

Figure 3.22: Landsat ETM+ image of ZI from 08/06/2009. Scale is 50 km across the image, and north is aligned with the long axis.

Although no breakup was seen in the MODIS imagery 2009-2011, a crack at the hinge line can be clearly seen forming in July 2009 (Figure 3.22), which may be the result tidal forcing causing vertical displacement of the ice tongue, as observed through the ice of radar interferometry by Rignot et al. (1997).

The floating ice tongue of ZI is the largest in Greenland, comprised of a compressed melange of calved icebergs, consolidated by the formation of sea ice between the clasts (Rignot et al., 2000), seen in Figure 3.22. Negative mass balance calculations indicate that the ice tongue of ZI is in a state of retreat (Rignot et al., 1997).

3. 1. 12 Nioghalvfjerdsfjorden (79N)

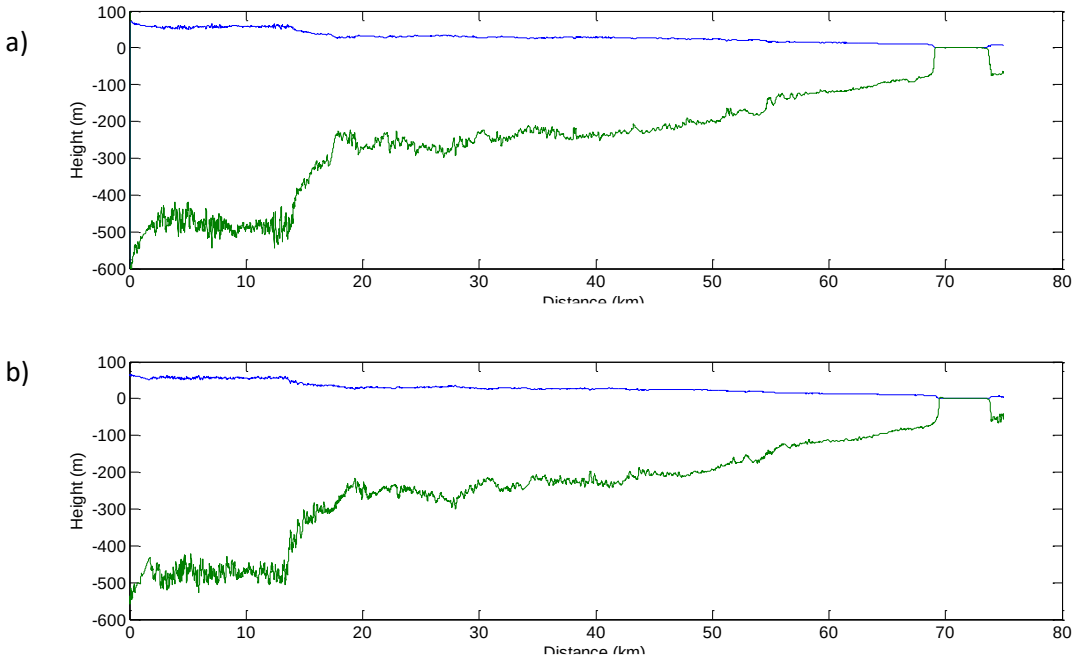

Figure 3.23: Pro-glacial profiles derived from freeboard (blue line) and bottom depth (green line) for 79N, in the years (a) 2009; (b) 2010.

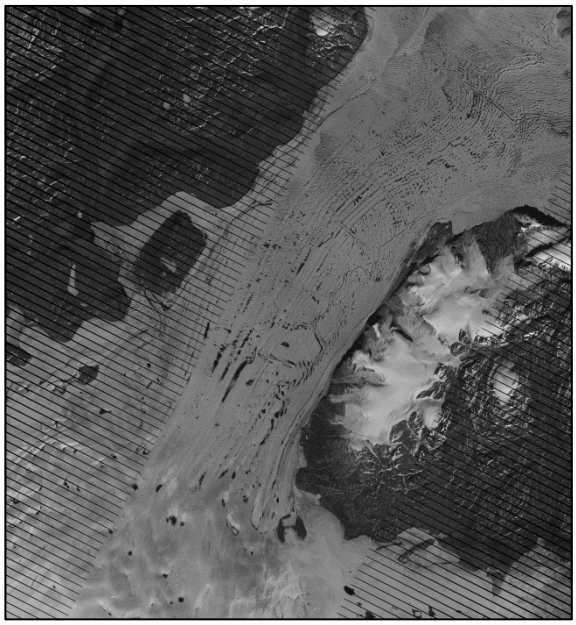

Figure 3.24: Landsat ETM+ image of 79N from 30/06/2010. Scale is 60 km across the image, and north is aligned with the long axis.

In Figure 3.21 above, the 100 – 300 m thick, 70 km long floating tongue of 79N can be seen. The termini of 79N and ZI have not shown any calving events during the 2009-2011 study period. 79N and ZI terminate into the same embayment, where historical records suggests they used to converge (Koch, 1928), but which is now choked with calved ice (Box and Decker, 2011).

The structural integrity of the floating ice tongues of 79N and ZI are maintained by a region of semi-permanent fast-ice, referred to as the Norske Øer Ice Barrier (NØIB) (Schneider and Budéus, 1997). The size and shape of this feature varies inter-annually, extending between 70 and 150 km from the coast (Reeh et al., 2001).

3. 1. 13. Petermann Glacier (PM)

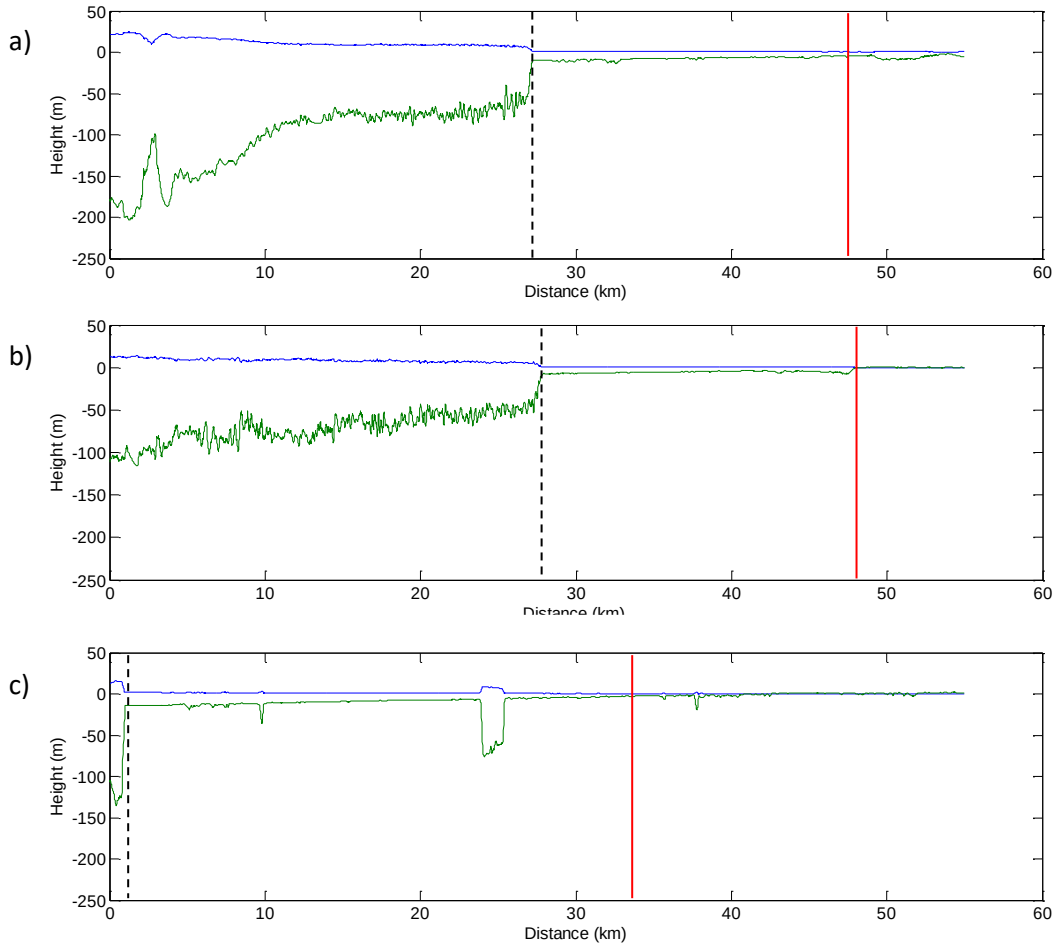

Figure 3.25: Pro-glacial profiles derived from freeboard (blue line) and bottom depth (green line) for PM, in the years (a) 2009; (b) 2010; (c) 2011.

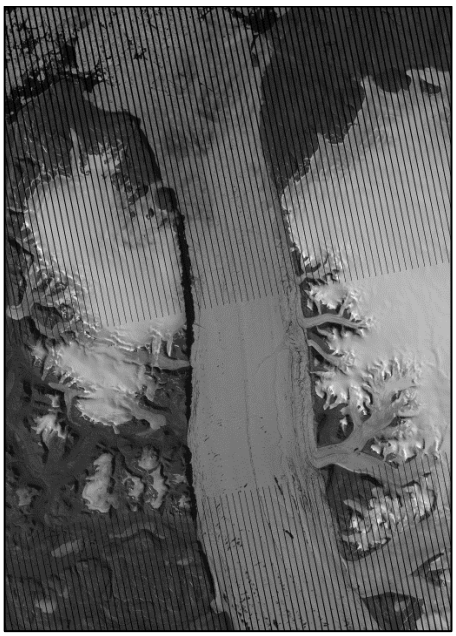

Figure 3.26: Landsat ETM+ image of PM from 28/06/2010. Scale is 50 km across the image, and north is aligned with the long axis.

The pro-glacial melange of PM is 9 – 20 m thick at the calving margin with an extent of 20 – 27 km and a surface slope of ¯ 0.04°. The floating tongue of PM glacier broke up between 3/8/10 and 5/8/10 (Mayer and Herzfeld, 2008), as can be clearly seen in Figure 3.24 above. No substantial sikussak or melange structures are identified; instead, the fjord is filled with seasonal sea ice, seen as the slightly darker region of ice at the head of the fjord in Figure 3.26.

3. 2. Melange variables

This table lists the morphological variables found through analysis of the melange profiles: thickness at the calving front, surface slope angle from smoothed melange profiles, and extent from the calving front. Extent is shown as the distance between the red and black dashed lines on the melange profiles in Section 3. 3.

Glacier	Date	Thickness (m)	Extent (km)	Slope (°)
KNS	2010	35.0	4.5	-0.21
KNS	2011	52.9	13.5	-0.21
HH	2009	115.5	32.5	-0.60
HH	2010	146.1	20.5	-0.83
HH	2011	135.5	27	-0.87
KL	2010	122.8	13	-0.72
KL	2011	99.3	15	-0.57
JI	2009	168.6	33	-0.56
JI	2010	125.5	30	-0.38
JI	2011	172.3	35	-0.45
KS	2010	33.1	7	-0.08
KS	2011	22.7	1.5	-0.05
RI	2010	122.7	13.5	-0.36
RI	2011	77.8	8.5	-0.20
UM	2009	35.3	14.5	-0.11
UM	2010	34.4	8.5	-0.10
DJ	2009	110.1	13.5	-0.48
DJ	2010	98.7	11	-0.41
DJ	2011	97.3	15.2	-0.42
II	2009	35.8	2.9	-0.18
II	2010	47.2	4.6	-0.24
II	2011	15.3	0	-0.07
TG	2009	14.5	3.5	-0.17
TG	2010	16.0	2.5	-0.20
TG	2011	54.7	3	-0.75
ZI	2009	N/A	N/A	N/A
ZI	2010	N/A	N/A	N/A
79N	2009	N/A	N/A	N/A
79N	2010	N/A	N/A	N/A
PM	2009	10.9	0.5	-0.04
PM	2010	8.7	0.5	-0.03
PM	2011	20.1	0.5	-0.04

Table 3.1: Melange variables derived from ATM melange profiles (thickness, slope, extent). N/A values are given where no pro-glacial melange structures were identified.

3. 3. Environmental variables

This table shows the environmental variables which were deemed most likely to affect the form and longevity of melange structures given the proposed dependence on winter formation and spring break-up. Winter and spring SSTs and SATs were obtained from ERA Interim data, from which the annually summed positive and freezing degree days (PDD and FDD respectively) were calculated, and the Freezing Index derived after Reeh et al. (1999).

Glacier	Date	Winter SST (°C)	Spring SST (°C)	Winter SAT (°C)	Spring SAT (°C)	Sum PDD	Sum FDD	Freezing Index
KNS	2010	0.18	1.77	-1.84	3.38	266	99	0.05
KNS	2011	-0.31	0.81	-5.61	-0.99	173	192	0.06
HH	2009	2.62	1.19	-4.52	1.42	225	140	0.06
HH	2010	3.80	3.44	-3.18	1.29	232	133	0.05
HH	2011	2.57	0.91	-4.86	1.40	222	143	0.05
KL	2010	-1.69	-1.57	-8.85	-0.88	168	197	0.10
KL	2011	-1.69	-1.68	-8.70	-0.17	164	201	0.08
JI	2009	-1.67	0.43	-11.75	-0.87	145	220	0.10
JI	2010	-1.63	1.01	-6.08	1.96	199	166	0.09
JI	2011	-1.36	-0.19	-9.33	-2.74	136	229	0.08
KS	2010	-1.76	-0.39	-10.39	-1.82	175	190	0.11
KS	2011	-1.43	-1.24	-10.05	-5.66	131	234	0.09
RI	2010	-1.76	-0.39	-10.39	-1.82	175	190	0.11
RI	2011	-1.43	-1.24	-10.05	-5.66	131	234	0.09
UM	2009	-1.67	-0.58	-15.08	-4.80	123	242	0.13
UM	2010	-1.76	-0.39	-10.39	-1.82	175	190	0.11
DJ	2009	-1.62	-1.00	-10.28	-1.45	193	172	0.13
DJ	2010	-1.64	-1.47	-8.71	-1.15	173	192	0.14
DJ	2011	-1.59	-1.43	-7.56	-1.07	195	170	0.12
II	2009	-1.67	-0.58	-15.08	-4.80	123	242	0.13
II	2010	-1.76	-0.39	-10.39	-1.82	175	190	0.11
II	2011	-1.43	-1.24	-10.05	-5.66	131	234	0.09
TG	2009	-1.54	-1.44	-22.59	-6.37	96	269	0.17
TG	2010	-1.58	-1.52	-18.98	-5.18	92	273	0.17
TG	2011	-1.55	-1.46	-20.52	-7.88	94	271	0.18
ZI	2009	-0.78	-0.78	-24.28	-7.88	62	303	0.27
ZI	2010	-0.78	-0.78	-24.18	-6.66	67	298	0.24
79N	2009	-0.08	-0.08	-24.57	-8.94	72	293	0.24
79N	2010	-0.08	-0.08	-24.48	-6.90	74	291	0.22
PM	2009	-1.61	-2.15	-28.57	-10.00	49	316	0.36
PM	2010	-1.61	-1.72	-28.21	-7.38	38	327	0.48
PM	2011	-1.61	-1.63	-28.49	-11.56	65	300	0.27

Table 3.2: Environmental variables of sea surface temperatures (SST) and surface air temperatures (SAT), annually summed positive and freezing degree days (PDD/FDD), and the fast-ice index (FI). Winter values are averaged daily temperatures from December to February, and spring values are average daily temperatures from March to May.

4. Analysis

4. 1. Sikussak vs. Melange

There are three different types of pro-glacial structures which have been identified in Section 3. 1. at the calving front of Greenland's tidewater glaciers.

Sikussaks are identified in front of the majority of glaciers (KL, JI, KS, RI, UM, DJ, II, TG), and are characterised by a seasonal rigidity observed in the MODIS imagery. They tend to be thickest and roughest near the glacier terminus, sloping away with surface slope angles between ⁻0.1 – ⁻0.5°, indicating that these structures trap calved material and large bergs close to calving front. Thickness varies from ~20 – 175 m, and extent ranges from 1.5 – 35 km.

Non-sikussak melange structures are identified in front of HH and KNS glaciers, where no period of seasonal rigidity is identified in MODIS imagery. The dimensions of these structures are similar to that of sikussaks, ~35 – 150 m thick, and ~5 – 35 km long, with surface slopes ranging from ⁻0.2 – ⁻0.8°. However, they do not tend to reach peak thickness at the glacier calving front, and appear from the profiles to be a composed of a more chaotic mixture of material. These observations are indicative of a looser melange, where the material drifts down-fjord away from the calving front.

In the far north (PM, 79N and ZI), large floating ice tongues are identified, in the cases of ZI and 79N restrained by multi-year sea ice, which helps to maintain stability and promote growth (Higgins, 1991). These structures are much larger, approximately 100 – 500 m thick and 20 – 70 km long.

The following analysis includes those glaciers which appear from consideration of the thickness profiles and observations of MODIS imagery to have some form of pro-glacial ice melange. These observations and the evidence from the thickness profiles indicate that ZI, 79N and PM do not have an area of resistive ice melange in front of their termini. ZI and 79N have much thicker, multi-year fast ice, and PM has seasonally forming fjord ice, but very little pro-glacial melange or sikussak. Therefore, ZI and 79N are excluded from the following analysis of ice melange and sikussak as they are deemed to have a distinctly different pro-glacial structure, and PM is tentatively included, but with consideration that it may also require individual analysis.

The structural attributes of melange/sikussak thickness at calving front, basic slope shape, and extent (measured from the calving face) will be used as the variables from which relationships with environmental, glacio-dynamic and topographic factors will be investigated. The thickness and slope attributes were derived from curve fitting analysis of the IceBridge thickness data, and the extent

was derived from a combination of IceBridge and MODIS imagery, and is shown in the results section for each year, and each glacier.

4. 2. Environmental controls

4. 2. 1. Latitude

It is well established that climatic controls have a significant influence on the terminal environment of tidewater glaciers (Nick et al., 2009; Dowdeswell et al., 2000), and it might be assumed that this is partially through the effect of atmospheric and oceanic forcing on pro-glacial melange and sikussak structures. Additionally, it has been considered by many authors since Lauge Koch (1928) that sikussak structures are limited to distinct locations, delimited as the far north in early definitions, but later definitions include sikussak locations much further south (Syvitski et al., 1996; Dowdeswell et al., 2000; Reeh et al., 2001). The spatial distribution of sikussak is thought to vary with climate (Reeh et al., 1999). This can be tested spatially, using latitude as a proxy for climate (Hanna et al., 2008). Therefore, an initial comparison of latitude with the each of the variables of sikussak structure is made.

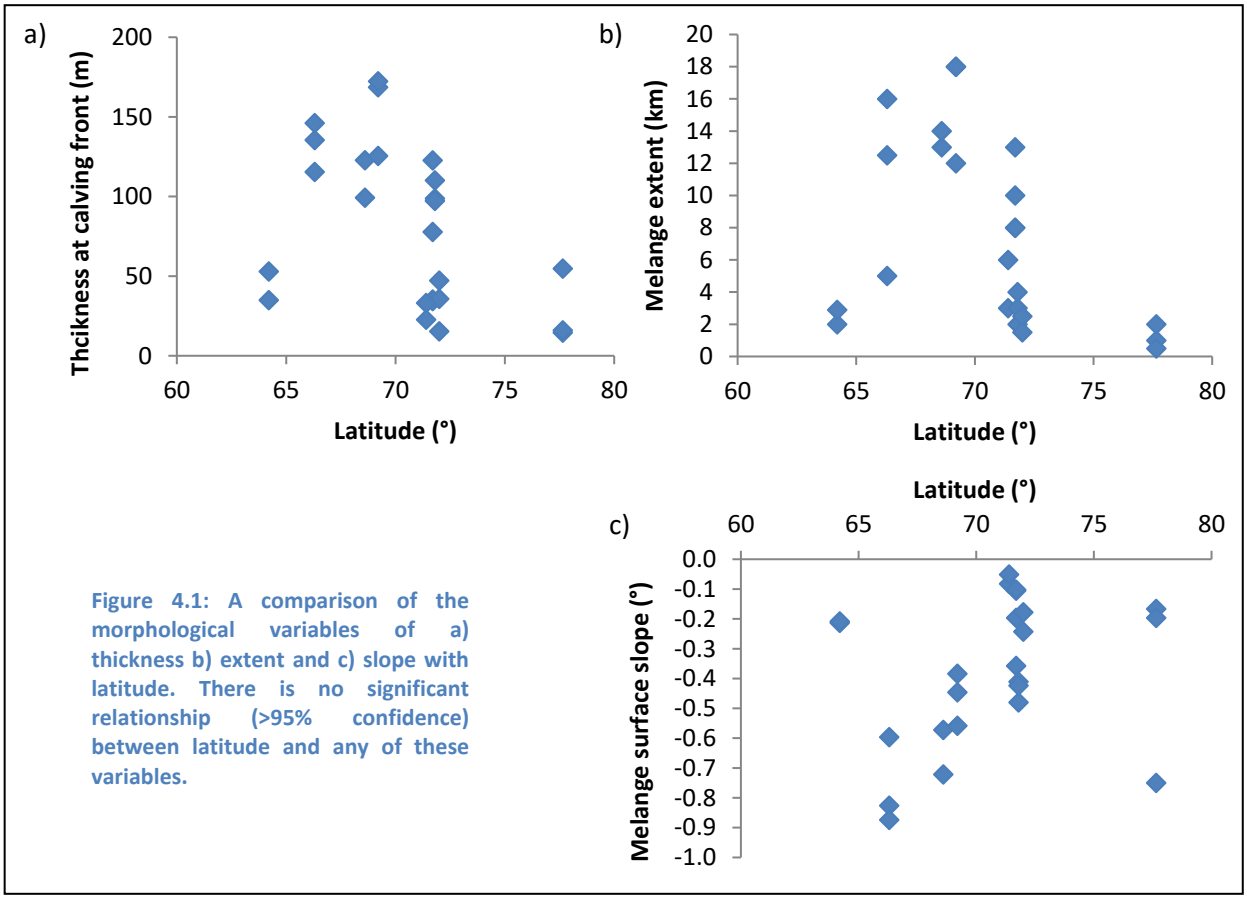

Figure 4.1: A comparison of the morphological variables of a) thickness b) extent and c) slope with latitude. There is no significant relationship (>95% confidence) between latitude and any of these variables.

However, Figure 4.1 above shows no significant (>95% confidence) relationships between latitude and melange thickness, extent or slope, which indicates that these variables must be controlled by non-environmental factors.

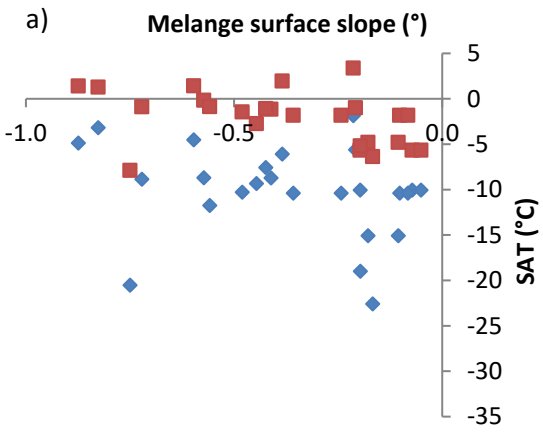

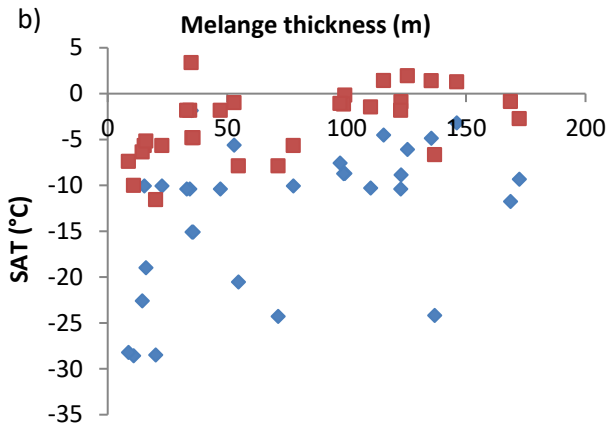

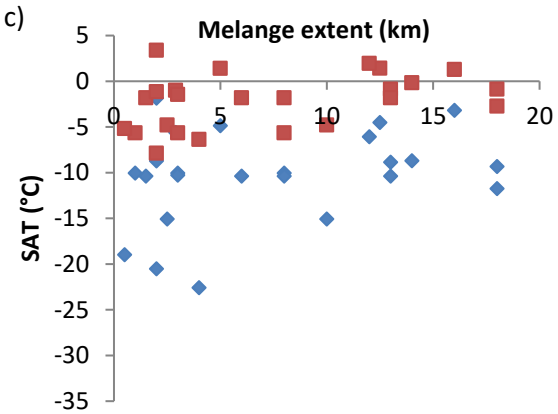

Figure 4.2: Relationship between winter (JFM) (blue diamonds) and spring (AMJ) (red squares) surface air temperature and melange a) slope b) thickness and c) extent. There is no significant relationship (>95% confidence) between SAT and any of these variables.

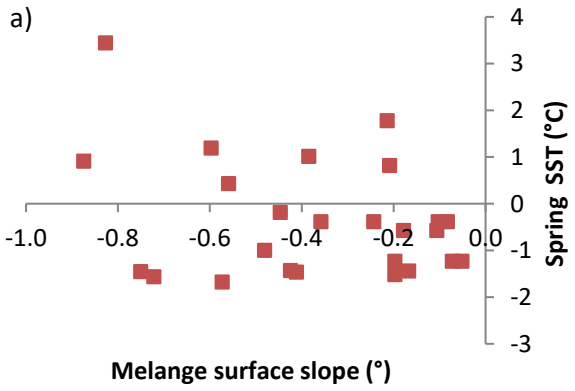

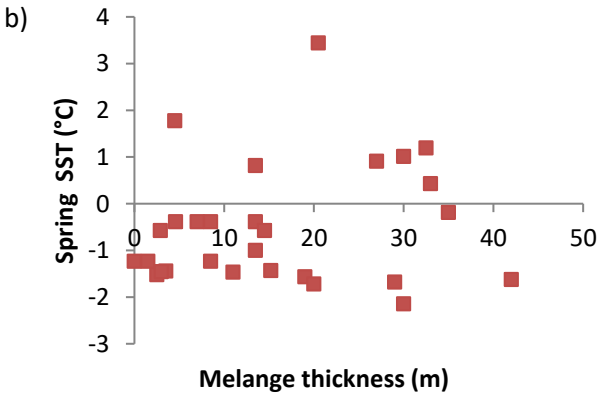

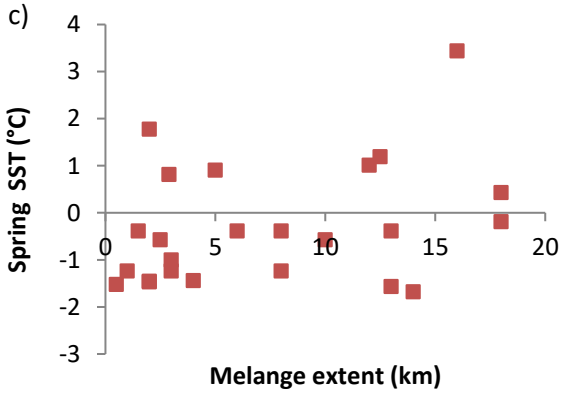

Figure 4.3: Relationship between spring (AMJ) sea surface temperature and melange a) slope b) thickness and c) extent. There is no significant relationship (>95% confidence) between SST and any of these variables.

4. 2. 2. SAT/SST

Since the IceBridge data from which the melange variables were derived was collected in spring, this time period was selected to attempt to identify any concurrent environmental controls affecting the morphological characteristics of the pro-glacial structures. Additionally, it has been shown from observation of MODIS data that sikussak structures become seasonally rigid during the winter (JFM) period, and so this was also investigated in order to identify whether the thickness and shape to which the sikussak built up was controlled by the coldness of the winter.

In Figures 4.2 and 4.3 above, winter (January – March) and spring (April – June) SATs and spring SSTs are compared with melange slope, thickness and extent. It is not possible to make a useful comparison between the structural characteristics of the melange and winter SST, as during the winter freeze-up when the sea surface is covered with ice, a standard value of -2°C, the freezing point of water, is assumed. Therefore only spring (April-June) SSTs are used.

Evaluation of Figures 4.5 and 4.6 indicates that analysing the effect of seasonal environmental factors in isolation is of limited value, as there is little correlation evident. Since the environmental forcings at different times of year affect the mobilisation and freeze-up dates of melange (Fox and Squire (1991), an alternative measure is required to evaluate the seasonal cycle as a whole.

4. 2. 3. Fast-ice Index

Reeh et al. (1999) used a fast-ice index based on relative numbers of degree-days above and below the freezing point of sea water (*DG+* and *DG-* respectively) to investigate the effect of temporal and spatial temperature changes on the growth and decay of fast-ice in Greenland fjords. This fast ice index may be expressed as:

$$FI = \frac{\sqrt{DG-}}{DG+}$$

The larger the value of FI, the greater likelihood there is of fast-ice persisting through the summer calving season (Reeh et al. 1999). This equation is based on the assertion of Assur (1956) that the seasonal growth of ice is related to the annual number of degree days below the freezing point of sea water (~-1.6°C) since freeze-up was initiated. Ice growth continues through the freeze-up period until the air temperature crosses a -12°C threshold to higher temperatures in the spring, when ice starts to weaken and thin (Assur, 1956). In this way, the thickness of ice is highly related to the relationship between the length of the calving season (ablation period ~ June-December) and the freeze-up season (~January-June). This can account for a long, cold winter in which the sikussak mass

is maintained, and a short, warmer calving season in which material is rapidly built up in front of the glacier.

Copland et al. (2007) use number of positive degree days (PDD) per year as a direct proxy for summer melting of the Ayles Ice Shelf of Ellesmere Island in Arctic Canada, just north of PM Glacier. They propose that this is a more valuable measure for understanding ice shelf health than mean monthly or annual temperatures. Additionally, climate reanalysis in the work of Copland et al. (2007) indicates that, similar to the findings of Reeh et al (1999), a distinct threshold in the number of PDD may exist for ice shelf calving identified at 200 yr^{-1}. In years which exceeded this value, ice shelf calving increased noticeably. Freezing degree days (FDD) are an alternative measure, indicating the extent to which the ice shelf has cooled.

Multi-year ice tends to promote the development of floating ice tongues at the terminus, as present at ZI and 79N glaciers, and semi-permanent fast-ice, identified as sikussak in Section 3.1, increases the stability of calving fronts to a lesser extent. A threshold of FI = 0.1 was identified by Reeh et al. (1999), above which semi-permanent fast-ice persisted, and below which fast-ice was impermanent or non-existent (Reeh et al. 1999).

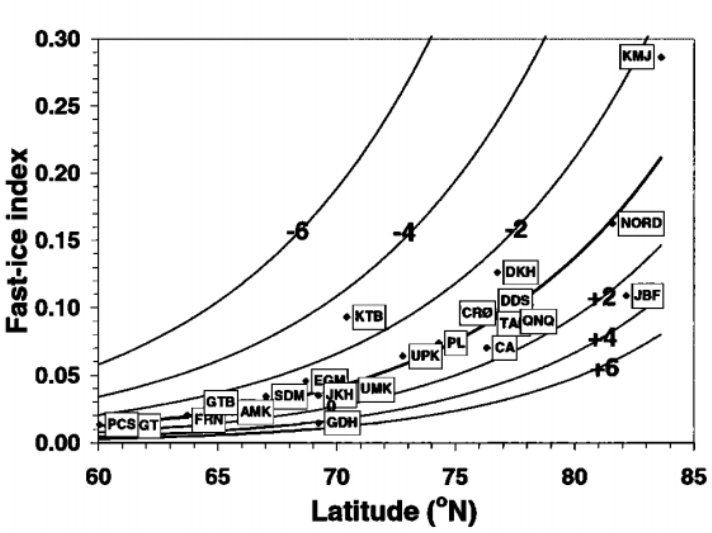

Figure 4.4: Greenland Fast-ice index for the decade 1951-1960. The thick black line represents an exponential least-squares fit to the data, and the thinner black lines represent FI fits for climate deviations ±6°C from the temperature in 1999 (Reeh et al., 1999).

In Figure 4.5, below, the fast-ice index proposed by Reeh et al (1999) has been applied to the locations of the glaciers of this study. Three time periods have been selected for this analysis: 1980-1989, shown on the graph as red squares; 1990-1999, shown as green triangles; and 2000-2009, shown as blue diamonds. A general trend of a decreasing fast-ice index for all locations of this study indicates a gradual increase in the length of the calving season (positive degree days) relative to the period of freeze-up (freezing degree days).

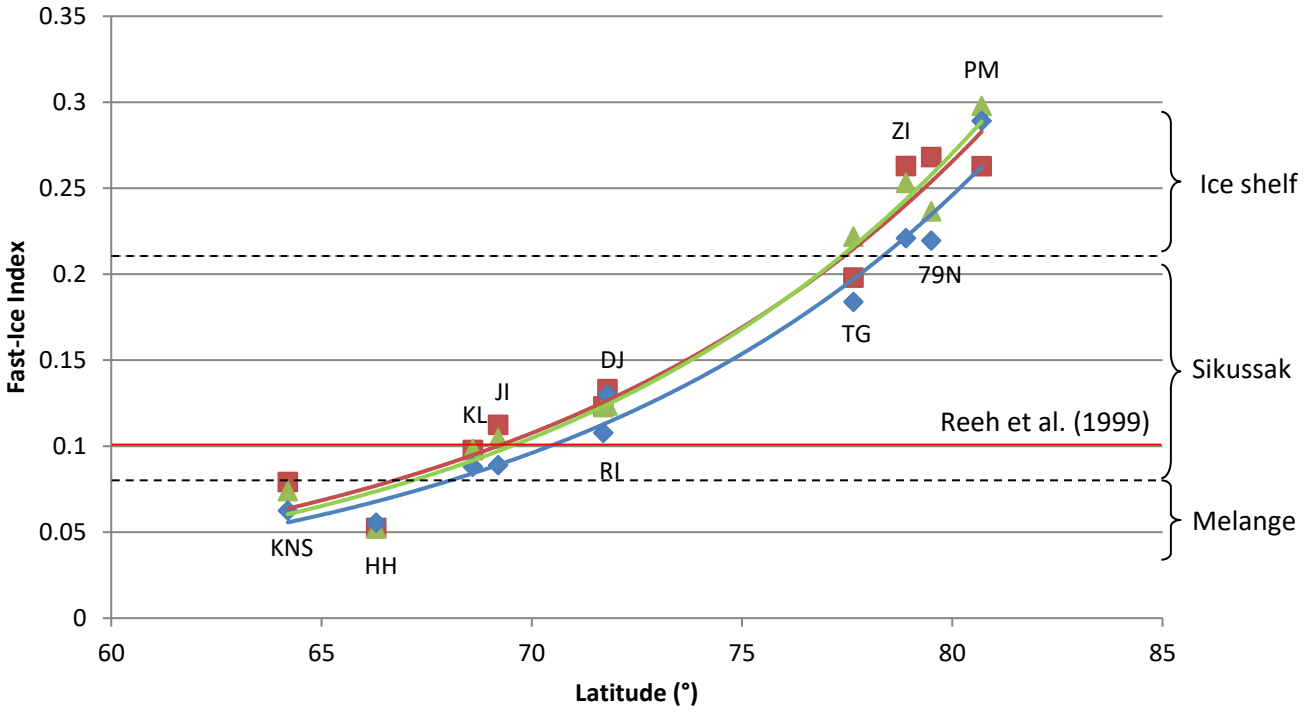

Figure 4.5: Fast-ice index using average PDD values for the periods 1980-1989 (red squares), 1990-1999 (green triangles) and 2000-2009 (blue diamonds). The trend lines represent an exponential least squares fit to each set of data. The thick red line shows the proposed fast-ice threshold from Reeh et al. (1999). Dashed black lines represent new proposed boundaries for melange, sikussak and ice shelf pro-glacial structures based on observations in this study.

According to Reeh's analysis, where the FI=0.1 represents a fast ice threshold in Greenlandic fjords, KNS, HH and KL glaciers are below the limit of fast ice in fjords. JI is above this threshold in the 1980s and 1990s, but warmer temperatures mean that it drops below to the threshold in the 2000s, coincident with the breakup of its floating ice tongue (Johnson et al., 2004). KL has also experienced rapid retreat due to calving instability (Joughin et al., 2008b). This indicates that there may indeed be some correlation between the FI index of Reeh et al. (1999) and the stability of the floating tongues of Greenlandic tidewater glaciers. Above the proposed threshold of Reeh et al. (1999), all glaciers studied have some form of seasonal or multi-year fast ice at their terminus.

However, although the FI = 0.1 threshold proposed by Reeh et al (1999) appears to align with the point at which instabilities are initiated, slightly different threshold values are now proposed which fit more closely with observations of sikussak rigidity made from the 13 glaciers investigated in this study.

A slightly lower value of FI = 0.08 is proposed as the threshold below which seasonal sikussak is not found, as observations from KL and JI using MODIS imagery indicate that these two glaciers both have seasonal sikussak at their terminus, and thus should be above the threshold for fast-ice.

Additionally, a new threshold is proposed at FI = 0.21, above which the fast-ice which forms in Greenlandic fjords is multi-year, rather than seasonal in nature, forming the ice shelves and extensive floating tongues identified in the IceBridge ATM data from ZI, 79N and PM glaciers (Section 3.1, Results).

These FI thresholds may be converted into latitudinal zones in which different forms of pro-glacial structures are expected to be found, based on the co-ordinates of the glaciers of this study which fall into the categories of melange, sikussak and ice shelf. The FI thresholds shown in Figure 4.5 correspond to <66.5°N as the region where fast-ice cannot be maintained, 68.5° - 77°N as the region with seasonal fast-ice, and >78°N as the region with multi-year floating tongues or ice shelves restraining the glaciers.

As stated by Reeh et al. (1999), and assuming an upper fast-ice threshold for maintaining permanent fast ice, a temperature increase of a few degrees may bring the glaciers of northern Greenland, including PM, ZI and 79N, below the FI necessary for maintaining permanent fjord ice, thereby threatening the stability of their floating tongues (Figure 4.4). The 2010 disintegration of the floating tongue of PM, the 1997 break-up of the Norske Øer Ice barrier which restrains ZI and 79N (Reeh et al., 2001), and the 13-fold acceleration of Hagen glacier in northeast Greenland during the past decade (Moon et al., 2012), may therefore be attributed to a climatic shift, resulting in disintegration of multi-year fast ice, under this analysis. However, these events may alternatively be attributed to the decadal cycle of break-up and re-formation which has been proposed for the multi-year fast-ice structures of northern Greenland (Thomsen et al, 1997).

Farther south, JI and KL lie very close to the lower threshold of semi-permanent fast-ice (FI = 0.08) identified through observations of the glaciers of this study. If the trend of decreasing FI observed in Figure 4.5 for the time period 1980 -2009 continues into the next decade, it is expected that JI and KL will drop below the FI = 0.08 threshold proposed for seasonal sikussak formation in this study. Additionally, it is predicted that RI, UM, KS and II will fall below the original FI = 0.1 threshold proposed by Reeh et al. (1999). Since this threshold appears to align with observations of instability, rapid retreat due to calving instabilities may be initiated at these glaciers during the next decade.

4. 2. 4. Forcing from the NAO

Since the FI index is based upon the ratio between annually summed PDD and FDD, an investigation is now made into the environmental forcings which affect this ratio.

Figure 4.6 below shows contoured SAT PDD for 2009/2010/2011, and it is clear from these data that there is a sharp change in the number of PDD between 65 and 70°N along the east coast, whereas the change is much more gradual along the west coast, which may cause a less abrupt latitudinal threshold for types of fast-ice structures found in the western fjords. This indicates that pure latitudinal patterns are likely to be skewed by the relative warmth of the southeast coast, and that analysis must consider the two coasts separately in order to identify any latitudinal patterns.

Although the synchronicity in terminal behaviour may be seen between glaciers in the same region, such as the synchronous thinning of HH and KL in 2003 (Howat et al., 2008), it is more difficult to attribute a common climatic forcing to rapid terminus changes in distant glaciers. However, although the warming in 2003 was focused on the southeast coast, some recorded warm years have a more extensive warm anomaly, such as 2005 (Hanna et al., 2008), where warm SATs affected the majority of the ablation zone of the ice sheet.

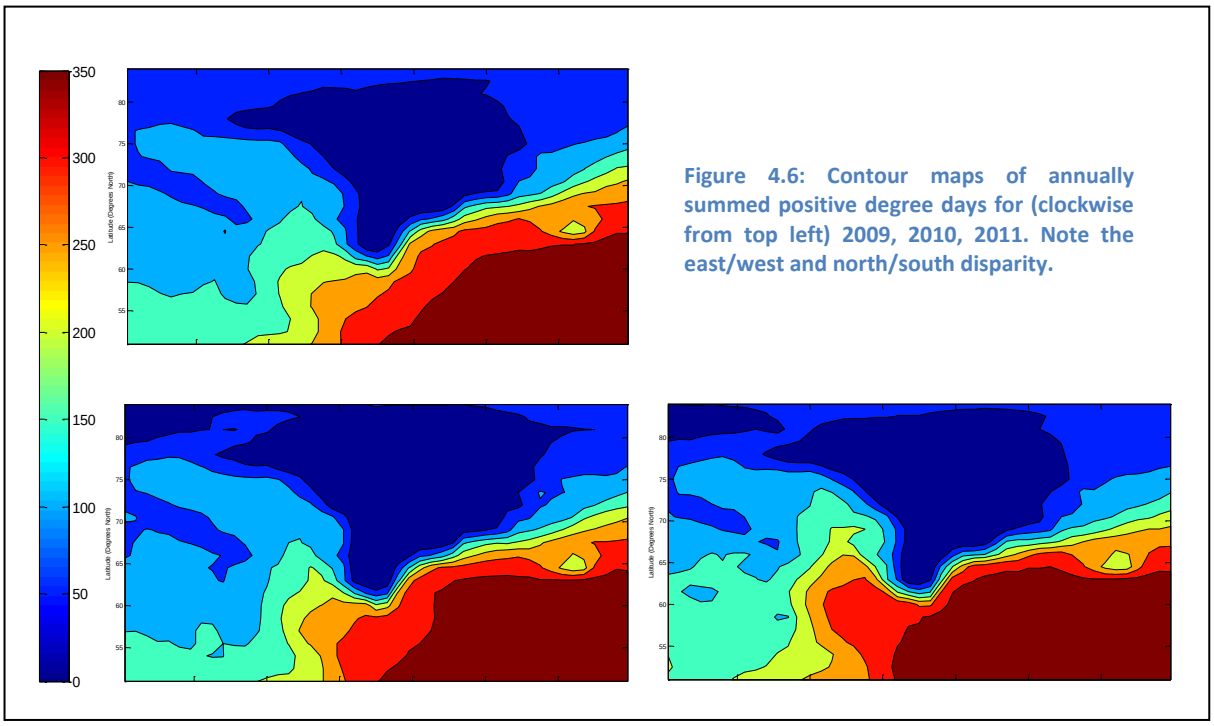

Figure 4.6: Contour maps of annually summed positive degree days for (clockwise from top left) 2009, 2010, 2011. Note the east/west and north/south disparity.

The lower bound of sikussak formation (68.5°N) is very close to the 69°N threshold below which rapid and synchronous changes in terminus dynamics were observed along the East coast (Seale et al., 2009; Nick et al., 2009). This indicates that the factors affecting the location of sikussak formation may well be the same as those which control tidewater glacier dynamics. As discussed in Section 1.3, oceanic and atmospheric currents have an important influence on the warmth of water and accompanying air masses which reach the coast of Greenland. Therefore, the relationship between the FI index and NAO variations is investigated (Figure 4.7, next page).

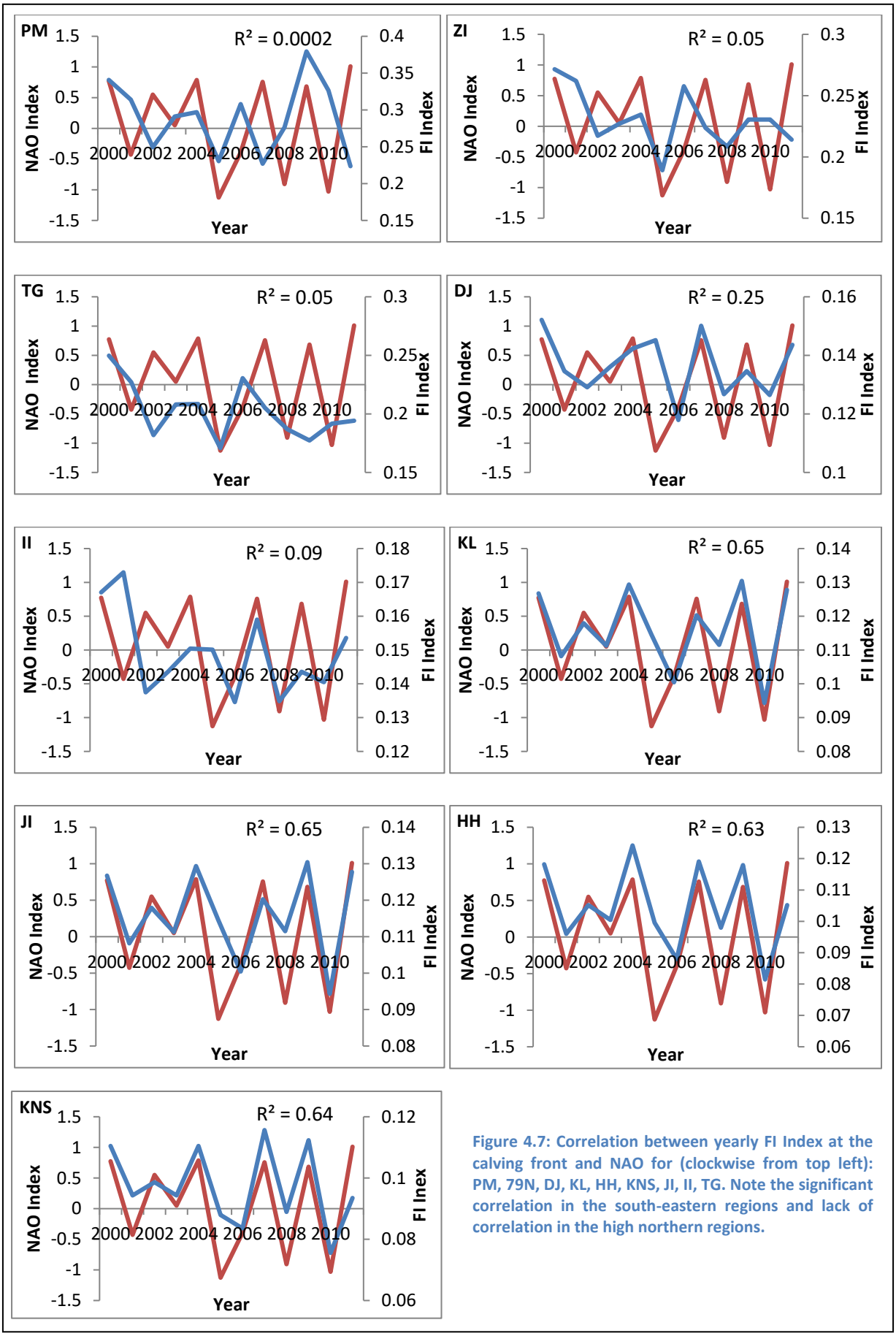

Figure 4.7: Correlation between yearly FI Index at the calving front and NAO for (clockwise from top left): PM, 79N, DJ, KL, HH, KNS, JI, II, TG. Note the significant correlation in the south-eastern regions and lack of correlation in the high northern regions.

These graphs show a significant correlation (>95% confidence) between yearly FI index and NAO index for HH, KL, KNS and JI regions, whereas II, TG, DJ, PM, and ZI show no significant correlation. This pattern is expected given that it is the southern regions, and south-eastern in particular, which are influenced by the Irminger Current. This supports the observations of Christoffersen et al. (2011), who, among others, assert that warm waters reaching the coast of south-east Greenland are well-correlated to variations in the NAO. This would suggest that warm water in fjords affects air temperature, and thus the fast-ice index, or may alternatively be an indication that warm water inflow to fjords is accompanied by warmer air flow, as shown by Christoffersen et al. (2011).

The fast-ice index is based upon the hypothesis that seasonal sikussak formation is dependent upon both a sufficiently warm and active summer season, and a winter which is cold enough to form sea ice in the fjords, which bonds the clasts together and causes the characteristic seasonal rigidity. This analysis indicates that environmental factors constitute a condition which needs to be met in order to enable sikussak structures to develop and persist. Figure 4.5 indicates that there exists a distinct climatic zone in which sikussak may be found within Greenland fjords, which corresponds to approximately 68.5 - 77°N. At KNS and HH, below 66.5°N, the fast-ice index and MODIS observations indicate that there is insufficient seasonal rigidity to establish a winter sikussak. Instead, there is a persistent presence of loose, unconsolidated melange which will have little seasonal effect of suppressing calving or maintaining the integrity of the calving face.

Therefore, there are latitudinal limits to the region in which sikussak can be found, and environmental controls are therefore a requirement for sikussak formation. However, the lack of statistically significant relationships (>95% confidence) in Figures 4.1 – 4.3 indicates that environmental factors do not influence the melange morphological variables of thickness, slope and extent, and the alternative controls on melange and sikussak morphology are therefore investigated in Section 4. 5.

4. 3. Glacio-dynamic forcing

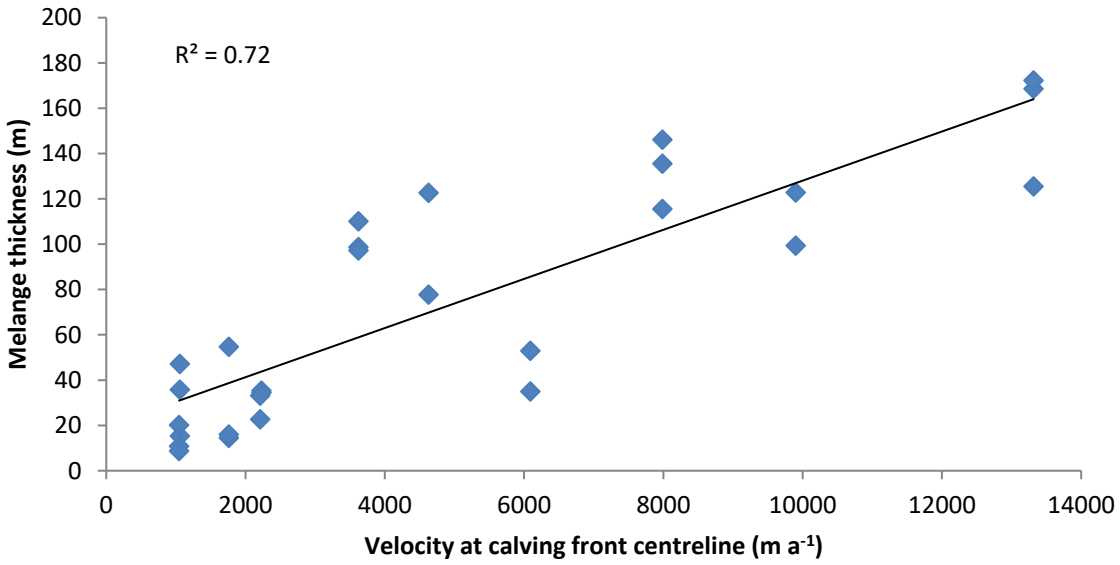

Figure 4.8: Velocity at calving front centreline compared with melange thickness at the calving front. Note strong positive relationship between velocity and thickness at calving front, which indicates that faster glaciers build up a thicker pro-glacial structure.

Figure 4.8 shows the positive correlation between glacier flow velocity and melange thickness at the calving front is statistically significant to a confidence of 99%. Since calving rate directly related to ice velocity (van der Veen, 1996), the strong positive relationship shown in Figure 4.8 indicates that a higher calving flux (an effect of a greater volume of ice crossing the grounding line) causes a much thicker melange structure to build up in front of the glacier.

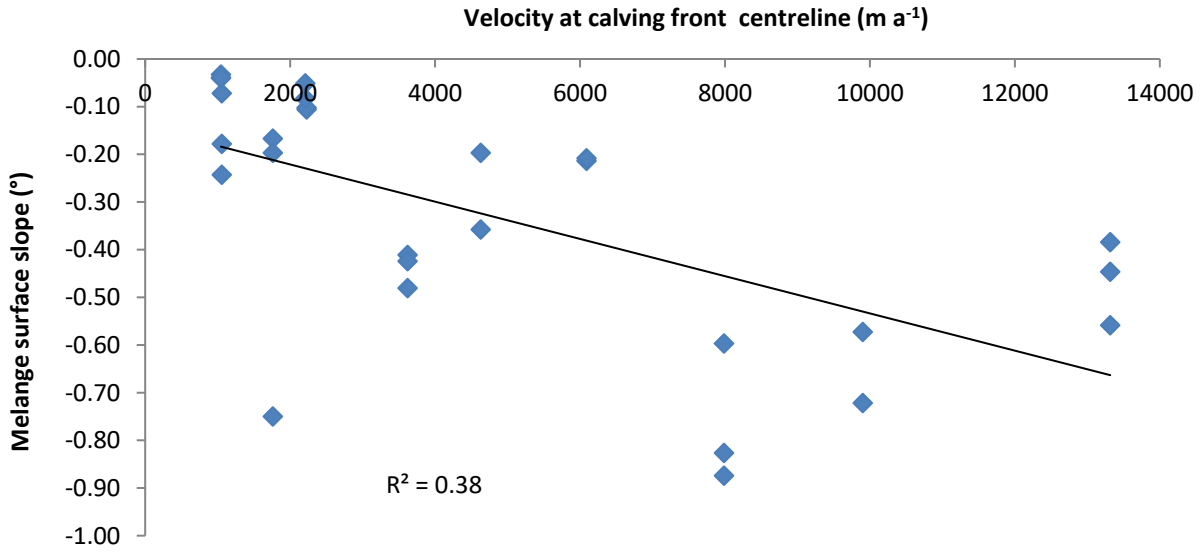

Figure 4.9: Velocity at calving front centreline compared with melange slope angle. Note the significant negative relationship, which indicates that the melange slope angle tends to be steeper in front of faster flowing glaciers.

Figure 4.9 shows a negative correlation between velocity at calving front and melange slope angle, significant to 95% confidence. This indicates that at faster-flowing glaciers, the melange is more steeply stacked against the calving front. This may be attributed to a 'bulldozing' effect, where increased glacier velocity causes the structure to build up more steeply against the calving face as the material is pushed down-fjord (Amundsen et al., 2010).

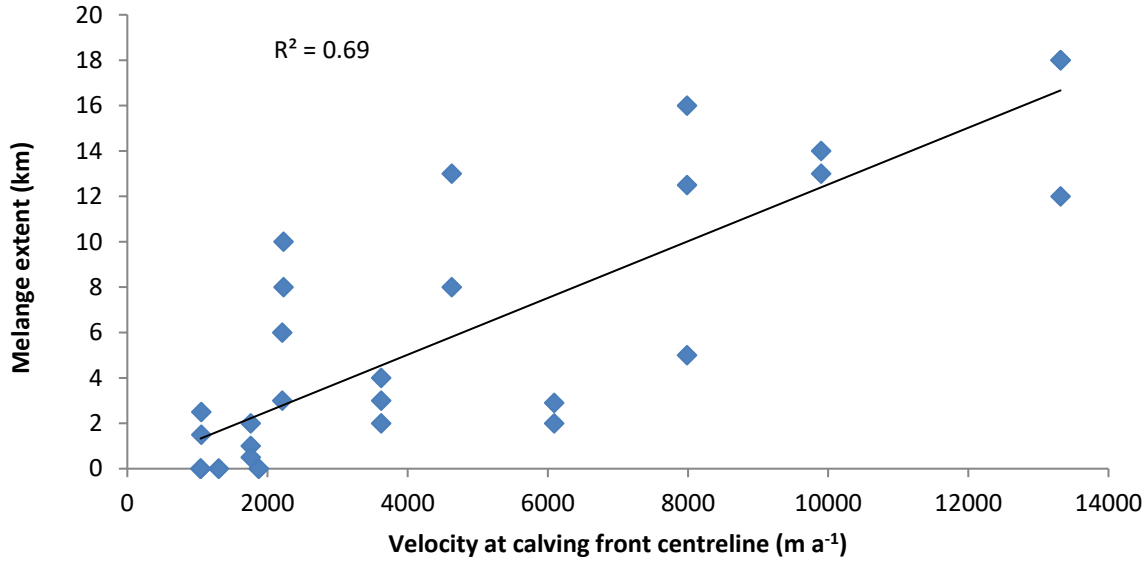

Figure 4.10: Velocity at the centreline compared with melange extent. PM Glacier has been excluded as an outlier, based on comparison of width and velocity relationship (Figure 4.16, below).

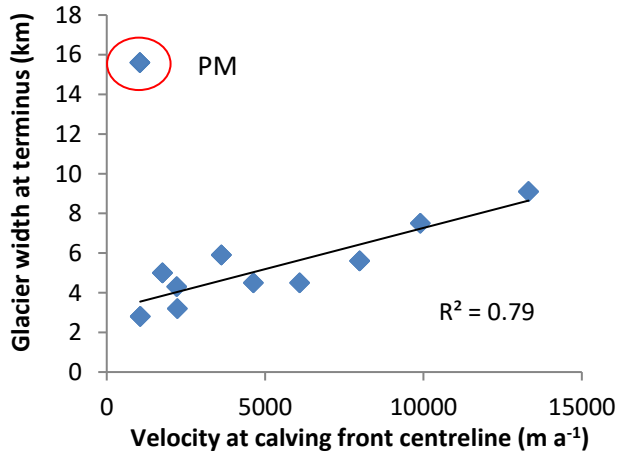

Figure 4.11: Graph showing relationship between glacier velocity and width at the terminus. Note PM Glacier has been excluded as an outlier.

Figure 4.10 shows a strong positive relationship between glacier velocity and width at the centreline, significant to 99% confidence. This suggests that flow velocity is influenced by sidewall friction, which is in turn controlled by width. PM glacier does not show the expected relationship between width and velocity (Figure 4.11), as it flows very slowly for such a wide glacier. This indicates that PM has a different type of force balance, due to a stronger bed or the constraining effect of the large floating ice shelf which resisted flow until its breakup in 2010. Therefore, the values for PM are disregarded for this section of the analysis.

Once PM is excluded as an outlier, the rest of the glaciers show a good (>90% confidence) correlation between the melange morphological variables and glacier width (as shown in Figures 4.12 – 4.14 below). This relationship is simply explained by the fact that fast glaciers are wide, but additionally indicates that it is not constriction from the sides, but rather inputs to the system, which affect melange/sikussak thickness – faster, wider glaciers generate more material and therefore have larger sikussaks.

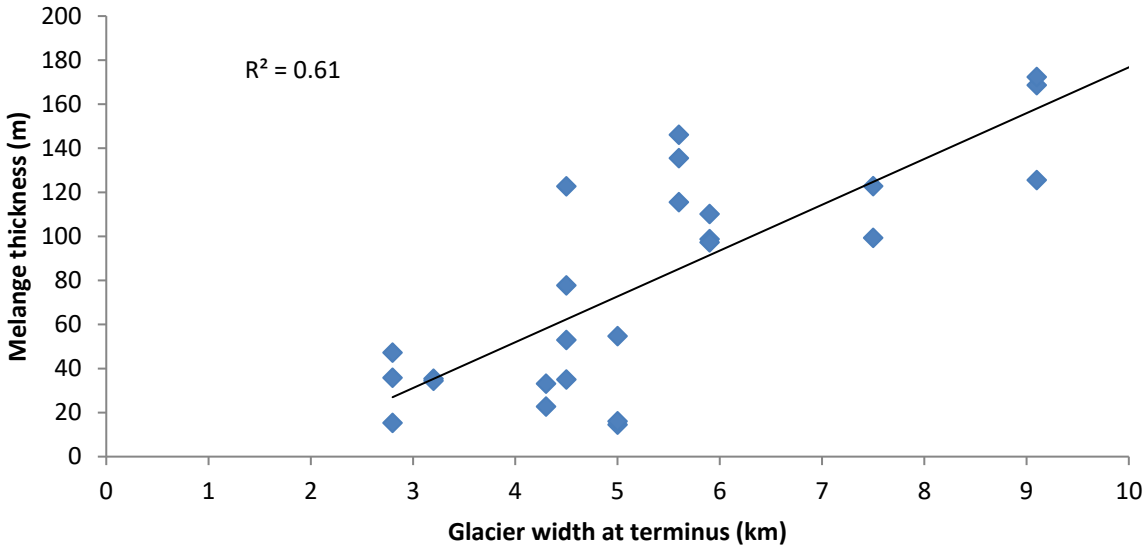

Figure 4.12: Comparison of glacier width with melange thickness at calving front. The trend indicates that melange thickness tends to increase with greater glacier width.

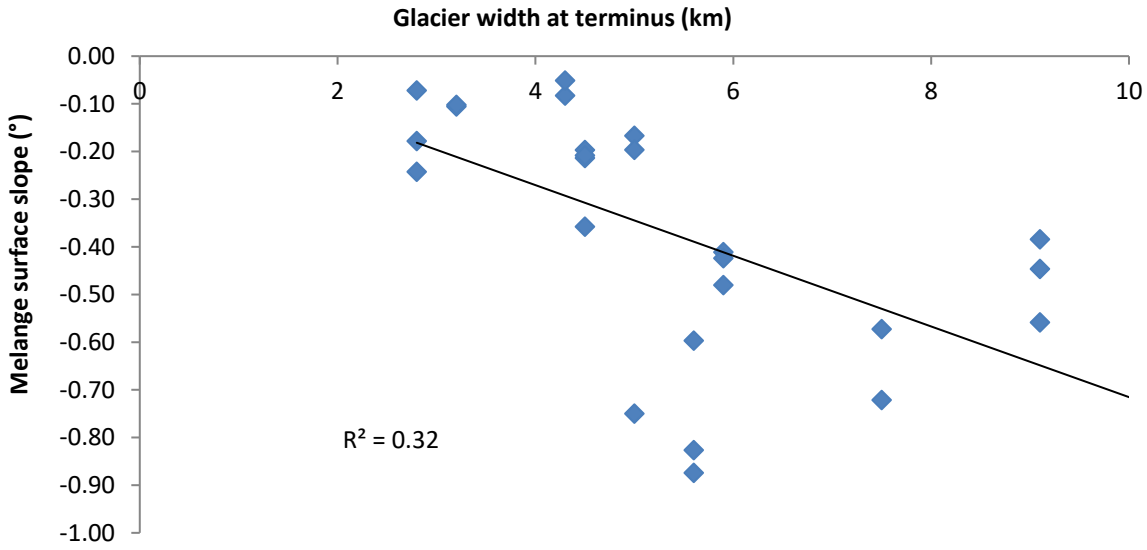

Figure 4.13: Comparison of glacier width with melange slope. The negative correlation indicates that melange slope tends to get steeper with greater glacier width.

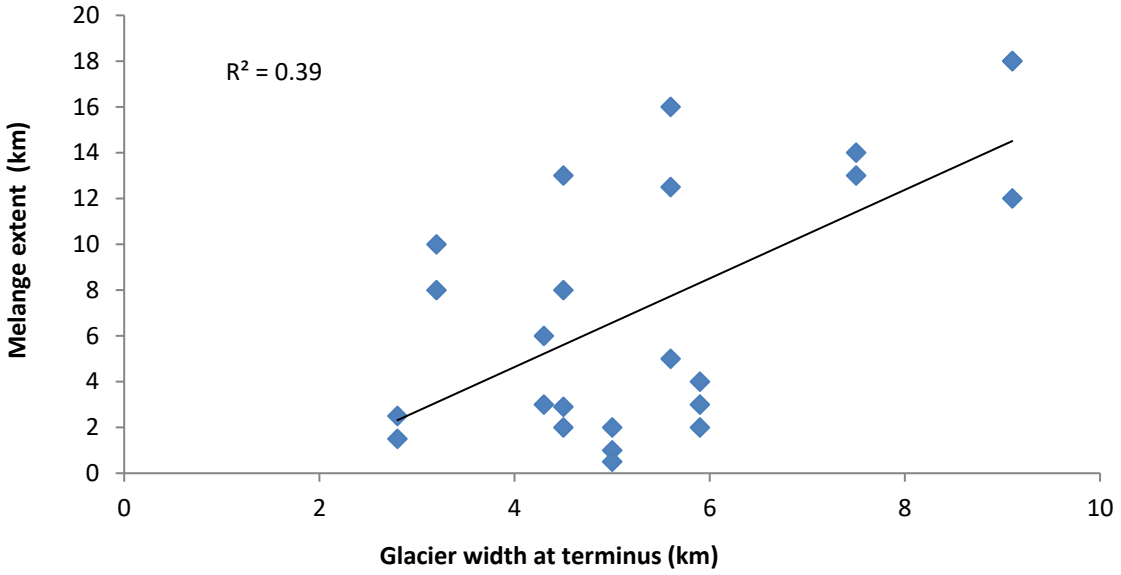

Figure 4.14: Comparison of glacier width with melange extent. The trend indicates that melange tends to extend further with greater glacier width.

Figure 4.15 shows that melange thickness and slope are strongly correlated, and this relationship is significant to 99% confidence. A greater thickness of ice at the calving front is likely to rapidly decline away from the face, whereas a thinner melange is likely to have a lower surface slope. Older, multi-year fast-ice structures tend to have a lower surface slope as shown by the thickness profiles of the pro-glacial environment of ZI and 79N glaciers (Section 3.1). This indicates that multi-year ice tends to spread out year on year, perhaps through a process of gravitational spreading, similarly to ice shelves. Thickness and slope are therefore highly dependent on the speed and volume of ice calved from the glacier. Additionally, the degree of definition between the sikussak and sea ice/sea level provides an indication of the rigidity of the material. A distinct break of slope indicates a more coherent structure, whereas a gradual decline indicates that the material is looser and more mobile.

A correlation is also seen between melange thickness and extent in Figure 4.16, significant to 99% confidence. This positive relationship shows that thicker melange structures tend to be more extensive, which indicates that the melange extent is also affected by the amount of glacier ice deposited pro-glacially. However, there are indications from MODIS observations that additional factors affect the length of the melange structure, and these will be investigated in Section 4.5.

The interpretation that sikussak thickness is highly dependent upon the volume of glacier ice calved off at the terminus indicates that there may be a stabilising feedback between glacier velocity, which is directly related to calving flux, and sikussak formation. Therefore, a hypothesis is proposed that faster glaciers build up a thicker sikussak at their terminus through higher calving rate and a hypothesised 'bulldozing effect', which consequently has a stabilising effect on the terminus.

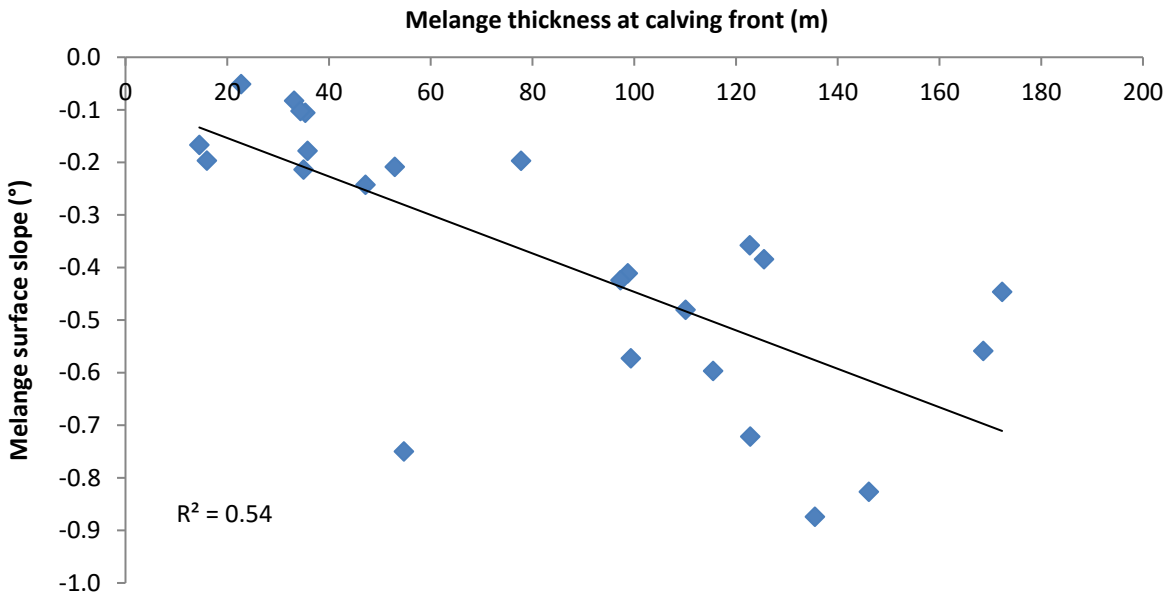

Figure 4.15: Relationship between the melange thickness and surface slope. The significant relationship (99% confidence) indicates that melange structures which are thick at the calving front tend to slope steeply away, whereas those which are thinner at the calving front tend to be much flatter.

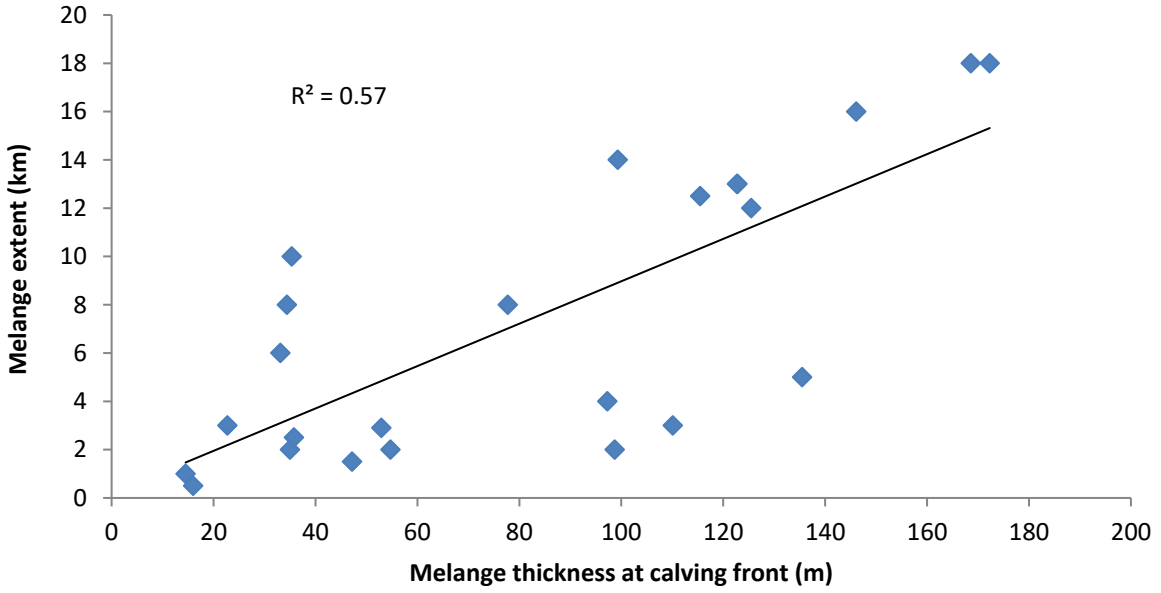

Figure 4.16: Relationship between melange thickness and extent. The significant relationship (95% confidence) indicates that as those melange structures which are thicker at the calving front also tend to be more extensive.

4. 4. Back-stress effects

The effect of sikussak on glacier dynamics has so far not been studied in detail. However, it is important to understand the shear strength of sikussak structures as the stabilising feedback between sikussak structures and glacier velocity is only important if the back-stress exerted by the sikussak on the glacier calving face is sufficient to either restrain flow or inhibit calving.

The potential back-stress from pro-glacial ice melanges ($p_{melange}$) was calculated from near-terminus velocity changes by Walter et al. (2012). These authors suggest that the effective back-stress at the terminus is a function of the balance of stresses at the calving front, considering the strength and thickness ($h_{melange}$) of the melange comparative to the thickness of the glacier terminus (h_{ice}).

Walter et al. (2012) estimate the pressure due to the presence of the ice melange ($p_{melange}$). This calculation is based on an observation of a ~1.5m d^{-1} 'ramped' step-change in ice flow velocity, $u_1(x)$, near the terminus coincident with the disintegration of the pro-glacial ice melange without any coincident calving events. From this, it is inferred that the ice melange directly restrains ice flow, and this capacity is quantified through a calculation of its buttressing pressure using Equation 8 (Walter et al., 2012) below:

$$p_{melange} = \frac{u_1(x_0)\bar{\eta}}{L} \quad [8]$$

Where L = longitudinal coupling length and $\bar{\eta}$ = average effective viscosity. Using the stress exponent m = 3, values for $p_{melange}$ of ~30-60 kPa are calculated, of a similar magnitude to tidal perturbations (~20 kPa). Walter et al. (2012) did not have a value for sikussak thickness, and this force is therefore a stress average which takes calving face thickness into account. The driving stress of Store Glacier (~200 kPa) is an order of magnitude greater than $p_{melange}$. From this, it is surmised that the force $p_{melange}$ exerts a seasonal back-stress of a similar magnitude to the resistance from basal drag or tidal variations (Walter et al., 2012).

Unfortunately, the IceBridge mission did not survey Store Glacier, and so the thickness of the melange structure for this glacier is not directly known. However, the strong correlation between velocity at the calving front and thickness of pro-glacial ice melange shown in Figure 4.8 indicates that the melange thickness is a linear function of ice velocity [h_m= f (u)], and this function can therefore be used to infer a thickness of ~90 m for the sikussak at Store Glacier.

Walter et al. (2012) estimated the effect of sikussak without knowing its thickness. The sikussak thickness data gathered by this study enables the sikussak/melange strength at each glacier to be determined, under the assumption that the ice is failing or shearing by compression, as it builds up. Under this assumption, the melange shear strength ($\tau_{melange}$) can be estimated as:

$$\tau_{melange} = \frac{p_{melange} \times h_{ice}}{h_{melange}}$$

[9]

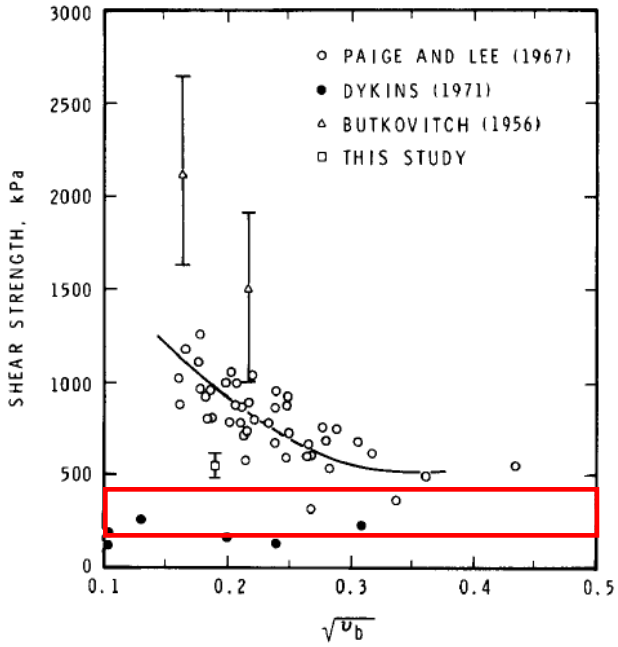

Figure 4.17: Shear strength as a function of the square root of brine volume. In red is shown the range of melange shear strengths calculated for Store Glacier. (Frederking and Timco, 1984)

This calculation is based upon the range of back pressures calculated by Nick et al. (2010) and Walter et al. (2012), and therefore a range of possible values for melange shear strength are calculated. These values range from 200-400 kPa. When compared to the work of Frederking and Timco (1984), these values lie in the lower bounds of estimated shear strength (Figure 4.17), indicating that sikussak fracture strength may be comparable to briny and porous sea ice.

Once $\tau_{melange}$ has been calculated from the Store Glacier data, this can be applied to the glaciers of this study to derive buttressing pressure using the equation:

$$p_{melange} = \frac{h_{melange}}{h_{ice}} \times \tau_{melange}$$

[10]

These values are shown in Table 4.1, below.

Glacier	Date	$h_{melange}$	$h_{melange}$ average	h_{ice}	$p_{melange}$	$p_{melange}$ average
KNS	2010	35		600	17.5	
KNS	2011	52.92	44.0	600	26.5	22.0
HH	2009	115.5		600	57.8	
HH	2010	146.1		600	73.1	
HH	2011	135.5	132.4	600	67.8	66.2
KL	2010	122.8		500	73.7	
KL	2011	99.32	111.1	500	59.6	66.6
JI	2009	168.6		4000	12.6	
JI	2010	125.5		4000	9.4	
JI	2011	172.3	155.5	4000	12.9	11.7
KS	2010	33.13		1600	6.2	
KS	2011	22.71	27.9	1600	4.3	5.2
RI	2010	122.7		902	40.8	
RI	2011	77.75	100.2	902	25.9	33.3
UM	2009	35.33		900	11.8	
UM	2010	34.39	34.9	900	11.5	11.6
DJ	2009	110.1		800	41.3	
DJ	2010	98.73		800	37.0	
DJ	2011	97.27	102.0	800	36.5	38.3
II	2009	35.79		650	16.5	
II	2010	47.17		650	21.8	
II	2011	15.33	32.8	650	7.1	15.1
TG	2009	14.51		800	5.4	
TG	2010	16		800	6.0	
TG	2011	54.72	28.4	800	20.5	10.7

Table 4.1: Values for melange and ice thickness at the calving front ($h_{melange}$ and h_{ice} respectively), and $p_{melange}$ calculated for each glacier.

Table 4.1 shows that the strongest melange structures are at HH and KL glaciers, and the weakest at KS and TG. These values apply to melange strength at a discrete point in time, based on the assumption of fixed melange thickness and strength. However, the melange strength likely evolves throughout the winter as a function of ice sheet growth (Reeh et al., 1999), and is therefore a constantly changing value. It has been suggested that this affects the seasonal velocity fluctuations of tidewater glaciers (Johnson et al., 2004), though even those glaciers without a substantial sikussak appear to undergo these seasonal speed-ups, indicating that the back-stress afforded by seasonal melange rigidity is clearly not an overriding factor in these dynamics.

	2009	2010	2011
KNS	210.1	265.1	561.1
HH	1186.4	1348.9	1022.9
KL		1072.4	889.9
JI	2680.6	2128.6	3523.4
KS		680.8	531.9
RI		1892.0	1892.0
UM	512.5	505.9	
DJ	91.5	160.6	116.1
II	379.9	484.7	171.2
TG	54.5	59.0	186.9

Table 4.2: Cross-sectional areas of the melange and sikussak structures for each of the glaciers of this study in the years 2009-2011.

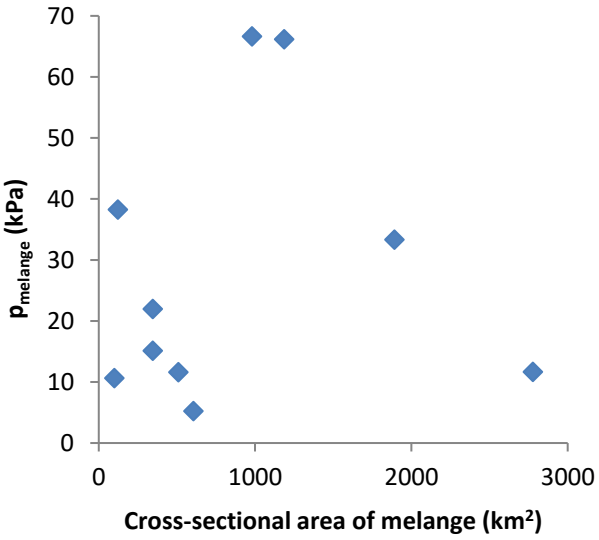

Figure 4.18: Comparison of back-stress exerted by pro-glacial melange and melange cross-sectional area.

In Table 4.6, the cross-sectional area of the sikussak, calculated using the thickness data obtained from Operation IceBridge, is given for each glacier. This is then compared with the $p_{melange}$ values derived from the previous analysis, from which no significant correlation is found. This indicates that these values of $p_{melange}$ are not dependent on the size of the sikussak, only the thickness at the calving front.

This analysis therefore has several weaknesses. Firstly, it fails to make any differentiation between coherent melange structures and what is hypothesised to be much weaker, loose melange in front of the glacier. Secondly, it is based on the ratio between the thickness of the melange and the thickness of the glacier. Consequently, it does not take into account the thickness further away from the glacier front or the distance away from the calving front which the glacier extends, and is therefore not incorporating the effect of accumulated shear strength where a greater volume of material may transfer greater stress onto the glacier front from the walls of the fjord.

4. 5. Topography

It has been proposed that topography exerts an appreciable control on the location of multi-year stability of calving fronts in glacial fjords (Warren, 1991), and that this mechanism may also apply to sikussak (Syvitski et al., 1996). If sikussak structures are similarly dependent on channel geometry, this indicates that the structures develop some form of cohesion, and are dependent on the fjord walls for stability. However, it must be recognised that in some cases it may be that sikussak remains in enclosed fjord areas not due to constraining topographic effects, but rather because this represents a more sheltered environment from which the sikussak is not so readily evacuated (Syvitski et al., 1996).

As previously stated, a sharply delineated sikussak front (in both the thickness data and in the satellite imagery) indicates coherence not present for looser melange structures (Figure 4.19a). This also suggests that, when rigid, sikussak may start to behave like a granular ice shelf (Joughin et al., 2008b), with the capacity to transfer stresses from the fjord walls onto the calving front.

a)

b)

Figure 4.19: Landsat ETM+ images of Kangerdlugssuaq Glacier terminus flowing into Kangerdlugssuaq Fjord in (a) 12/07/01 and (b) 15/08/05. Note the sharply delineated calving front in image (a), the limit of which seems controlled by the location of a break in fjord geometry. Image (b), taken later in the calving season of a different year, shows a loss of rigidity, resulting in the melange mass moving further out into the fjord, seemingly no longer constrained by topography. North is aligned with the short axis and the scale is approximately 30 km across the images.

MODIS imagery shows that the KL sikussak extent seems to be related to the location of a topographic pinning point (shown in Figure 4.19a) at a fjord confluence approximately 15 km from the glacier terminus in years 2000-2011. The sikussak remains as a coherent mass during its period

of seasonal rigidity before this widening of the fjord and material only extends out into the rest of the fjord during periods of weakened melange, when ice is evacuated through wind and wave action (Figure 4.19b). This seems likely to be controlled by the stability afforded by side-wall friction in the narrower section of the fjord.

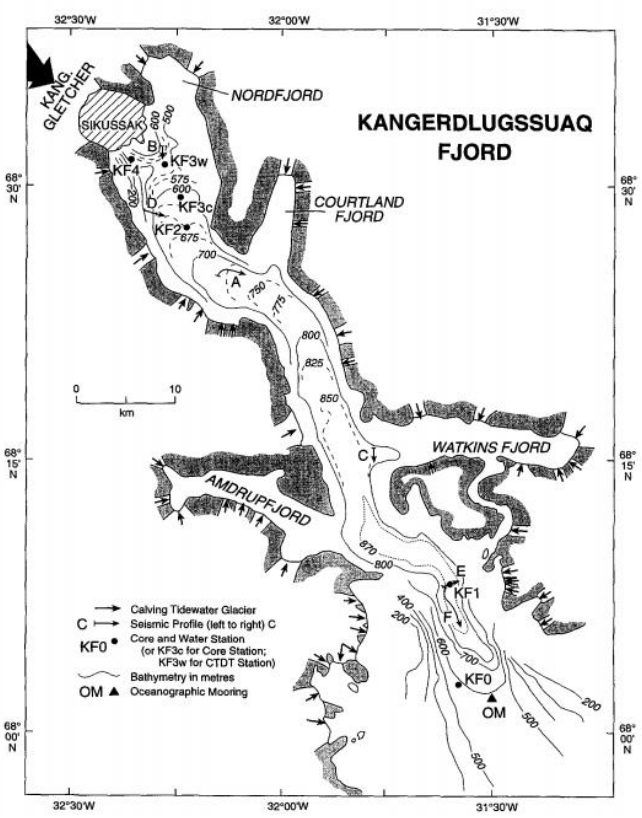

Figure 4.20: Sketch of Kangerdlugssuaq Fjord and Kangerdlugssuaq pro-glacial sikussak. Note the different location of the glacier calving front, but similar extent of sikussak to recent observations (Syvitski et al., 1996).

Figure 4.26 (from Syvitski et al., 1996), shows the extent of the sikussak in the early 1990s to the same location it is now, despite the fact that the calving front has retreated. This indicates the importance of the fjord pinning point to the sikussak of this glacier. Analysis by Dwyer (1995) states that the sikussak has remained in this position for the preceding two decades also, which would be an uncommon degree of stasis unless stability afforded by the fjord topography to some extent.

From analysis of the melange profiles in Section 3.1, it does not appear that the formation of sikussak is dependent on a large, grounded iceberg at its furthest extent, as no large icebergs are identified at the limit of the sikussak along any of the ATM flight lines. Additionally, the icebergs within the sikussak matrix, which can be seen from the data in Section 3.1, do not appear to be large enough to ground on the floor of the fjord, unless a major topographic obstruction, such as a sill, exists in the cavity beneath the sikussak. Therefore, the most likely control on rigid sikussak extent appears to be sidewall friction.

It is interesting to compare the topographic dependence of HH and KL, as the glaciers discharge into very similar fjord systems, with a short constricted section ending in a wider fjord confluence, which then discharges into the sea. HH is similarly constrained by the fjord topography during times when it shows occasional rigidity (Figure 4.21a). For the majority of the time, however, loose, unconsolidated mixture is evident in front of the calving face (Figure 4.21b). This rigidity is sporadic, rather than seasonal, and as can be seen from the melange cross-section in Section 3 and Figure

4.21b, the material is not built up against the calving face, but is rather spread out loosely along-fjord.

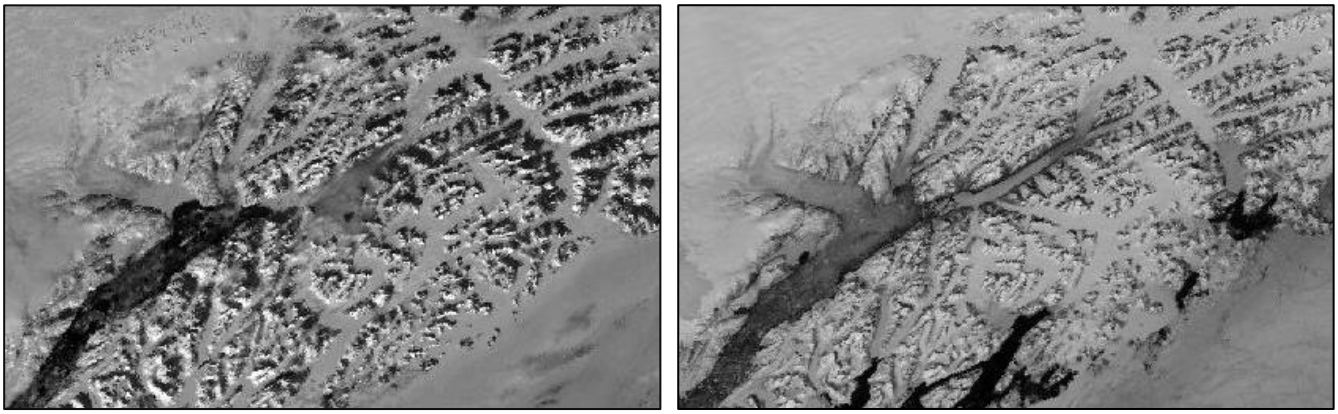

Figure 4.21: MODIS imagery showing Helheim Glacier and pro-glacial ice melange discharging into Sermilik Fjord from (a) 20/03/2001 and (b) 11/05/2005. North is aligned with the short axis and scale is ~150 km across the image.

Observations from Landsat and MODIS imagery of the other glaciers of this study indicates a widespread dependence on fjord topography for both sikussak and melange structures. However, the reason for this dependence is inferred to be different depending on the rigidity of the structure. Rigid sikussaks show the same dependence on fjord topography as tidewater glaciers (Warren, 1991), and appear to be deriving stability from the fjord walls. Looser melange structures seem to have little dependence on topographic effects, which explains the highly variable extents of pro-glacial melange structures, such as those shown at HH, but analysis from MODIS imagery indicates that loose melange is dispersed more quickly when exposed to wind, wave and tidal action in open water. Therefore sheltered embayments and protected fjord systems are conducive to a greater residence time of loose melange prior to evacuation (Syvitski et al., 1996).

Therefore, from analysis of sikussak profiles, it seems unlikely that this grounding of large icebergs (Syvitski et al., 1996) is an important formation mechanism, as it does not appear typical that sikussaks have a large iceberg at their furthest extent, although it is recognised that these features may not be captured by the IceBridge flight line. It seems much more likely that the second hypothesis of Syvitski et al. (1996) (that sikussaks form in oceanographically-isolated environments) has a greater effect upon loose melange structures. There appears to be an additional dependence on the stability afforded by fjord walls for rigid sikussaks which was not suggested by Syvitski et al. (1996). This is highly analogous to the effect of additional shear strength afforded by fjord walls proposed by Warren (1991), and indicates that rigid sikussaks may act in a similar way to ice shelves.

5. Discussion

5. 1. Observations

What is evident from this study is that sikussak structures are much thicker and pervasive than widely thought, and may therefore have more important influences in the sensitive terminal environment of tidewater glaciers than previously considered. Sikussak thickness at the calving front has a range between ~15-170 m. This is shown to exert a substantial back-stress on the glacier calving face, estimates ranging from 5.2 kPa at KS to 66.6 kPa at KL. Observations made in this study indicate that this back-stress effect, is however, dependent upon rigidity created when the calved melange, comprised of a mixture of large tabular bergs and smaller bergy bits, is cohered into a rigid structure by the formation of sea ice between the clasts. Therefore, it is now recommended that the term 'sikussak' be adopted and applied exclusively to this seasonally rigid structure, which has a unique influence in the seasonal suppression of calving. The term 'melange' is retained in this study as a general term to refer to any mixture of ice types, sikussak included.

5. 2. Categorisation

Reeh et al. (1999) attempted to categorise the stability of fast-ice based on an index using annually summed degree days above and below the freezing temperature of water. This is more useful than simply using mean annual temperature, or spring and winter temperatures in isolation, because it incorporates the ratio between the effect of calving occurring in summer and that of freeze-up occurring in winter. This has been identified as critically important in the formation of sikussak structures, which are dependent on calving for production of material, and winter freeze-up which seasonally binds the clasts.

Using this fast-ice index adapted from the work of Reeh et al. (1999), average FI values for the decades of 1980, 1990 and 2000 were extracted. Reeh et al. (1999) suggested that values less than FI=0.1 are too warm to support permanent sikussak. The set of glaciers which fall below this threshold are KNS and HH, with KL and JI on the threshold, passing below by the most recent decade. This seems, therefore, to be a useful primary categorisation, as JI and KL have exhibited rapid retreat due to calving instabilities during the last decade, and KNS and HH have been identified as those glaciers which do not establish a permanent sikussak during the winter months. However, according to observations from MODIS imagery, KL and JI do establish seasonal fast-ice, although it is not present year-round as it is at more northern glaciers. The threshold proposed by Reeh et al.

(1999) is therefore proposed to be the point at which calving instabilities are precipitated, and an alternative FI threshold is suggested in this study, at FI = 0.08, which fits better with observations of seasonal rigidity. Additionally, an upper bound of seasonal fast ice is proposed at FI = 0.21, above which fast-ice ceases to be seasonal, and instead multi-year ice is observed, as at ZI and 79N. However, neither sikussak nor multi-year ice is identified pro-glacially to PM, and it is recognised that the multi-year ice which protects the floating tongues of ZI and 79N glaciers may be dependent upon the Norske-Øer Ice Barrier which is highly location-specific.

Based on the co-ordinates of the glaciers of this study, the proposed FI thresholds corresponds to <66.5°N as the region where fast-ice cannot be maintained, 68.5° - 77°N as the region with seasonal fast-ice, and >78°N as the region with multi-year fast ice. Inevitably, there are gaps between these regions where the pro-glacial structures have been characterised. A more comprehensive study which incorporates a greater number of glaciers from a more diverse range of locations around the circumference of the GrIS would remedy this shortfall.

Although categorisation using climatic indices is useful in order to identify the broad latitudinal zones in which sikussak is to be found, it has limited application in characterising sikussak morphology. This is due to the fact that sikussaks are highly dependent upon the additional factors of ice velocity (from which calving flux may be inferred) and fjord topography.

Calving flux is a useful way in which to establish a primary categorisation of melange structures, as this varies in a set of discrete ways across the glaciers of this study. At high northern latitudes (>78°N), calving occurs infrequently relative to the glaciers farther south, indicating the presence of thick, multi-year land-fast ice. In the mid-latitudes (68.5° - 77°N), calving occurs during a yearly calving season which runs from approximately June-October each year, though this varies with the seasonal cycle of SATs at each glacier. This indicates the presence of a seasonally rigid sikussak, which suppresses calving for at least a few months each year. Finally, at the low latitudes (<66.5°N), calving is nearly constant, and the pro-glacial melange structures achieve rigidity sporadically, if at all.

5. 3. Controls

It is important to identify the controls which affect the sikussak variables of thickness, slope and extent in order to identify where and why sikussak structures build up, and the changes which will affect their continuing presence. Sikussak and melange structures are essentially transitional

structures, and therefore dependent upon factors from both the glacier feeding calved ice and the sea ice supporting this material.

From the analysis in Section 4, it is possible to determine a hierarchy of controls on sikussak formation. Analysis of the FI index indicates that environmental variables constitute an important condition which has to be met in order to enable sikussak growth, but the poor correlations seen in Figures 4.1 – 4.3 indicate that the controls on sikussak morphology have to be found elsewhere.

Calving flux is a primary control on sikussak thickness, indicating that this variable is controlled by the amount of material which deposited in the pro-glacial environment, and how quickly. The variation in surface slope angle across the different melange structures suggests that the shape which the melange settles to is not merely a function of calving flux, however. Analysis in Section 4.3 identified that the slope shape, or how steeply the melange is stacked against the calving face, is a function of how cohesive the material is. Rigid sikussaks tend to be more steeply stacked against the calving face than loose melange. This is attributed to the fact that loose melange will settle into a flatter shape as the clasts are free to move against each other, whereas sikussaks are held together in the shape in which icebergs are calved off from the glacier calving face, and are therefore likely to be steeper, with a sharper definition between the melange and fjord ice/ sea water. Additionally, it is observed that older structures tend to be longer and flatter, indicating that sikussak may be able to flow from gravitational settling in a manner similar to ice shelves.

Investigation of the effect of topography in Section 4.5 indicates that the length of the sikussak structures is not merely a function of thickness and slope, as the sikussak may reach an abrupt end at a break in fjord topography. This is seen in the case of KL, where a rigid sikussak cannot be maintained across the larger width at a fjord confluence. It is hypothesised that rigid sikussaks are dependent on the stability afforded by friction along fjord walls, whereas loose melange structures are more often found in narrow fjord systems and protected embayments due to the sheltering effect that these locations have from wind, wave and tidal processes.

5. 4. Force balance

It appears from analysis in Section 4.4 that the back-stress applied on the glacier calving face is sufficient to affect ice flow velocity as well as the rate of calving. There is presumed to be a difference in the back-stress applied from rigid sikussaks and loose melange structures, although this cannot be surmised from calculations of back-stress which are based solely on measurements of melange thickness at the calving face, and it is therefore suggested that calculations based on a

consideration of melange volume and rigidity would be more appropriate. Additionally, although the presence of a pro-glacial sikussak is an important control on seasonal suppression of calving (thereby enabling winter advance of the calving front), additional factors, including seasonal meltwater inputs, also affect seasonal variations in flow and calving (Walter et al., 2012).

This analysis suggests that there is a stabilising feedback between the growth of sikussak structures during the glacier calving season and the flow velocity of the glacier feeding it. This is shown in Section 4.2 by the significant positive correlation between glacier velocity and sikussak thickness and extent, which indicates that at faster glaciers, a thicker sikussak builds up. Calculations in Section 4.3 based on the work by Walter et al. (2012) indicate that thicker sikussaks exert a greater back-stress on the calving front.

5. 5. Implications for future change

There has been a long history of observations of change in the pro-glacial environments of Greenland's tidewater glaciers since 1945, when Koch observed uninhibited iceberg calving from the glaciers of North Greenland in 1938, which in 1933 had been restrained by thick, multi-year ice packed against the calving front (Wadhams, 1981). It has also been noted by Dowdeswell et al. (2000) that sikussak was likely much more extensive during the YD and LIA cold events, as a result of generally lower temperatures.

If the trend observed in Figure 4.5 continues into the next decade, as expected under predicted future climatic warming (IPCC, 2007), the lower limit of seasonally rigid sikussak is expected to rise by at least one degree of latitude, to 67.5°N. Under this scenario, JI and KL will move out of the zone of seasonally rigid sikussak, and will therefore no longer be affected by the proposed stabilising feedback afforded by these structures. This is likely to result in an extension of the calving season, and consequently contribute to a substantial increase in the calving flux of these glaciers. Flow instabilities are predicted to be initiated at KS, RI, UM and II, which are expected to fall below the threshold proposed by Reeh et al. (1999).

Similarly, those zones of multi-year fast-ice north of 78°N may experience a transition to seasonal sikussak if the upper threshold of sikussak formation also shifts northwards. Evidence of break-up of large areas of multi-year fast ice in the high northern latitudes at PM, 79N and Hagen Glacier indicates that this process may already be underway.

Although it might appear that the predicted future climatic warming will cause the zones of sikussak and multi-year fast-ice to shift north, this interpretation is dependent on atmospheric and oceanic factors being homogenous across latitudinal bands. However, it is clear from the analysis of the NAO effect on warm water intruding across the continental shelf of south-east Greenland that the oceanographic factors which affect the south-eastern coast are dependent upon location-specific oceanographic and atmospheric patterns, including the NAO and the Irminger Current. The correlation between the lower limit of sikussak formation and the 69°N limit of the Irminger Current on the east coast supports this analysis, and these forcings will not necessarily transfer in a predictable way to the western and northern coasts.

5. 6. Study Limitations

Due to the limited nature of this study, only 13 glaciers were investigated, 3 of which were discounted as not having sikussak or melange structures in the early stages of the analysis. This leaves a dataset of 10 glaciers, which is relatively few, but sufficient to develop key new insights into the relationship between sikussak structures and the glaciers which they abut. This study was constrained by the availability of data from the IceBridge mission data on which a large proportion of the results are based. It was therefore limited to those glaciers from which data was gathered down the long-profile by flight-lines down-glacier. Additionally, although consideration was put into gathering data from those glaciers for which the maximum amount of good data was available, some glaciers were limited to only two out of the three years of this study due to poor data availability.

It was not possible to derive winter SST from the ERA-Interim data due to formation of sea ice over the sea surface in winter. It was additionally limiting to use only sea surface temperatures in the analysis of oceanographic influence, as it is well established that much of the warm water which affects the termini of tidewater glaciers in Greenland is transferred across the continental shelf at depth due to its dense and highly saline nature (Christoffersen et al., 2011).

Future study could be undertaken to better constrain the latitudinal boundaries of the zones of melange, sikussak and multi-year land-fast ice. The Operation IceBridge data collection is ongoing, and so more years will become available for analysis in the future. It would be interesting to investigate how the morphology of pro-glacial melange and sikussak evolves over a longer time period, in order to evaluate the influence of climate change on these structures. Additionally, comparing sikussak observations to annual and seasonal changes in ice velocity may yield some interesting insights into the relationship between sikussak and glacio-dynamics. Finally, a better

consideration of the structural rigidity and volume of melange structures is required in order to better constrain estimates of their back-stress effect.

6. Conclusion

This study recommends that the term 'sikussak' be adopted in glaciological literature to refer to a shelf-like seasonal feature comprised of ice bergs and bergy bits, held together by sea ice. This term is included in the broader heading of 'melange', which is used to refer to any mixture of ice types, and may be either loose or rigid.

It is found that sikussak rigidity may be defined using a fast-ice index, developed from the work by Reeh et al. (1999), based on the ratio between annually summed degree-days above and below the freezing point of sea water. From this, rough latitudinal areas where multi-year fast ice, seasonal sikussak, and loose melange are found may be delimited. Sikussak structures are found to exist within a distinct latitudinal zone between 68.5 and 77°N in the fjords of Kangerdlugssuaq Gletscher, Jakobshavn Isbrae, Kangerlussuaq Sermerssua, Rink Isbrae, Umiamako Isbrae, Daugaard-Jensen Glacier, Ingia Isbrae and Tracy Glacier. Below 67.5°N, sea ice does not seasonally form to bond the clasts into a rigid structure, and so loose melange structures are found in Kangiata Nunata Sermia and Helheim Gletscher fjords. Above 78°N, multi-year land-fast ice is found at Zachariae Isstrom and Nioghalvfjerdsfjorden, although this is not observed at Petermann Glacier.

Although environmental factors define the latitudinal zone where melange and sikussak structures may be found, the primary control on the morphology of these pro-glacial structures is ice velocity, which is proportional to calving flux under steady-state conditions. Thus, the thickness and extent of these melange and sikussak structures is a primarily a function of the volume of glacier ice which is calved. Fjord topography is identified as a secondary control on melange and sikussak extent. Thinner sections of fjord afford rigid sikussak stability from side-wall friction, and protect loose melange from the effect of winds, waves and tides.

Sikussak structures are found to exert a back-stress on the glacier calving front in the range 5-65 kPa. Unsurprisingly, thicker sikussaks exert a greater back-stress on the calving front, and this is thought to reduce calving and restrain flow during the period of seasonal rigidity.

It is now proposed that there is a stabilising feedback between sikussak formation and glacier velocity, whereby rapid glacier flow with a high calving flux results in a thicker sikussak building up at the calving front, which exerts a greater back-stress on the calving front, inhibiting calving. If the latitudinal zone of sikussak formation moves northward by one degree of latitude, Kangerdlugssuaq and Jakobshavn Isbrae, two of the most prolific exporters of ice in the GrIS, will no longer be in the zone of sikussak formation, and their calving flux no longer mitigated by this stabilising feedback. This has important implications for the future mass balance of the GrIS.

7. References

ADTIC: U. S. Arctic, Desert, Tropic Information Centre (1955) *Glossary of arctic and subarctic terms* Maxwell Air Force Base, Alabama: Air University, Research Studies Institute. (ADTIC Publication A-105)

Ahn, Y., and Box, J. E. (2010) Glacier velocities from time-lapse photos: technique development and first results from the Extreme Ice Survey (EIS) in Greenland *Journal of Glaciology* 56 (198): 723-734

Amundsen, J. M., Fahnestock, M., Truffer, M., Brown, J., Luthi, M. P., Motyka, R. J. (2010) Ice melange dynamics and implications for terminus stability, Jakobshavn Isbrae, Greenland *Journal of Geophysical Research* 115 (F01005):1-12

Andresen, C. S., Straneo, F., Ribergaard, M. H., Bjork, A. A., Andersen, T. J., Kuijpers, A., Norgaard-Pedersen, N., Kjaer, K. H., Schjoth, F., Weckstrom, K., Ahlstrom, A. P. (2012) Rapid response of Helheim Glacier in Greenland to climate variability over the past century *Nature Geoscience* 5: 37-41

Andrews, J. T., Milliman, J. D., Jennings, A. E., Rynes, N., Dwyer, J. (1994) Sediment thicknesses and Holocene glacial marine sedimentation rates in three East Greenland fjords *The Journal of Geology* 102 (6): 669-683

Assur, A. (1956) *Airfields on Floating Ice Sheets for Routine and Emergency Operations: SIPRE Report* Snow Ice and Permafrost Research Establishment, Corps of Engineers, U.S. Army.

Bamber, J. L., Alley, R. B., Joughin, I. (2007) Rapid response of modern day ice sheets to external forcing *Earth and Planetary Science Letters* 257 (1-2): 1-13

Bassis, J. N., and Walker, C. C. (2012) Upper and lower limits on the stability of calving glaciers from the yield strength envelope of ice *Proceedings of the Royal Society A*

Benn, D. I., Warren, C. R., Mottram, R. H. (2007) Calving processes and the dynamics of calving glaciers *Earth-Science Reviews* 82: 143-179

Box, J. E., and Decker, D. T. (2011) Greenland marine-terminating glacier area changes: 2000-2010 *Annals of Glaciology* 52 (59): 91-98

Bradley, R. S., and England, J. H. (2008) The Younger Dryas and the Sea of Ancient Ice *Quaternary Research* 70: 1-10

Christoffersen, P., Mugford, R. I., Heywood, K. J., Joughin, I., Dowdeswell, J. A., Syvitski, J. P. M., Luckman, A., Benham, T. J. (2011) Warming of waters in an East Greenland fjord prior to glacier retreat: mechanisms and connection to large-scale atmospheric conditions *Cryosphere* 5 (3): 701-714

Christoffersen, P., O'Leary, M., van Angelen, J. H., van den Broeke, M. (2012) Partitioning effects from ocean and atmosphere on the calving stability of Kangerdlugssuaq Glacier, East Greenland *Annals of Glaciology* 53(60): 1-8

Copland, L., Mueller, D. R., Weir, L. (2007) Rapid loss of the Ayles Ice Shelf, Ellesmere Island, Canada *Geophysical Research Letters* 34 (L21501): 1-6

Dowdeswell, J. A., Whittington, R. J., Jennings, A. E., Andrews, J. T., Mackensen, A., Marienfield, P. (2000) An origin for laminated glacimarine sediments through sea-ice build-up and suppressed iceberg rafting *Sedimentology* 47: 557-576

Dwyer, J. L. (1995) Mapping tide-water glacier dynamics in East Greenland using Landsat data *Journal of Glaciology* 41 (139): 584-595

Echelmeyer, K. A., and Kamb, B (1986) Stress-gradient coupling in glacier flow. II. Longitudinal averaging of the flow response to small perturbations in ice thickness and surface slope *Journal of Glaciology* 32 (111): 285-298

Fausto, R. S., Ahlstrom, A. P., Van As, D., Boggild, C. E., Johnsen, S. J. (2009) A new present-day temperature parameterization for Greenland *Journal of Glaciology* 55 (189): 95-105

Fox, C., and Squire, V. A. (1991) Strain in shore fast ice due to incoming ocean waves and swell *Journal of Geophysical Research* 96 (C3): 4531-4574

Frederking, R. M. W., and Timco, G. W. (1984) Measurement of shear strength of granular/discontinuous columnar sea ice *Cold Regions Science and Technology* 9: 215-220

Frederking, R. M. W., and Timco, G. W. (1986) Field measurements of the shear strength of columnar-grained sea ice *In: Proc. 8th IAHR Symposium on Ice,* Vol. I, pp 279-292, Iowa City, U.S.A, 1986.

Freuchen, P. (1915) General observations as to natural conditions in the country traversed by the expedition *Meddelelser om Grønland* 58: 284-340

Fricker, H. A., Bassis, J. N., Minster, B., MacAyeal, D. R. (2005) ICESat's new perspective on ice shelf rifts: The vertical dimension *Geophysical Research Letters* 32 (L23S08): 1-5

Geirsdottir, A., Miller, G. H., Wattrus, N. J., Bjornsson, H., Thors, K. (2008) Stabilization of glaciers terminating in closed water bodies: Evidence and broader implications

Germe, A., Houssais, M-N., Herbaut, C., Cassou, C. (2011) Greenland Sea sea ice variability over 1979-2007 and its link to the surface atmosphere *Journal of Geophysical Research* 116 (C10034): 1-14

Hakkinen, S. and Rhines, P. B. (2004) Decline of subpolar North Atlantic circulation during the 1990s *Science* 304: 555-559

Hanna, E., Cappelen, J., Fettweis, X., Huybrechts, P., Luckman, A., Ribergaard, M. H. (2009) Hydrological response of the Greenland ice sheet: the role of oceanographic warming *Hydrological Processes* 23: 7-30

Hanna, E., Huybrechts, P., Steffen, K., Cappelen, J., Huff, R., Shuman, C., Irvine-Fynn, T., Wise, S., Griffiths, M. (2008) Increased runoff from melt from the Greenland ice sheet: A response to global warming *Journal of Climate* 21 (2): 331-341

Higgins, A. K. (1991) North Greenland glacier velocities and calf ice production *Polarforschung* 60 (1): 1-23

Holland, D. M., Thomas, R. H., De Young, B., Ribergaard, M. H., (2008a) Acceleration of Jakobshavn Isbrae triggered by warm subsurface ocean waters *Nature Geoscience* 1: 659-664

Howat, I. M., Box, J. E., Ahn, Y., Herrington, A., McFadden, E. M. (2010) Seasonal variability in the dynamics of marine-terminating outlet glaciers in Greenland *Journal of Glaciology* 56 (198): 601-613

Howat, I. M., Joughin, I., Fahnestock, M., Smith, B. E., Scambos, T. A. (2008) Synchronous retreat and acceleration of southeast Greenland outlet glaciers 2000-06: ice dynamics and coupling to climate *Journal of Glaciology* 54 (187): 646-660

Howat, I. M., Joughin, I., Tulaczyk, S., Gogineni, S. (2005) Rapid retreat and acceleration of Helheim Glacier, east Greenland *Geophysical Research Letters* 32 (L22502): 1-4

IPCC (2007) *Climate Change 2007: The Physical Science Basis. Contribution of Working Group I to the Fourth Assessment Report of the Intergovernmental Panel on Climate Change* [Solomon, S., D. Qin, M. Manning, Z. Chen, M. Marquis, K.B. Averyt, M. Tignor and H.L. Miller (eds.)]. Cambridge University Press, Cambridge, United Kingdom

Johnson, J. V., Prescott, P. R., Hughes, T. J. (2004) Ice dynamics preceding catastrophic disintegration of the floating part of Jakobshavn Isbrae, Greenland *Journal of Glaciology* 50 (171): 492-504

Joughin, I. (2002) Ice-Sheet Velocity Mapping: A Combined Interferometric and Speckle-Tracking Approach *Annals of Glaciology* 34: 195-201

Joughin, I., Das, S., King, M. A., Smith, B. E., Howat, I. M., Moon, T. (2008a) Seasonal speedup along the western flank of the Greenland ice sheet *Science* 320: 781-783

Joughin, I., Howat, I. M., Alley, R. B., Ekstrom, G., Fahnestock, M., Moon, T., Nettles, M., Truffer, M., Tsai, V. C. (2008b) Ice-front variation and tidewater behaviour on Helheim and Kangerdlugssuaq Glaciers, Greenland *Journal of Geophysical Research* 113 (F01004): 1-11

Joughin, I., Howat, I. M., Fahnestock, M., Smith, B., Krabill, W. Alley, R. B., Stern, H., Truffer, M. (2008c) Continued evolution of Jakobshavn Isbrae following its rapid speedup *Journal of Geophysical Research* 113 (F04006): 1-14

Joughin, I., Smith, B. E., Howat, I. M., Scambos, T., Moon, T. (2010) Greenland flow variability from ice-sheet-wide velocity mapping *Journal of Glaciology* 56 (197): 415-429

Koch, L. (1926) Ice cap and sea ice in North Greenland *Geographical Review* 16 (1): 98-107

Koch, L. (1928) Contributions to the glaciology of North Greenland *Meddelelser om Grønland 65 (2): 181-464*

Koch, L. (1945) The East Greenland Ice *Meddelelser om Grønland 130 (3): 1-374*

Krupnik, I., Aporta, C., Gearhead, S., Laidler, G. S., Holm, L. K., eds., (2010) *SIKU: Knowing Our Ice: Documenting Inuit Sea Ice Knowledge and Use* Springer, New York.

Kurtz, N., and Harbeck, J. (2012) Operation IceBridge sea ice freeboard, snow depth, and thickness data products manual

Kwok, R., and Cunningham, G. F. (2008) ICESat over Arctic sea ice: Estimation of snow depth and ice thickness *Journal of Geophysical Research* 113 (C08010): 1-18

Kwok, R., Toudal Pederson, L., Gudmandsen, P., Pang, S. S. (2010) Large sea ice outflow into the Nares Strait in 2007 *Geophysical Research Letters* 37 (L03502): 1-6

Laidler G. J (2007) *Ice, Through Inuit Eyes: Characterizing the Importance of Sea Ice Processes, Use, and Change Around Three Nunavut Communities* PhD Thesis. Department of Geography, University of Toronto.

Larour, E., Rignot, E., Aubrey, D. (2004) Modelling of rift propagation on Ronne Ice Shelf, Antarctica, and sensitivity to climate change *Geophysical Research Letters* 31 (L16404): 1-4

Lloyd, J., Moros, M., Perner, K., Telford, R. J., Kuijpers, A., Jansen, E., McCarthy, D. (2011) A 100 yr record of ocean temperature control on the stability of Jakobshavn Isbrae, West Greenland *Geology* 39 (9): 867-870

Luckman, A., Murray, T., de Lange, R., Hanna, E. (2006) Rapid and synchronous ice-dynamic changes in East Greenland *Geophysical Research Letters* 33 (L03503): 1-4

MacAyeal, D. R., Freed-Brown, J., Zhang, W. W., Amundsen, J. M. (2012) The influence of ice melange on fjord seiches *Annals of Glaciology* 53 (60): 45-49

Maslinik, J. A., Serreze, M. C., Barry, R. G. (1996) Recent decreases in Arctic summer ice cover and linkages to atmospheric circulation anomalies *Geophysical Research Letters* 23 (13): 1677-1680

Mayer, H., and Herzfeld, U. C. (2008) The rapid retreat of Jakobshavns Isbrae, West Greenland: Field observations of 2005 and structural analysis of its evolution *Natural Resources Research* 17 (3): 167-178

Meier, M. F., and Post, A. (1987) Fast tidewater glaciers *Journal of Geophysical Research* 92 (B9): 9051-9058

Moon, T., Joughin, I., Smith, B., Howat, I. (2012) 21st-Century evolution of Greenland outlet glacier velocities *Science* 336: 576-578

Motyka, R. J., Hunter, L., Echelmeyer, K. A., Connor, C. (2003) Submarine melting at the terminus of a temperature tidewater glacier, LeConte Glacier, Alaska, U.S.A. *Annals of Glaciology* 36: 57-65

Munchow, A., Falkner, K. K., Melling, H., Rabe, B., Johnson, H. L. (2011) Ocean warming of Nares Strait bottom water off NW Greenland 2003-09 *Oceanography*24 (3): 114-123

Murray, T., Scharrer, K., James, T. D., Dye, S. R., Hanna, E., Booth, A. D., Selmes, N., Luckman, A., Hughes, A. L. C., Cook, S., Huybrechts, P. (2010) Ocean regulation hypothesis for glacier dynamics in southeast Greenland and implications for ice sheet mass changes *Journal of Geophysical Research* 115 (F03026): 1-15

Nick, F. M., van der Veen, C. J., Vieli, A., Benn, D. I. (2010) A physically based calving model applied marine outlet glaciers and implications for the glacier dynamics *Journal of Glaciology* 56 (199): 781-794

Nick, F. M., Vieli, A., Howat, I. M., Joughin, I. (2009) Large-scale changes in Greenland outlet glacier dynamics triggered at the terminus *Nature Geoscience* 2: 110-114

Paige, R. A., and Lee, C. W. (1967) Preliminary studies on sea ice in McMurdo Sound, Antarctica, during "Deep Freeze 65" *Journal of Glaciology* 6 (46): 515-528

Petersen, G. H. (1977) Biological effects if sea-ice and icebergs in Greenland pp. 319-329 In: M. J. Dunbar (ed.) *Polar Oceans*. Arctic Institute of North America, Calgary.

Pounder, E. R., and Little, E. M. (1959) Some physical properties of sea ice *Canadian Journal of Physics* 37 (4): 443-473

Rasmussen, K. J. V. (1915) Report of the First Thule Expedition 1912 *Meddelelser om Grønland* 58: 284-340

Reeh, N., Mayer, C., Miller, H., Thomsen, H. H., Weidick, A. (1999) Present and past climate control on fjord glaciations in Greenland: Implications for IRD-deposition in the sea *Geophysical Research Letters* 26 (8): 1039-1042

Reeh, N., Thomsen, H. H., Higgins, A. K., Weidick, A. (2001) Sea ice and the stability of north and northeast Greenland floating glaciers *Annals of Glaciology* 33: 474-480

Ribergaard, M. H. (2011) Oceanographic investigations off West Greenland *NAFO Scientific Council Documents* 11/001

Rignot, E., Buscarlet, G., Csatho, B., Gogineni, S., Krabill, W., Schmeltz, M. (2000) Mass balance of the northeast sector of the Greenland ice sheet: a remote sensing perspective *Journal of Glaciology* 46 (153): 265-273

Rignot, E. J., Gogineni, S. P., Krabill, W. B., Ekholm, S. (1997) North and northeast Greenland Greenland ice discharge from satellite radar interferometry *Science* 276: 934-937

Rignot, E., and MacAyeal (1998) Ice-shelf dynamics near the front of the Filchner-Ronne Ice Shelf, Antarctica, revealed by SAR interferometry *Journal of Glaciology* 44: 405-418

Seale, A. (2009) *South-east Greenland Ice Sheet short term response to environmental conditions* MPhil Dissertation. Scott Polar Research Institute, University of Cambridge.

Seale, A., Christoffersen, P., Mugford, R. I., O'Leary, M. (2011) Ocean forcing of the Greenland Ice Sheet: Calving fronts and patterns of retreat identified by automatic satellite monitoring of eastern outlet glaciers *Journal of Geophysical Research* 116 (F03013): 1-16

Schneider, W., and Budeus, G. (1997) A note on the Norske Ø Ice Barrier (Northeast Greenland), viewed by Landsat 5 TM *Journal of Marine Systems* 10: 99-106

Sohn, H-G., Jezek, K. C., van der Veen, C. J. (1998) Jakobshavn Glacier, West Greenland: 30 years of spaceborne observations *Geophysical Research Letters* 25 (14): 2699-2702

Stein, M. (2005) North Atlantic subpolar gyre warming – impacts on Greenland offshore waters *Journal of Northwest Atlantic Fisheries Science* 36: 43-54

Stern, H. L., and Heide-Jorgenden, M. P. (2003) Trends and variability of sea ice in Baffin Bay and Davis Strait, 1953-2001 *Polar Research* 22 (1): 11-18

Straneo, F., Curry, R. G., Sutherland, D. A., Hamilton, G. S., Cenedese, C., Vage, K., Stearns, L. A. (2011) Impact of fjord dynamics and glacial runoff on the circulation near Helheim Glacier *Nature Geoscience* 4: 322-327

Straneo, F., Hamilton, G. S., Sutherland, D. A., Stearns, L. A., Davidson, F., Hammill, M. O., Stenson, G. B., Rosin-Asvid, A. (2010) Rapid circulation of warm subtropical waters in a major glacial fjord in East Greenland Nature Geoscience 3: 182-186

Syvitski, J.P.M, Burrell, D.C., Skei, J.M. (1987) *Fjords: Processes and Products* Springer Verlag, NY.

Syvitski, J. P. M., Andrews, J. T., Dowdeswell, J. A. (1996) Sediment deposition in an iceberg-dominated glacimarine environment, East Greenland: basin fill implications *Global and Planetary Change* 12: 251-270

Thomsen, H. H., Reeh, N., Olesen, O. B., Boggild, C. E., Starzer, W., Weidick, A., Higgins, A. K. (1997) The Nioghavfjerdsfjorden glacier project, North-East Greenland: a study of ice sheet response to climatic change *Geology of Greenland Survey Bulletin* 176: 95-103

van der Veen, C. J. (1996) Tidewater calving *Journal of Glaciology* 42 (141): 375-385

Vieli, A., Funk, M., Blatter, H. (2001) Flow dynamics of tidewater glaciers: a numerical modelling approach *Journal of Glaciology* 47 (157): 595-606

Wadhams, P. (1981) The ice cover in the Greenland and Norwegian Seas *Reviews of Geophysics and Space Physics* 19 (3): 345-393

Walsh, K. M., Howat, I. M., Ahn, Y., Enderlin, E. M. (2012) Changes in the marine-terminating glaciers of central east Greenland, 2000-2010 *The Cryosphere* 6: 211-220

Walter, J. I., Box, J. E., Tulaczyk, S., Brodsky, E. E., Howat, I. M., Ahn, Y., Brown, A. (2012) Oceanic mechanical forcing of a marine-terminating Greenland glacier *Annals of Glaciology* 53 (60): 181-192

Walters, R. A. (1989) Small-amplitude, short-period variations in the speed of a tide-water glacier in south-central Alaska, U.S.A. *Annals of Glaciology* 12: 187-191

Warren, C. R. (1991) Terminal environment, topographic control and fluctuations of West Greenland glaciers *Boreas* 20: 1-15

Wiseman, W. J., Owens, E. H., Kahn, J. (1981) Temporal and spatial variability of ice-foot morphology *Geografisk Annaler* 63A: 69-80

Zwally, H. J., Yi, D., Kwok, R., Zhao, Y. (2008) ICESat measurements of sea ice freeboard and estimates of sea ice thickness in the Weddell Sea *Journal of Geophysical Research* 113 (C02S15): 1-17